GEOPHYSICAL MAPPING OF GEOLOGICAL STRUCTURES AS POTENTIAL SITE FOR GOLD MINERALIZATION AT GOLDEN PRIDE NZEGA GREENSTONE BELT TABORA SOUTH OF LAKE VICTORIA TANZANIA

BY

NKYA ABRAHAM TUMSIFU

I56/70141/2011

A Dissertation Prepared and Submitted to the University of Nairobi in Partial Fulfilment for the Award of Degree of Masters of Science in Geology (Mineral Exploration).

DECEMBER, 2013

UNIVERSITY OF NAIROBI

DECLARATION

I hereby declare, that this dissertation is my original work and it has not been submitted for a degree in any other university or for any other award.

SIGNED ……. DATE …….

NKYA ABRAHAM TUMSIFU

The dissertation has been submitted for examination with my knowledge as University supervisors.

SIGNED ……DATE …….

PROF. J.O. BARONGO.

School of Physical Science

Department of Geology

P.O. Box 30197-00100

University of Nairobi (Kenya)

SIGNED ……DATE …….

DR. E. DINDI.

School of Physical Science

Department of Geology

P.O. Box 30197-00100

University of Nairobi (Kenya)

DEDICATION

I dedicate this dissertation to my lovely wife Esther and daughter Abigail. I also dedicate this work to my mother, Elivida Daniel Kisaka for putting in place strong foundation in my academic life by sacrificing and making sure my school fees are paid in time.

ABSTRACT

The study area is located southeast of Lake Victoria in Nzega greenstone belt Tanzania. It represents inferred late Archean orogenic gold deposits and is hosted in intensely deformed meta-sedimentary rocks. Nzega greenstone belt of the Nyanzian Super-group comprises felsic volcanics, Banded Iron Formation (BIF), and subordinate mafic volcanics and sedimentary rocks. Archean mineralization is hosted by BIF or felsic tuffs. Mineralisation is hosted within an east-west striking, steeply dipping, and brittle-ductile shear zone within a sequence of volcani-clastic and siliclastic rocks of Archean age.

Aeromagnetic data are fully analyzed and interpreted where the analysis and interpretation are mainly devoted towards outlining significant surface and subsurface tectonic trends and their relationship with anomalous zones. According to the qualitative interpretation of the geological and aeromagnetic data, shaded relief maps, upward continuation together with vertical derivatives, analytical signals technique significantly improve the interpretation of magnetic data in terms of discriminating between shallow and deep magnetic sources within the study area.

The lineament structural map is constructed through the signatures of the contours and shaded relief of the total aeromagnetic data, analytical signal and horizontal derivatives. Euler de-convolution was applied to the aeromagnetic anomaly map to delineate geologic contacts. The depth estimates calculated for these major magnetic anomalies range between 1.6 and 2.1 km. Lineament structural map and magnetic depth map values have been utilized to conduct the interpretation of the main subsurface structures affecting the study area, which correlate with the previous studies of aero radiometric anomalous zones all over the study area. The obtained results show the most significant structural trends affecting the distribution of the anomalies in the present study area.

Three main tectonic trends are outlined from the total aeromagnetic and shading relief maps. These trends were defined as NE, NW and E-W; the prominent N-S trending fault identified from the aeromagnetic data and also found on the surface geological map of the study area shows its reactivation. These trends apparently control the distribution of gold mineral occurrence in the area. Furthermore, most of the mineralization occurrences of Nzega greenstone belt have showed an intimate association with interpreted high magnetic zones and lineaments. It is also evident that lithological units affected by high lineament density have hosted some of the gold occurrences.

ACKNOWLEDGEMENTS

I would like to thank all the people who contributed in various ways to the successful completion of this work. I am indebted to the Geological Survey of Tanzania, particularly Mr. Minja for providing most of the datasets required for the research.

My gratitude goes to my supervisors Prof. J. Barongo and Dr. E. Dindi who meticulously went through all my work and gave invaluable advice. I really appreciate your letting me be! Without you this would not have been possible.

I acknowledge the support and encouragement of my friends and colleagues in the University of Nairobi student community. Last but not least, to my wife Esther and daughter Abigail and all members of my family. I say thank you for your support, understanding and long-suffering.

TABLE OF CONTENTS

DECLARATION ..... **i**

DEDICATION ..... **ii**

ABSTRACT ..... **iii**

ACKNOWLEDGEMENTS ..... **iv**

LIST OF TABLES ..... **ix**

1 CHAPTER ONE: INTRODUCTION **1**

1.1 Introduction **1**

1.2 Research Background **3**

1.3 Motivation for this Research **5**

1.4 Research Problem **5**

1.5 Research Objective **6**

1.6 Specific Objectives **6**

1.7 Research Questions **6**

1.8 Thesis/Dissertation Structure **7**

1.9 Location and Access **9**

1.10 Physiography and Drainage **10**

1.11 Historical Exploration and Mining in Tanzania **12**

1.12 Modern Gold Exploration and Mining **14**

2 CHAPTER TWO: LITERATURE REVIEW **17**

3 CHAPTER THREE: THE GEOLOGY **26**

3.1 Regional Geology **26**

3.2 Regional Geological Setting of Lake Victoria Gold Fields **33**

3.3 Local Geology **37**

3.4 Mineralization in the Lake Victoria Gold Fields **39**

4 CHAPTER FOUR: MATERIALS AND METHODS 40

4.1 Pre -field work 40
4.1.1 The study of Geological map by Barth (1990) 40

4.2 Post-field work 41

4.3 Resources/Materials 41
4.3.1 Airborne Magnetic data 41
4.3.2 Geological map 41
4.3.3 Software and Hardware 42

4.4 Aeromagnetic Data Processing 42
4.4.1 Data Processing 42
4.4.1.2 Geo-referencing 42
4.4.1.3 Removal of earth's normal magnetic field 43
4.4.1.4 Image Enhancement 43
4.4.1.5 Shaded Relief Grey-Scale Map 44
4.4.1.6 Colour Shaded Relief Image 44
4.4.1.7 Vertical Derivatives 46
4.4.1.8 Reduction to pole 46
4.4.1.9 Analytical Signal 46

5 CHAPTER FIVE: DATA PROCESSING AND INTERPRETATION 47

5.1 Introduction 47

5.2 Qualitative Interpretation 48

5.3 Quantitative interpretation 49
5.3.1 Interpretation of aeromagnetic data 49
5.3.2 Structural features from aeromagnetic imagery 57

5.4 Structural features 58
5.4.1 Interpretation of magnetic lineaments 58
5.4.2 Geological features indicative of mineralization from the geological map 65
5.4.2.1 Lithology 65
5.4.2.2 The granite-greenstone contact 66
5.4.2.3 Geological structural from the geological map 66

5.5 Quantitative Interpretation of Magnetic data 68
5.5.1 Trend Analysis 68
5.5.2 Depth estimation 68

5.6 The structural map of the study area deduced from magnetic interpretation 73

6 CHAPTER SIX: DISCUSSION AND CONCLUSIONS 75

6.1 Discussion 75

6.2 Conclusions 77

7 CHAPTER SEVEN: RECOMMENDATIONS 78

REFERENCES 79

APPENDICES 87

LIST OF FIGURES

Figure 1-1: Outline of the dissertation 8
Figure 1-2: Sketch map showing the study area in Tanzania south of Lake Victoria. Note that the indicated gold-occurrence comprises active and abandoned mines, prospect, and active local digging sites. Gold deposits indicated on map include: Tulawaka (TU), Geita (GT), Bulyanhulu (BU), Buck Reef (BF), Buzwagi (BZ), Golden Pride (GP), North Mara (NM) 9
Figure 1-3: Physiographic map of Nzega 11
Figure 3-1: Geological Map of Tanzania (from Hester, 1998) 30
Figure 3-2: Geologic Section of Tanzania (from Hester et al, 1998) 31
Figure 3-3: Stratigraphic Column of the Geology of Tanzania (Barth 1990) 32
Figure 3-4: Overview map of greenstone belts (in green) and major gold deposits in the Lake Victoria Goldfields, northern Tanzania. Gold deposits indicated on map include: Tulawaka (TU), Geita (GT), Bulyanhulu (BU), Buck Reef (BR) 34
Figure 3-5: Interpretation of Regional Geological Map of Lake Victoria Gold Field (after Borg, 1994). 36
Figure 3-6: Geological map of Tanganyika from Degree Sheet 28-Nzega North-West (after Handle, 1956) 38
Figure 4-1: The HSV colour model (after Foley et al; 1990) H.S.V represent Hue, Saturation and Value, respectively Figure: The HSV colour model. 45
Figure 5-1: Total Magnetic Intensity (TMI) with Lines indicating identified magnetic faults. . 51
Figure 5-2: Analytical signal images with identifying the N-S magnetic faults anomalies. 52
Figure 5-3: Vertical derivative images identifying magnetic faults anomalies. 53
Figure 5-4: Horizontal derivative image of the study area amplified deep anomalies 54
Figure 5-5: Second vertical derivative images 55
Figure 5-6: Upward continuation images 56
Figure 5-7: Shading relief map of total magnetic intensity, to show the main structural trends affecting the study area: A) N-S, B) NW- SE, C) ENE and D) NE-SW trends. 60
Figure 5-8: The interpreted structural lineament map of the study area according to analytical signaland horizontal derivative 61
Figure 5-9: The interpreted structural lineament map of the study area to show surface and subsurface geologic structures 62
Figure 5-10: The interpreted structural lineament map of the study area from shaded relief image map 62
Figure 5-11: Geology and Structural Interpretation of shaded relief image map 64
Figure 5-12: Lithological map of the study area compiled from the Geological Survey of Tanganyika. 67
Figure 5-13: Magnetic depth coloured map as a result of Euler de-convolution of the total aerial magnetic intensity data. 70
Figure 5-14: Plot of the Euler solutions of the magnetic anomaly and structural index one representing linear intrusive). 71
Figure 5-15: Estimated locations of Magnetic contacts/structures according Euler de-convolution methods 72
Figure 5-16: Structural map from the synthesis of geology, structure and aeromagnetic interpretation. 74

LIST OF TABLES

Table 1-1: A listing of gold and base metal mines in Tanzania (after Hester, 1998): 13

Table 1-2: Resource data from different mining being obtained by public news releases (after Hester, 1998):.....15

Table 1-3: Significant new gold discoveries made since the mid 1990s (after Hester, 1998):' .16

1 CHAPTER ONE: INTRODUCTION

1.1 Introduction

The area under study is located in the southeastern part of Lake Victoria. It represents an inferred late Archaean orogenic gold deposit and is hosted in intensely deformed meta-sedimentary rocks. A major problem in this regard is that the regional structure and distribution of fault zones within the greenstone belt is not understood and therefore the researcher is trying to interpret the aeromagnetic data to find out these geological structures.

Magnetics is a geophysical survey technique that exploits the considerable differences in the magnetic properties of minerals with the ultimate objective of characterizing the Earth's sub-surface. The technique requires the acquisition (Horsfall, 1997) of measurements of the amplitude of the magnetic field at discrete points along survey lines distributed regularly throughout the area of interest. The magnetic field, whose amplitude is measured, is the vector sum of;

- The Earth's main field which originates from dynamo action of conductive fluids in the Earth's deep interior (Merrill et al., 1996);
- An induced field caused by magnetic induction in magnetically susceptible earth materials polarized by the main field (Doell and Cox, 1967);
- A field caused by remanent magnetism of earth materials (Doell and Cox, 1967); and,
- Other (usually) less significant fields caused by solar, atmospheric (Telford et al., 1976) and cultural influences.

It is the induced and remanent fields that are of particular interest to the regolith geoscientist because the magnitudes of these fields are directly related to the magnetic susceptibility, spatial distribution and concentration of the local crustal materials. Fortunately, only a few minerals occur abundantly enough in nature to make a significant contribution to the induced and remanent fields. The most important of these is magnetite and, to a lesser extent, ilmenite and pyrrhotite (Clarke, 1997; Telford et al., 1976).

Once the main field and the minor source effects are removed from the observed magnetic field data via various data reduction and processing methods, the processed data serve as an indicator of the spatial distribution and concentration of the magnetically significant minerals. At this point, the data are enhanced and presented (Milligan and Gunn, 1997) in readiness for their analysis.

Most importantly, the analysis ultimately leads to an interpretation (Gunn et al., 1997, Mackey et al., 2000) of structure, lithology, alteration, regolith and sedimentary processes, amongst many other factors. The geological ingredients that can be interpreted from magnetic surveys are those that influence the spatial distribution, volume and concentration of the magnetically significant minerals. It is important to realize that the magnetic data serve only as an indicator because it is generally not possible to ascertain a definitive, unambiguous and direct lithological or structural interpretation.

The magnetic field is usually measured with a total field magnetometer. The most common instrument in use today is the caesium vapour magnetometer. Observations are made at regular intervals (generally between 1 to 7 meters) along a series of traverse lines of constant azimuth and spacing. Observations are similarly made along tie lines oriented perpendicular to the traverse lines. Tie lines are necessary to assist in the removal of temporal variations in the main field.

Tie lines are usually spaced ten times further apart than traverse lines. Data may be acquired close to ground level (ground magnetic) either via a person carrying a magnetometer or with a magnetometer mounted on a motor vehicle. Alternatively, airborne magnetic (aeromagnetic) which is the data used in this research can be acquired via mounting the magnetometer on a fixed wing aircraft or a helicopter. Fixed aircraft acquisition is preferred due to the lower cost; however, helicopters are necessary where the terrain is rugged.

While data are being collected along the survey lines, a base station magnetometer also measures the magnetic field at a stationary point. These data serve as an estimate of the temporal variation of the main field, which is subtracted from the survey data. The base station magnetometer is also used to identify magnetic storm events (where the magnetic field is varying rapidly due to disturbances in the ionosphere/magnetosphere). On such occasions, data acquisition is suspended (or data re-acquired) because the estimate of the temporal variation is less accurate at a distance from the base station.

1.2 Research Background

The present study shows the relationships between surface and subsurface structural trends and the distribution of magnetic minerals. Therefore, the aeromagnetic survey aims to investigate the subsurface structural setting as it is a powerful tool in delineating the regional geology (lithology and structure) of buried basement terrain. The detailed aeromagnetic map is proven to be very effective in cases where the geology of the studied area is clearly known (Aero-Service, 1984).

According to Reford (1962), the earth's magnetic field, acting on magnetic minerals in the crust of the earth, induces a secondary field, which reflects the distribution of these minerals. The main field, which is the inducing magnetic field, varies slowly from one place to another. However, the crustal field which is the portion of the magnetic field associated with the magnetism of crustal rocks containing both magnetism caused by induction from the Earth's main magnetic field and from remanent magnetization, varies more rapidly. The airborne magnetometer records these variations in the total magnetic field. The regional correction removes the greater part of the primary field of the earth, so that the local variations of the secondary field are emphasized.

Although several familiar minerals have high susceptibilities (magnetite, ilmenite, and pyrrhotite), magnetite is by far the most common. Rock susceptibility, almost always, is directly related to the percentage of magnetite present. Spatial variations of the crustal field are usually smaller than the main field, nearly constant in time and place depending on the local geology, where the local magnetic anomalies are the targets in magnetic prospecting. Also, the magnetic method is employed, although not always successful, to map topographic features of the basement surface that might influence the structure of overlying sediments.

In addition, large-scale aeromagnetic surveys have been conducted to locate faults, shear zones and fractures. Such zones may serve as potential hosts for a variety of minerals, and may be used as a guidance exploration for the epigenetic, stress-related mineralization in the surrounding rocks (Paterson and Reeves, 1985). The qualitative interpretation of aeromagnetic survey data illustrates directly the geological information by looking at the map without any calculations (Grant and West, 1965). The very high gradient on an aeromagnetic map usually indicates the difference in magnetic susceptibility such as that between granite (acidic rock), andesite (intermediate rock) and basalt (basic rock); a condition called "intrabasement". The case of some variation of contour gradient on an aeromagnetic map usually indicates vertical movements (faults); a condition called "suprabasement" (Dobrin, 1976).

A considerable amount of qualitative interpretation of magnetic maps consists of recognizing and delineating anomaly patterns. These can be classified, especially on the so called regional maps covering comparatively large areas, into some basic shapes and their modifications. The following list is not exhaustive but will be found to be adequate in analysis of most regional magnetic maps:

- Circular feature or features of roughly the same extent in all directions;
- Long, narrow anomaly features, so called lineaments;
- Dislocations when one part of an anomaly pattern is displaced with respect to the other part;
- Extensive high intensity areas (sheets) with no regular pattern of contours but considerable relief in the field values;
- 'Quiet' areas with little relief in the field values showing no distinctive pattern areas;

Naturally, the various patterns do not necessarily occur isolated from each other but may be found superimposed. Experience shows that each pattern has its distinctive geological counterpart although the exact nature of this may differ from area to area. For instance, circular patterns are often associated with granitic as well as basic intrusions or with ore bodies, while long, narrow patterns are very frequently due to dikes, tectonic shear zones, isoclinally folded strata with magnetic impregnation or long ore bodies. Dislocations are indicative of geological faults. Large gabbro intrusives greenstone belts, etc, will typically give rise to sheets of anomalies.

In many instances, quartzite rock formations, monzonite, limestone, etc; can be delineated by typical quiet areas with low field values, but this is not invariably the case since, for example, many limestones with scarn minerals or quartzite with magnetic impregnation as well as monzonites can be associated with fairly high magnetic anomalies. The interpretation of various anomaly patterns on a magnetic map in terms of rocks must be made in conjunction with available field geological observations. Conversely, the availability of a magnetic map is of the greatest use in constructing the geology of sparse rock outcrops.

1.3 Motivation for this Research

Identification of prospective areas for gold mineralization within the Nzega greenstone belt will stimulate foreign investment in the area resulting in job creation in gold mining and downstream industries in Tanzania. This will contribute to economic development and improve living standards of the local people of Nzega and other impoverished rural areas. An investigation of the usefulness of Geo-soft package software V 6.3, Surfer V 9.9, as well as Geographic Information System (GIS) techniques in the study area is considered important due to the following observations:

- Most mineral deposits with field recognizable surface expressions in the Tanzania greenstone belts have already been found and exploited. There is, therefore, a need to find new deposits, or to identify extensions of known ore bodies by re-mapping the greenstone belt.

- Modern mining and extractive techniques now permit efficient exploitation of large, low grade deposits which have been overlooked in the past, or simply not considered as viable as compared in the past.

- The success of the Tanzania gold mining industry has largely been sustained by a high gold price, improved investment methods and exploration or development in and around existing mines. No important gold camps have been discovered in the Nzega greenstone belt apart from the Resolute Mining Company whose ore resources/reserves are almost coming to an end.

1.4 Research Problem

The Golden Pride Gold Mine is located in NW Tanzania, 750 km north-west of the port of Dar-es Salaam and 200 km south of Lake Victoria in Nzega district at latitude 4^0 13' 18"S and 4^0 30' 18"S longitude 33^0 11' 02"E and 33^0 30' 02"E (Figure 1.2). It occurs within the Nzega greenstone belt at the southern end of the Lake Victoria Greenstone Terrane. The study area, Nzega in the south east of Lake Victoria gold fields is one of the prospective regions for gold and other base metal mineralization where presently gold is being extracted by Golden Pride Mine.

The nature of gold and mineralized host rock in the area is still controversial. A major problem in this regard is that the regional structure and distribution of fault zones within the Nzega greenstone belt are currently not understood. The first geological map of the area was published in 1956. However, surface geological mapping could not be sufficient to explain the control and nature of gold mineralization of the area.

Therefore, an account should be taken to reveal deep tectonic features, which are unknown and to establish the relationship between lithology and structure of the low grade metamorphic terrain (Nzega greenstone terrain) to assess the control on gold mineralization. These problems were addressed by applying different techniques including integrated analysis of all the acquired aeromagnetic data, and known mineralization occurrence data.

1.5 Research Objective

The overall objective of the proposed research is to demarcate the buried geological structures and to identify the important trends in the magnetic anomaly field and to establish the inter-relationship between lithology and tectonic structure of the area. This is to be achieved through the interpretation of the aeromagnetic survey data of the Nzega greenstone belt which hosts gold and the application of Oasis Montaj as well as Geographical Information System (GIS) techniques.

1.6 Specific Objectives

- To identify and delineate structures that are associated with the Nzega greenstone belt from high resolution aeromagnetic data using various enhancements filters.

- To establish the relationship of geologic structures to major tectonic structures, intrusions, volcanic activity and implication to tectonic activity in the Nzega greenstone belt.

- To assess the inter-relationship between lithology and tectonic structure of the area.

1.7 Research Questions

The following research questions are addressed in this study:

- Can structural and lithological relationship assist in the identification of potential mineralization site in the low metamorphic terrain of Nzega greenstone belt?

- What are the dominant structural settings of the Nzega greenstone belt?

- Is there any relationship between surface and subsurface structures/ lineaments?

1.8 Thesis/Dissertation Structure

Figure 1.1 provides an outline of the thesis and this outline is briefly described below. Chapter One provides an introduction, background and motivation for the study; this is followed by the study objectives and research questions.

Chapter two provides a comprehensive literature review that begins with a provision of other peoples works in Lake Victoria region in general and relating to the Nzega greenstone belt. Gaps on what is missing to other peoples work on the area were also identified and used in Nzega greenstone belt aeromagnetic data interpretations.

Chapter three outlines in detail the geology, including both the regional and local geology of the study area. The geological structures identified on the geological maps were also looked careful to relate to the structures marked by magnetic data.

Chapter four outlines in detail the material and research methodology, In order to meet objectives of the research and to answer the research questions, several steps were carried out.including aeromagnetic data for Nzega greenstone belt was investigated, processed and interpreted.

Chapter five explains data processing and interpretation using Geo-soft package software V.6.3, Surfer V 9.9 and Geographical Information System (GIS). The completed total magnetic map was obtained where data in xyz format was gridded, and then contoured at minimum curvature gridding. Several techniques were employed in production of other different Maps for this study. The techniques which were employed are the Vertical derivatives, analytical signal, horizontal derivative, upward continuation and 3D Euler de-convolution.

Chapter six discusses the geological structures mapped using different image enhancement. The subsurface basement tectonic map of the studied area is constructed and depth to the top of the intrusive causative targets was calculated from the aeromagnetic map using Euler de-convolution method.

Chapter Seven points out some recommendations required to encounter the anomalies found in this study such as drilling and trenching, follow up ground geophysics surveys etc.

Chapter Eight highlights the synthesis and structural geological map compilation to see trending and possibilities of some regional tectonic evolution of the study area.

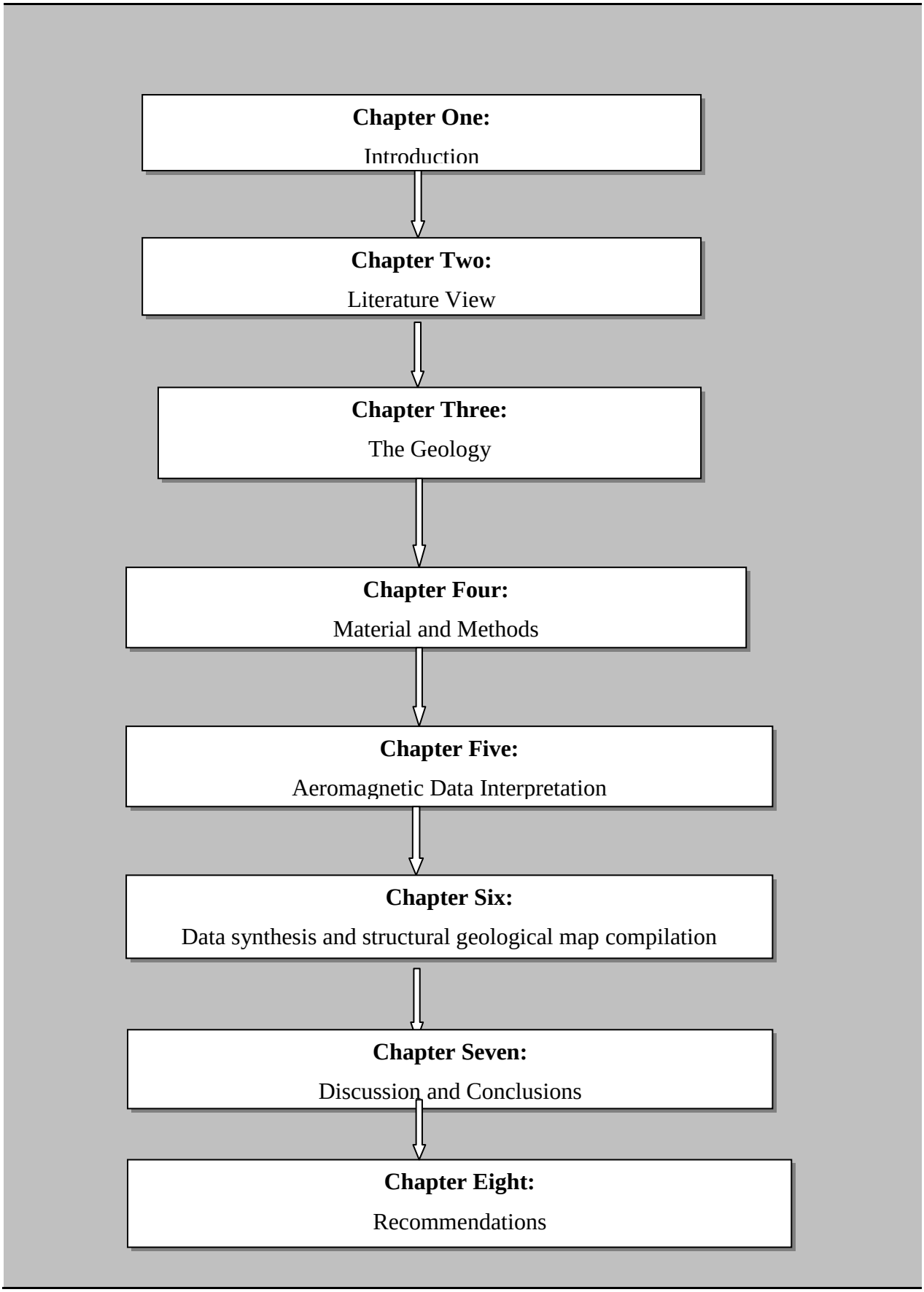

Figure 1.1: Outline of the Dissertation.

1.9 Location and Access

The Nzega greenstone belt is located in NW Tanzania 750 km north-west of the port of Dares Salaam and 200 km south of Lake Victoria in Nzega district, Tabora region latitude 4^0 13' 18"S and 4^0 30' 18"S longitude 33^0 11' 02"E and 33^0 30' 02"E (Figure 1.2). The Tabora region shares a border with Shinyanga region in the North, Singida region in the East, Mbeya and Rukwa regions in the South while the Western border is shared with Kigoma region (not shown on map). Most parts of the study area are accessible by roads.

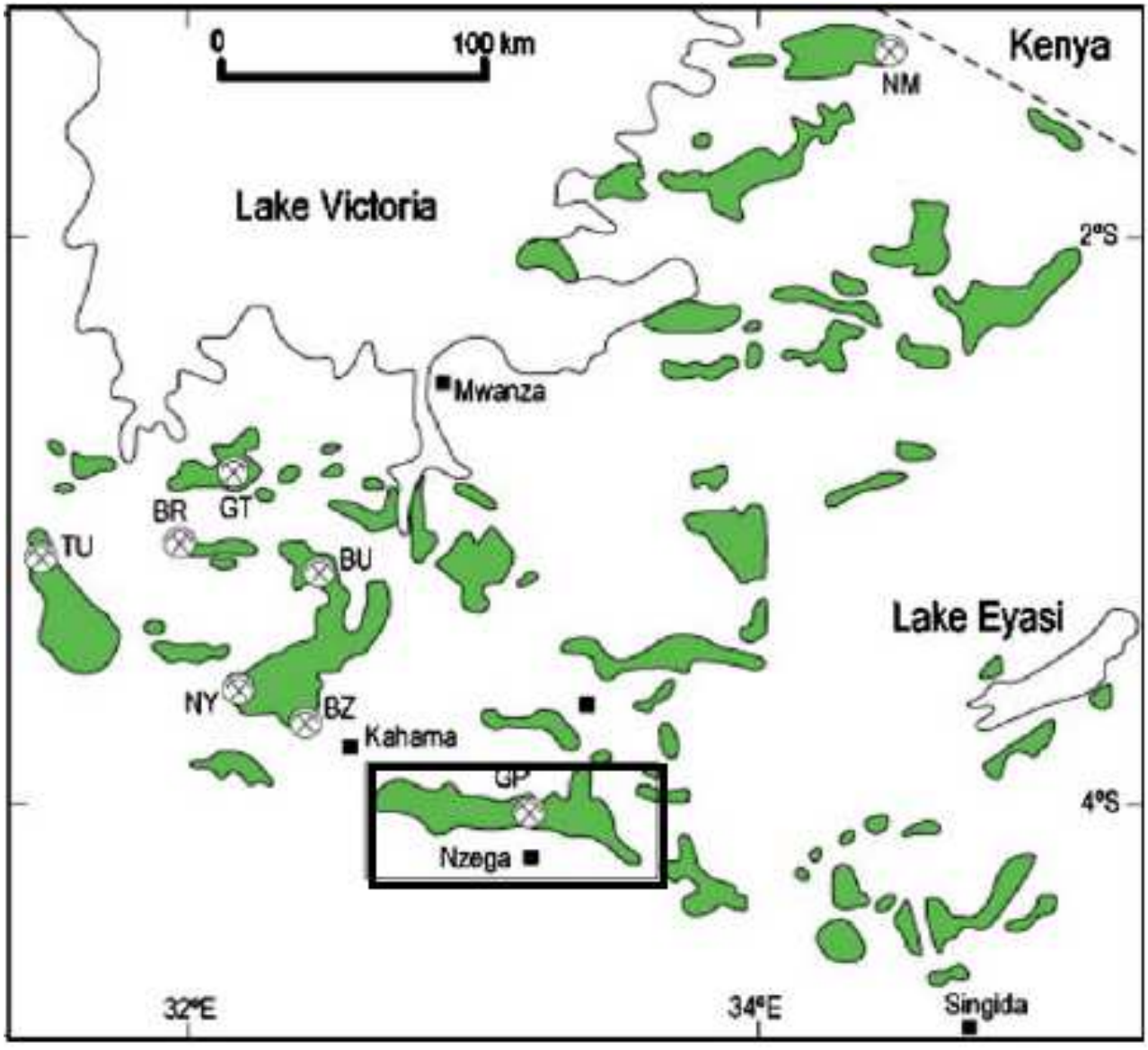

Figure 1-2: Sketch map showing the study area in Tanzania south of Lake Victoria. Note that the indicated gold-occurrence comprises active and abandoned mines, prospect, and active local digging sites. Gold deposits indicated on map include: Tulawaka (TU), Geita (GT), Bulyanhulu (BU), Buck Reef (BF), Buzwagi (BZ), Golden Pride (GP), North Mara (NM) Image adapted after Borg and Shackle ton (1997).

1.10 Physiography and Drainage

Topography generally ranges from 1200 m on the plains to 1500 m on the hills and ridges. Due to its resistance to weathering, hills and ridges comprise Banded Iron Formation (BIF). Low ground between ridges is either covered by red sandy loam (derived from the BIF) or by a thick layer of hard ferricrete.

On drainage, Nzega is drained by the two river systems of the Malagarasi and the Manonga - Wembere. The Malagarasi drains the southern and western parts of the region into Lake Tanganyika and out into the Atlantic. The Manonga drains into the inland Lake Eyasi. The extensive Malagarasi swamp covers the extreme western part of the region.

The sedimentary Bukoba formation forms a dominant ridge line which blocks the drainage to the west resulting in the swampy lowland and broad “Mbuga” filled valleys which penetrates deeply into the south - central area of the Tabora region. The flat low-lying areas are significant from hydrogeology point of view. They are flooded during the rainy season and potentially water logged during the rest of the year.

Most of the rivers are dry river beds during the dry season and even during the rainy season the rivers fill the bank or overflow during a very short period and recede rapidly. The main cause of these short peaks is the vegetation type of the region. Much of the miombo forest floor is bare of vegetative cover. The rainfall runs off the bare surface and very little water infiltrates into the subsurface soils.

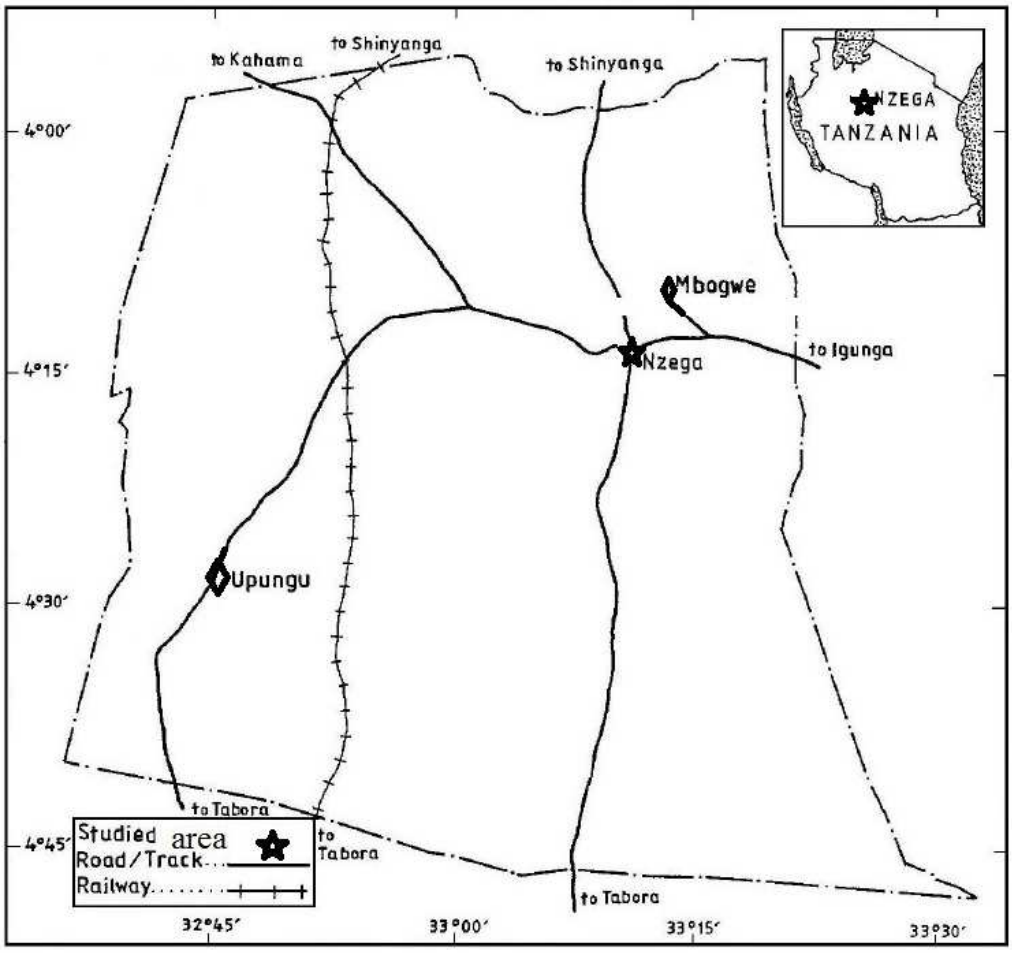

Figure 1-3: Physiographic map and the Location of study area Nzega.

1.11 Historical Exploration and Mining in Tanzania

The following overview is sourced from Smith (2004). The first recorded prospecting and mining in Tanzania was during the German colonial period in the Lake Victoria region, in the period around 1894-1895 (after Barth 1990).

Included within this colonial period was the development and exploitation of the Augusta-Victoria gold mine (also known as Jubilee Reef Mine) located on small scale independent gold mining flourished in the Northern Victoria gold fields of the Archean and the Proterozoic of the Western Rift, largely under German and British colonial control.

This period of exploitation extended from the turn of the century until independence in the early 1960's. With independence came state intervention, independent miners lost control of their mines and some were turned into military bases (e.g, Kiabakari) to "protect state assets".

Nationalization led to most mines falling into disrepair with the notable exception of the Williamson Diamond Mine, most mining remained at artisanal level until the opening of Tanzania to foreign investment in the early 1990's. Some of the historically important gold and base metal mines are as shown in Table 1:1 as follows (after Hester 1998).

Table 1-1 :A listing of gold and base metal mines in Tanzania (after Hester, 1998)

Location	Name	Operating Period	Production kgs Gold	Grade g/t Gold
Musoma –Mara greenstone belt	Buhemba	1913-1970	12,170	
	Nyasenero	1922-1970		
	Mrangi (Phoenix)	1932-1965	155	High grade
	Simba sirori	1920-1938	300	12-14
	Maji Moto	1928-1940	Small	
	Kiabakari	1933-1966	8,810	
	Mara Mine	1932-1970	1943	15.3
Geita-greenstone belt	Geita	1939-1966		
	Ridge 8	1938-1954	27,440	5
	Bismarck Reef	1913-1914		
	Prospect 30	1939-1953		
Rwamagaza greenstone belt	Buck Reef	1982-1990	100	7-10
	Mawe -Meru	1930-1952	2,300	27
Nzega greenstone belt	Canuck	1945-1953	230	6.2
Iramba-Sekenke greenstone belt	Sekenke	1909-1956	4,300	
Lupa District	New Saza	1939-1956	8,390	7.5
	Ntumbi Reef	1937-1965	1,709	12.1
Mpanda District	Mukwamba	1950-1961	2,177	1.56
Kilimafedha greenstone belt	Serengeti goldfield	1932 – 1955	300	

1.12 Modern Gold Exploration and Mining

Modern exploration (primarily gold) commenced earliest in the early 1990's with the relaxing of socialist ideals and the opening up of Tanzania to foreign investment.

1990-1995

The Government had, through its wholly owned Mining and Exploration Company Stamico (State Mining Co-operation) carried out limited exploration and mining during the Socialist period, largely on the coat tails of artisanal miners and with assistance from Russian and Chinese Government technical teams. By the late 1980's the Government had made available to foreign companies some of the properties it had developed (e.g. Bulyanhulu).

The United Nations Revolving Fund also carried out exploration, on behalf of the Government (1965–1995), to encourage the exploitation of Tanzania's mineral resources. The United National (UN) work culminated in the mid 1990's with an open auction to foreign exploration companies of the discoveries and data sets the UN had made. The assets included:

- Discovery of the Golden Ridge gold resource
- Extensions to the Geita colonial mines
- Extensions to the Canuck colonial mine

Foreign companies that were able to secure historical mines, United Nation discoveries, and Government Projects, quickly expanded the resources they acquired. Significant examples are listed in **Table 1:2** with resource data being obtained by public news releases.

Table 1-2: Resource data from different mining being obtained by public news releases (after Hester, 1998):

Project	**District**	**Majority Ownership**	**Current Resources**		
Bulyanhulu	Kahama	Barrick	15.0 million OZS	@	9.5 g/t (Au)
Golden Ridge	Kahama	Barrick	1.5 million OZS	@	2.2 g/t(Au)
Lone Cone (Geita Hill)	Geta	AngloGold	6.0 million OZS	@	2.5 g/t (Au)
Ridge 8	Geita	AngloGold	3.3 million OZS	@	5.5 g/t (Au)
Nyamigena	Mara	Placer	2.2 million OZS	@	3.5 g/t (Au)
Nyabirama	Mara	Placer	2.2 million OZS	@	3.5 g/t (Au)
Buck reef	Geita	Gallery	1.1 million OZS	@	4.6 g/t (Au)
Buhemba	Mara	Meremeta	0.8 million OZS	@	2.6 g/t (Au)

1995 – 2004

The rapid success of early entrants into Tanzania encouraged them to commit to larger exploration budgets and fuelled a rush of new companies that soon made their own contribution to the growing gold resource base of the country. Significant new gold discoveries made since the mid 1990's are listed below **(Table 1-3):**

Table 1-3: Significant new gold discoveries made since the mid 1990s' (after Hester, 1998):

Project	**District**	**Majority Ownership**	**Current Resources**		
Kukuluma	Geita	AngloGold	2.00 million OZS	@	4.0 g/t (Au)
Nyankanga	Geita	AngloGold	7.29 million OZS	@	4.0 g/t (Au)
Golden Ridge	Nzega	Resolute	2.79 million OZS	@	3.0 g/t (Au)
Buzwagi	Kahama	Barrick	1.60 million OZS	@	1.9 g/t (Au)
Mugusu	Geita	Barrick	0.20 million OZS	@	4.5 g/t (Au)
Tulawaka	Kahama	Barrick	0.81 million OZS	@	11.1 g/t (Au)
Nyakafuru	Kahama	Gallery	0.73 million OZS	@	6.3 g/t (Au)
Miyabi Hill	Kahama	Twigg	0.14 million OZS	@	2.1 g/t (Au)
Golden Horse Shoe	Geita	Tan Range	0.30 million OZS	@	3.5 g/t (Au)
Kitongo	Mwanza	Gallery	0.48 million OZS	@	2.0 g/t (Au)

2 CHAPTER TWO: LITERATURE REVIEW

Many exploration geologists have drawn attention to Tanzania especially in the Lake Victoria Gold Fields. Interpretation of magnetic survey data has provided a great deal of information in mineral exploration. Lithology, alteration and geological structures have been recognized in different geologic environments. Modern aeromagnetic surveys are very often of the total intensity amplitude of the proton magnetometer. The data are very often digitally recorded for automatic production of contoured maps.

One point to note or worth noting in this connection is that aeromagnetic profiles tend to give an impression of a single anomaly while actually there is more than one anomaly. This lack of resolution increases with increasing altitude at which the survey is carried out. Most aeromagnetic surveys are flown at a height between about 70 m and 200 m but much lower altitudes (30-35 m) are standard in Finland and Sweden. The anomaly resolution in the latter is vastly superior to that of high altitude surveys.

A consequence of the decreased resolution in high altitude aeromagnetic surveys is that, if the causative feature is actually composed of several geologic bodies at shallow depth, the interpretation gives consistently too large depth to the bodies. The difference can be quite considerable and this danger should be constantly being borne in mind in interpreting high altitude aeromagnetic data. The removal of the influence of terrain irregularities on magnetic surveys made at constant barometric height, a procedure called draping has been discussed by Mathew (1994) and Pilkington and Roest (1992).

Analyzing, interpreting and compiling geophysical data in conjunction with geologic observation can reveal the tectonic setting that helps understand the major tectonic mechanisms. Rifts, evolving to continental break up and the formation of new ocean basins are some of the most productive magnetic systems expressed at the surface of the earth. Understanding the process operating in these systems setting is critical to our knowledge of how planet works (Earth).

One of the earliest geological mappings of the Lake Victoria area was by Quennell et al in 1956, the map shows the older, Early-Archean Dodoma System overlain by the Nyanzian and Kavirondian Systems (Tanzania Craton), flanked by the Late Archean Usagaran and Ubendian Mobile Belts (Stockley, 1936; Grantham et al., 1945; Quennell et al., 1956). The Dodoman System comprises rocks of interlayer concordant granitoids, migmatites and schist belts in widespread belts of tonalite–trondhjemite granodiorite (TTG) and their gneissic equivalents (e.g. Quarter Degree Sheets (QDS) 161, 162, 178, 179).

According to the technical report Canaco Resources by Eur Geol Dr. Sandy M. Archibald (March 2011), a high resolution XPlorer magnetic and radiometric airborne survey was carried out over part of the Handeni property from 1st September to September 2nd 2010 by New Resolution Geophysics (NRG) Pretoria south Africa using a Euro copter AS350B2 helicopter a total of 935 line kilometers were surveyed. The survey was flown at an elevation of 25 m with a 90^0 east- west orientations an a line spacing of 100 m. Measurement collected was total magnetic field, first vertical derivatives, analytical signal, digital terrain model and total count radiometry. The local geological structure was defined by airborne geophysics. The dominant structure in the area was a doubly plunging synclinorium with a primary north western long axis. East-trending, low angle, south dipping thrust faults have been interpreted at Majiri, and from drilling at Magambazi North. North-northwest trending graphitic shears and east-northeast trending graphitic faults have also been mapped in the Magambazi area.

Hill top Resource report by G. S. Carter, (2010) showed that Java Investment Co. Ltd (JICL Consultants) commenced a ground magnetic survey over the Mrangi gold prospect in Musoma Mara greenstone belt on June 21, 2008 on behalf of Hill Top Resources Corporation. The surveys showed that there is a clear magnetic distinction between the north-eastern and south-western half of the grid separated by a magnetic low valley running from south-east to north-west part of the grid. The Mrangi total magnetic field indicated that a lineament trending NE-SW and running north east were observed. It was interpreted as a possible shear zone or fault although there is no clear evidence of displacement of magnetic units.

In July, 2003, an airborne magnetic horizontal gradient and radiometric survey was flown over the Itilima project located at Lake Victoria gold field by Fugro Airborne Surveys (Pty) Limited ("Fugro") to identify possible kimberlite target anomalies. Interpretation of these data by Paterson, Grant & Watson Limited ("PGW") identified airborne anomalies as potential kimberlites.

Selected anomalies by ("PGW") considered with potential to be signature of kimberlite pipe were presented with first order derivatives magnetic data. The anomalies found were classified as, anomaly source is distinct from the host rock, anomaly exhibits the characteristics of a pipe-like intrusive and target is proximal/similar to known kimberlites and named as priority one and priority two, as anomaly source appears distinct from the host rock; but is harder to differentiate; Also the PGW interpretation showed the presence of a diorite intrusive expressed by high magnetic values, the interpretation on radiometric data reveals a series of possible alteration zones.

Geo-tech Airborne Limited (2006) acquired airborne magnetic data over the Tusker project located at Lake Victoria gold fields in March 2004 at 75m line spacing and 40m terrain clearance. The second vertical derivative of reduced to pole magnetic data was able to map the magnetic mudstone / siltstone package, and show that stratigraphy has been deformed. The data also suggest that Tusker is at the intersection of a SE stratigraphic discontinuity, NS fault and NE fold and fault axis.

Paterson, Grant & Watson Limited, Alessandro Colla Scintrex Ltd. (1999) describes airborne magnetic and radiometric survey of the Calama area, northern Chile. The area is characterized by an active mining industry, mainly porphyry copper deposits. About 70% of it is under sedimentary cover. Magnetics and radiometric proved to be very successful in providing important new information on the extent and lithology of the different volcanic and intrusive units. Extensive structural mapping was derived from the data, and a previously unrecognized SW-NE fault system, potentially an important mineralization control, was delineated. Interpretation was carried out at both the 1:250,000 and 1:100,000 scales. The structural and lithology interpretation was carried out using the total magnetic field and the first vertical derivative maps. For outlining the different units, both the analytic signal and the apparent magnetic susceptibility were used. With the magnetic it was possible to define the major lithologic units and to extend them under covered areas. The more outstanding signatures observed were: the area has a vast incidence of volcanic units, of Jurassic, Cretaceous and Tertiary age.

The more magnetic and extensive are the Jurassic, Intrusive have a strong magnetic signature where they outcrop or are close to surface, generally high amplitude anomalies with circular shape. On the total magnetic field map they have strong dipolar signatures that distinguish them from the volcanics. Some of them were defined under the sedimentary cover or within the volcanics. It is significant that is possible to distinguish between various intrusive based on the magnetics.

In some cases, the radiometric data provide a stronger indication of the lithology and/or boundaries of the intrusive than the magnetic data. Sedimentary units were outlined according to weak, amorphous magnetic signatures. They are subordinate to the volcanic and intrusive units. Most of these areas are fault controlled and are related to basins delimited by vertical-movement faults. The radiometric interpretation was focused on outlining structures and contacts and on the delineation of radiometric signatures in areas defined as anomalous in terms of the occurrence of radiometric anomalies defined from the ternary radiometric image, coincidence with intrusive mapped from magnetics, and/or the presence of faults controlling the intrusions, or crosscutting faults without a clear intrusion mapped.

W. T. C. Sowerbutts from Goulty et al. (1984) in trying to map magnetic dyke using detailed vertical gradient magnetic survey of part of a small intrusion known as the Butterton Dyke with the aid of a microcomputer-based data gathering system. The results of over 16500 magnetic measurements resulted the reveal a detailed pattern of magnetic anomalies. From these it was observed it is possible to trace the course of two dykes for a distance of over 300 m, and identify places where they change direction and show small offsets. The advantage of making vertical gradient rather than total field magnetic measurements was a faster surveying speed and better resolution of near-surface anomalies.

Hunting Geology and Geophysics Ltd (1966) conducted airborne magnetic and electromagnetic survey of Lake Victoria Gold Fields in which they combined the A.B.E.M. rotary field method, which necessitates the use of two aircraft, with magnetometer observations. The magnetometer was a Gulf MK 111, measuring the relative magnetic total intensity. The flying height was 400 ft (122 m) with a plane separation of 900 ft (274 m). The airborne results obtained did not pertain directly to gold mineralization, but indicate major fault zones, carbonaceous or sulphide horizons, granite contacts and profound changes in lithology, providing a useful overall picture of the general geology of the area with major tectonic features from which many clues for gold mineralization can be obtained.

Airborne magnetic and electromagnetic surveys were flown in order to distinguish major fault zones, conducting horizons and profound changes in lithology. In promising areas, selected from the airborne results or from the presence of old mine workings, special grids were cut out and pegged. These grids were surveyed with magnetometer and E. M. Gun. The results, evaluated in contour and derived structural maps, revealed the important tectonic features of the areas.

This information formed the background for the final TURAM survey, which gave, in some instances direct indications of the mineralized quartz veins. This combination revealed also so many particulars of the structural pattern, that extensions of the deposits could be established and it became possible, to carry out trenching and drilling programmes successfully.

Geo-survey International worked in the area (Lake Victoria gold fields) during the period 1971 to 1980 and pointed out the super-terrane/terrane scale, greenstone lithologies are discriminated from gneisses and granitoids via the qualitative interpretation of mainly geophysical images and geological maps. Although the country-wide airborne magnetic and radiometric data were captured at widely spaced flight lines they were re-filtered and re-processed using advanced geophysical programs in an attempt to extract as much regional litho-structural information as possible.

Borg, 1994; Chamberlain, 2003; Kabete, 2008; and Borg, 1992) indicated that regional geological maps at 1:125,000 and 1:100,000 scales, in digital and/or hard form from the Geological Survey of Tanzania, were scanned and registered in the ARC1960 projection in respective UTM zones, consistent with the location of the lake Victoria area under interpretation. Additional geological information, including company exploration reports from the Ministry of Energy and Minerals, and reconnaissance and detailed geological mapping in selected, were also used in interpretation. First-pass definition of lithological associations with distinctive geophysical signatures can was extracted from aeromagnetic images. The shape and geometries of the strong positive and negative magnetic signatures were assigned to specific rock types from available geological maps. These were distinguished from moderately, weakly and non-magnetic lithomagnetic bodies, possibly paragneisses.

Geological mapping using regional airborne magnetic survey data revealed bedrocks underlying the Lake Victoria region that comprise alternating crustal blocks of strong E–W-trending linear, open to isoclinal, upright folded, litho-magnetic units that map out greenstone-abundant belts, more specifically belts with Banded Iron Formations and magnetite-quartzites. These were clearly separated from extensive belts of E–W-trending to NW–SE-trending highly magnetic and/or strongly radiometric, syn-orogenic and late-tectonic granitoids in weakly magnetic paragneissic rocks. A linear belt of alternate highly radiometric and/or strongly magnetic anomalies map a wide zone of linear, NW–SE-trending strongly magnetic and highly radiometric K-feldspar granitoids which formed swarms of intrusions in the southern part of the Lake Victoria Region and the entire Moyowosi–Manyoni and Dodoma Basement Super-terranes, in the Central Tanzania Region.

According to Doyle (1986), indicated that it is almost impossible to get a direct geophysical response from gold because of the low grades in deposits. However, indirect geophysical indications may occur through association of gold with particular host rocks, marker beds or structures which are, for example, of unusual magnetization, density, electric polarization, or conductivity/resistivity.

Barth (1990) working in the Lake Victoria area produced a geological map at a scale of 1:500,000 from geological compilation of 1:125,000 and 1:100,000 scale QDS maps available from the Geological Survey of Tanzania (Tanzania, 2005). The map shows the geology and selected mineral deposits of the Lake Victoria Goldfields. Barth (1990) subdivides the geology of this region from older to younger, into Archean granitoid shield, Archean greenstone belt, Proterozoic–Late Archean intrusive rocks, and Proterozoic and Cenozoic rocks including regolith, and Recent and proto-lake sediments.

Structural data on the map by Barth (1990) include only magnetic lineaments and mafic gabbroic dykes. The map by Barth was produced during the onset of modern exploration in Tanzania, and, as such, it highlights BIFs and late basins from other greenstones and associated regolith, and linear belts of late-kinematic granitoids in extensive granitoid gneiss basement. The map clearly shows many gold prospects and old mines, although their spatial relationship with structures cannot be interpreted from the map. This is despite the fact that the importance of structural controls on lode-gold deposits was already known in 1990 (e.g. Groves).

Reeves (1993), in a review of airborne geophysical mapping indicated that aeromagnetic compilation has been done at the continental scale in several areas in cooperation with other partners. The compilation of magnetic data is useful to study the structures at global and continental scale. However, aeromagnetic surveys are usually conducted at the national level and each has its own different specifications using a common reference datum to provide the opportunity to display magnetic signature and the continuity of geological structures in continental or regional scale without interruption at national boundaries.

West and Witherly (1995) used basic geophysical techniques to characterize the Syama gold deposit, initially discovered by geochemical methods. Magnetic and induced polarization (IP) surveys were used to identify rock types and basic structures and contacts while very low frequency electro-magnetic (VLF-EM) was used to define more detailed structures associated with the deposit. Radiometric was used to map the surface expression of sericitic alteration. Airborne magnetic and radiometric survey results confirmed the usefulness of the two methods for mapping geology and structure in greenstone belts of West Africa.

Additionally, the results were used to identify and rank prospective oxide reserve targets. However, potassium (K) concentrations unrelated to the subsurface geology in areas of transported laterite limited the success of the venture. This did not, however, impede the ability of basic geophysical techniques to provide very useful information relating to lithologies, structure and alteration. There are many examples of the gravity technique being used at all scales from the identification of prospective Gold (Au) districts to that of gold-related hydrothermal alteration at a local scale.

More recently, the development of airborne gravity gradient systems (e.g. BHP Billiton-Falcon, Bell Geo-space-Air FTG), have seen the gravity technique grow in application. Areas are now being flown where ground access was previously not possible and where rapid acquisition is required. Gravity is an effective technique for defining the geometry and structure of greenstones belts at a regional scale. Barrick showed that gravity has also proven effective in mapping intrusions in sedimentary and volcanic terrains for Carlin, Oxidized Intrusion Related (OIR) and Reduced Intrusion Related (RIR) systems. Structure and alteration can also be mapped, either directly by gravity in weathered environments or inferred in terrains where geological units of different density are offset and/or altered (Robert et al., 2007). Magnetite depletion is a characteristic of some Au deposits, resulting in zones of low anomalies; for example, ferromagnetic minerals in mafic volcanics are destroyed by carbonatization.

Barley and Goldfarb (1996) in a review of tectonic setting of mesothermal gold deposits observed that most of the giant gold deposits in the world are spatially associated with regional first-order structures, the deposits usually hosted by late-tectonic splay faults or shear zones. The first-order structures may have acted as major conduits for fluid transport from deep in the crust, while the secondary structures acted as the loci for mineral deposition with locally reduced fluid pressure. In general, mesothermal Au provinces are characteristically associated with regional structures.

Mesothermal Au deposits are found in structurally controlled sites within, or adjacent to orogenic belts (Barley and Goldfarb, 1996). The dominant orientation of gold-bearing structures in the Tanzanian craton is northwest and structures with this general orientation can be traced across the Tanzanian and Ugandan cratons and into the Democratic Republic of Congo. More subtle northeast trends may control the mineralization in BIF at Geita and Golden Ridge and are also clearly visible on airborne magnetic maps west of Bulyanhulu. North-south structures appear to be significant at the Nyakafura deposit as are east-west structures at Golden Pride.

In their study of Archean mineralization, Groves et al; (1998) pointed out that based on geological characteristics, which include (a) strongly deformed host rocks, (b) overall low sulphide volume, (c) abundant quartz–carbonate veining, (d) a carbonate–sulphide chlorite–sericite alteration assemblage in greenschist facies rocks and (f) a spatial association with large-scale compressional structures, the Golden Pride gold deposit can be classified as an orogenic gold deposit.

When they conducted a radiometric dating, Borg and Krogh (1999) obtained U–Pb age of 2,780±3 Ma from rhyolite pyroclastics in the adjoining greenstone belt that could potentially be associated with the rhyolitic volcanic rocks in the eastern end of the NGB. The rest of the belt is characterised by greenschist facies, fine-to medium-grained siliciclastic rocks interbedded with banded iron formations (BIFs). At the Golden Pride mine, a U–Pb age of 2,716±11 Ma was obtained from a homogenous zircon population derived from meta-sandstone interbedded with BIF (Chamberlain and Tosdal, 2007). The Nyanzian rocks are unconformably overlain by polymictic conglomerates and sandstones associated with the Kavirondian System.

In its explanation on Archean greenstone belt (GTK, 2003) pointed out that the granitoids overprint a crustal-scale sinistral shear zone evident from re-processed country-wide geophysical data and high-resolution aeromagnetic and radiometric data (e.g. There are E–W- to WNW–ESE-trending narrow corridors of non-magnetic and non-radiometric geophysical features that are coincident with greenschist–amphibolite facies granitoid-greenstone belts (e.g. epidote– amphibole chlorite schist belts: QDS 174 and 175), in the Dodoma Basement Superterrane). These are bounded by highly radiometric syn-late kinematic granitoids, and traversed by E–W- to NW–SE-trending anastomosing lithostructural fabrics, some drag folded along major NW–SE-trending tectonic boundaries between different domains in the Undewa–Ilangali Terrain. In addition, the Central Tanzania Region contains alternate belts of elongate E–W to NW–SE-trending magnetic anomalies, which map mafic–ultramafic rocks.

These strongly magnetic igneous rocks extend westerly from Mtera to Rungwe in the Dodoman Schist Superterrane, and further east of Lake Rukwa where they extend and crop out intermittently between Kapapa and east of Kigoma in the Eastern Ubendian terrane.

Borg (1990) and Shackleton 1997) have also worked in the area and stated that the greenstone belts in the Lake Victoria Gold are comprised of dominantly mafic volcanic rocks and (immature) sedimentary rocks that are assigned to the Late Archean Nyanzian Super group. The super group can roughly be divided into a Lower and Upper Series on the basis of a recognizable upward transition from mafic to felsic lavas, with minor tuffs and inter-bedded sedimentary rocks.

In an attempt to clarify gold occurrence, Alida (2007) and Robert et al. (2007) observed that apart from the use of geochemical methods for gold exploration within the Lake Victoria Gold Field (LVGF), the mesothermal gold deposits are known to be structurally controlled. Structural investigations (lineament derivations) have also proved to be a useful Au exploration tool in the LVGF and other mesothermal Au provinces.

In the previous studies of the lithological and structural inspection of drill core, together with pit mapping, from the Golden Pride gold deposit, Kabete et al. (2008) show that the mine stratigraphy mainly comprises a series of strongly foliated, lower- to middle-greenschist facies, interbedded sandstone and siltstone units. This sequence is intersected by intensely foliated (i.e. schistose) and carbonate-altered rocks that represent the Golden Pride Shear Zone (GPSZ), which divides the mine stratigraphy into a hanging wall and a footwall sedimentary sequence. In close spatial association with the GPSZ and related structural elements, a variety of intrusions crosscut the mine stratigraphy. Furthermore, BIF units occur within both the hanging wall and footwall sedimentary sequence.

This research project provides a comprehensive study of the geology and structural control of the Nzega greenstone belt to underpin the super-terrain-scale architecture of the greenstone belt, in order to highlight continuous litho-structural patterns, bounding faults/shear zones and associated higher-order splays, and their links to gold-endowed provinces (goldfields) with small to giant gold districts. High-resolution magnetic profiles are required, especially in the gold-endowed Lake Victoria Region, in order to define prospective gold districts within apparently poorly gold-endowed province.

3 CHAPTER THREE: THE GEOLOGY

3.1 Regional Geology

Tanzania craton is approximately 1000km by 500km in extent and forms part of a ring of Archean cratons surrounding the Congo basin (Figure 3-1). Limited geochronology dating has been done on the craton. Walrcen et al, (1994) established Pb-Pb ages of Ca 2720 Ma to the Tanzania craton. Bell and Dodson (1984) determine Rb-Sr isochron ages of Ca 255 Ma on post-orogenic granitoids indicating the lower age limit of the craton. The Tanzania craton is bound by early Proterozoic and younger mobile belts; the NW-N trending, Ubendian belt to the south west; the ENE trending Usagaran belt to the south south east and east; the Mozambique belt also to the east; the Kibaran to the north west and the Ruwenzory belt to the north Cahen and Snelling (1984); Goodwin (1991).

The craton is divided into lower basement in the central and southern parts and an upper basement at the north. The lower basement contains medium to high grade gneiss-migmatite and Dodoma schist belts, with the schist widely intruded and metamorphosed by 2.6 Ga old granitoid plutons. The upper basement consists of the older Nyanzian schist belts, comprsing mafic-felsic volcanic rocks, Banded Iron Formations (BIFs), greywacke are all intruded by approximately 2.8 Ga old granitoids Quinnel et al (1959). The geology of Tanzania is quite well understood on a regional scale as the country has been mapped by several generations of geologists from the beginning of the 20th century by colonial surveys, more recent aid programs in the 90's and this research continues to the present day under the present Tanzanian Geological Survey.

The following description of the geology of Tanzania is adapted from a review of the resource potential of Tanzania by Hester (1998). Most recently, Barth (1990) has produced a geological compilation map of the Victoria Gold Fields based upon geological field verification as well as geophysical and remote sensing interpretations. Barth's work was part of a large aid program completed by the Bundesanstalt fur Geowissenschaften und Rohstoffe (BGR) of Hanover, Germany, in the late eighties and early nineties**.** Historically, the rocks of Tanzania have been divided into systems which correspond to spatially and stratigraphically identifiable units which have age connotations within the normal geologic time scale.

Archean Era

A large Archean craton composed of granite and greenstones dominates the west-central portion of Tanzania and is named the Tanzanian Craton which is itself part of the African plate. The craton covers an area roughly 750x325 km in size. Some authors have included the Tanzanian cratonic rocks as part of the Mozambique Belt which extends along the eastern African coast from Mozambique to Sudan. An oldest sequence of highly metamorphosed Archean sediments (Dodoman system), forms a band across the southern portion of the craton and predate the granite and greenstone. Numerous greenstone belts are found in the north of the craton that typically have an E-W strike although N-S and NW-SE strikes locally dominate.

These greenstone rocks are divided into lower and upper sequences (Nyanzian system). The lower sequence comprises basaltic, andesitic and dacitic lavas, with minor inter-bedded tuffs and sediments. The sediments include Banded Iron Formation (BIF), re-crystallised cherts, shale and conglomerates. The upper sequence comprises felsic lavas and tuffs, ferruginous cherts, BIF and meta-pelites. The greenstones are usually of green schist facies and are of highest economic importance as they host the majority of Tanzania's gold resources. Conglomerates, coarse arkosic and feldspathic grits and quartzites (Kavirondian system) rest unconformably on the Nyanzian rocks in the north of the craton.

The granites of the Archean (Granite-Gneiss terrain) appear younger than the other Archean rocks and can be found throughout the craton. The western portion of the craton, is cut by a north-south dyke swarm which is visible on regional aeromagnetic data and this swarm extends northward through the main gold mining areas and into Lake Victoria. The dykes are of Karoo Age which corresponds to late Permian to Jurassic Period of the Paleozoic Era. A series of Mesozoic to Cenozoic Era aged carbonatites, kimberlites and related rocks occur as small bodies all across Tanzania**.**

Proterozoic Era

The Lower Proterozoic (Ubendian System) aged rocks of Tanzania are formed by lithologies of the Western Rift that wrap around the southwest of the Archeancraton in the form of a mobile belt. They comprise gneiss with minor mafic and ultramafic intrusives and late stage granites. The metamorphic grade is generally amphibolite to granulite facies. It is possible that many of the rocks of the Ubendian are reworked rocks from the Archean.

The Lupa and Mpanda gold and base metal mineral fields are located within the Ubendian system. The slightly younger Proterozoic rocks (Usagaran) that form the mobile belt on the southeast of the craton comprises granulites, gneisses and quartzites. Like the Ubendian, it is possible that many of the rocks of the Usagaran are reworked rocks from the Archean. Gold mineralization around the Iringa district (southern Tanzania) is within the Usagaran system. The upper Proterozoic rocks in the northwest of the country (Karagwe-Ankolean system) comprise weakly metamorphosed schists, phyllites, argillites and quartzites.

Palaeozoic Era

Rocks that span the boundary between the Proterozoic and Palaeozoic (Bukoban system) are found in the northwest of the country and cover part of the Nyamirembe properties. They comprise sandstones, quartzites, shales, red beds, dolomitic limestones, cherts and amygdaloidal lavas. Alluvial gold has been located in the Kibondo district that is comprised of Bukoban sediments. Sediments that dominate the southeast of Tanzania (Karroo) are the northern most extent of a sequence that is also found in South Africa. They comprise coarse sandstones, shales, siltstones and coal.

Mesozoic Era

The early Mesozoic is characterised by the formation of thick deltaic deposits from marinetransgressions. Limestones, sandstones, shales and marls (Upper Mesozoic) occur in coastalbasins and are syngenetic with the commencement of rifting. Carbonatite (rare earth elementmineralisation) and Kimberlite (diamond mineralisation) emplacement is associated with the late Mesozoic at branches along the eastern rift and Shinyanga districts, respectively.

Cenozoic Era

The formation of the rift systems (eastern and western) occurred primarily in the Cenozoic and was accompanied by sedimentation, volcanism (intermediate to basic alkalic rocks) and intrusive activity. Volcanoes can be seen in the Kilimanjaro region near a rift triple junction, with lakes (Tanganyika, Rukwa, Nyasa and Natron) defining the western and eastern rifts.

Tertiary Period and Miocene Epoch

There are widespread areas of laterite duricrust within the Lake Victoria Gold fields. The laterite tends to be composed of typical cemented iron pisolites that mantle rocky ridges especially where the ridges are composed of BIF. The mantles tend to be thickest near the ridges and typically have 10°-15° slopes that thin outward forming wedges draped around the ridge exposures.

Pleistocene Epoch

Wide areas of the Lake Victoria region that are generally topographically low are overlain by calcareous black organic hardpan soils (vertisols) that are termed “black cotton soils” or more commonly in Tanzania “Mbuga clay” and “mbuga”. These sediments have been interpreted to have been laid down in several periods as lake-bottom sediment accumulations by the previously larger proto-Lake Victoria. Other areas are underlain by sand and gravel deposits that represent cemented beach sediments. Both the presence of laterite and Mbuga clays will play a significant role in masking geochemical responses originating in the bedrock and must be taken into account while interpreting geochemical data for gold exploration.

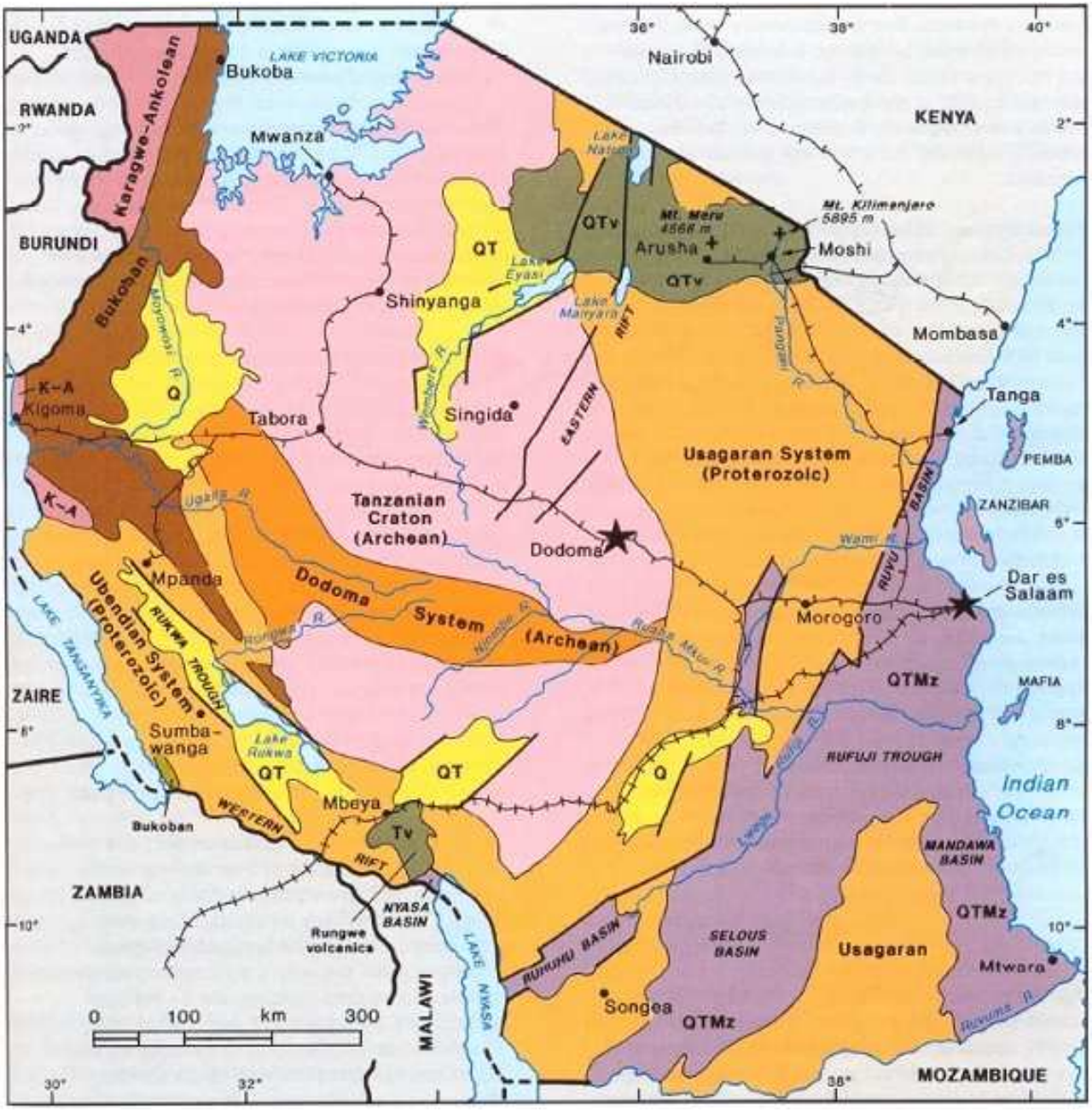

Figure 3-1: Geological Map of Tanzania (after Hester, 1998) showing mobile belts surrounding the Archean Craton.

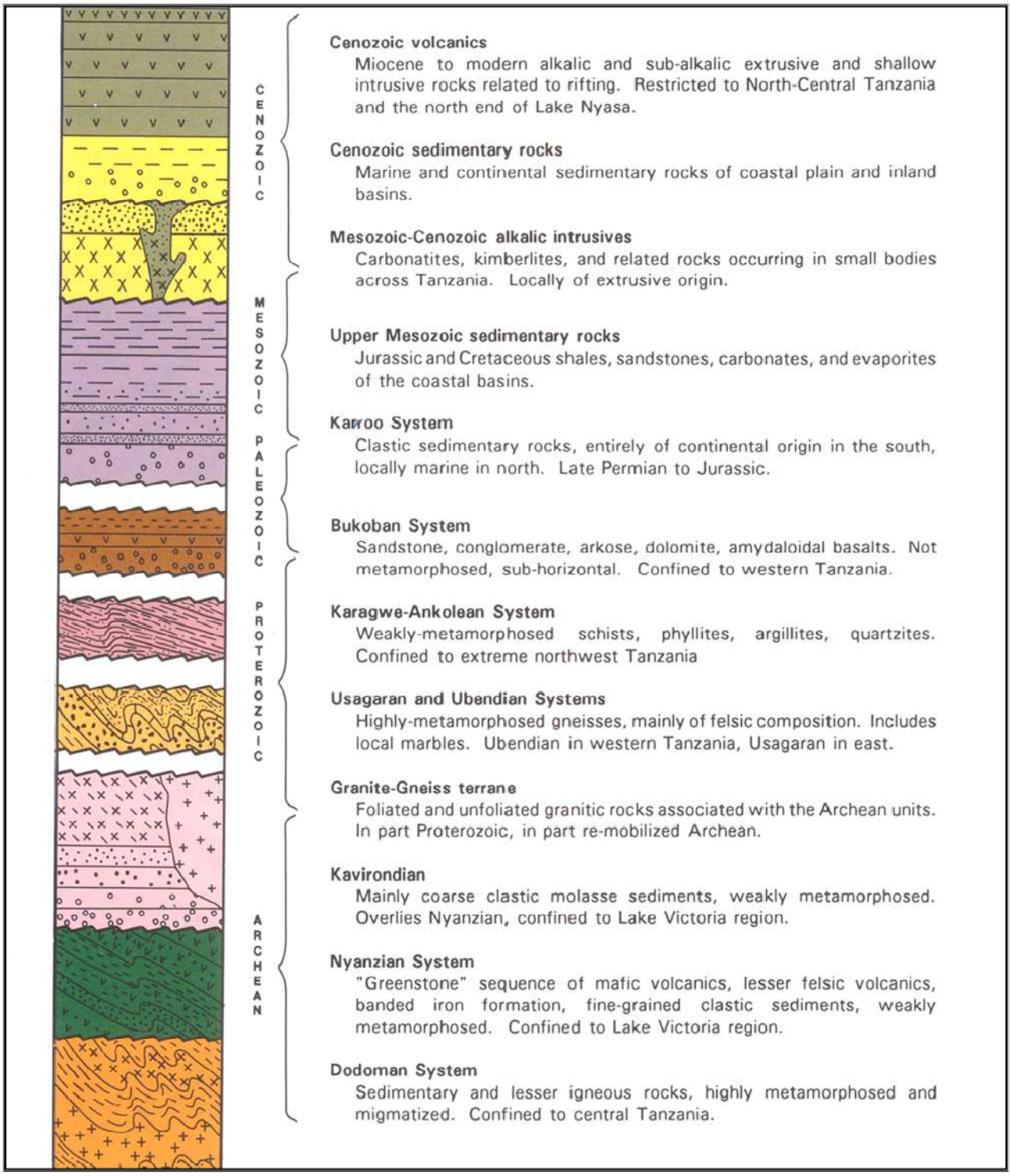

Figure 3-2: Geologic Section of Tanzania (after Hester et al, 1998)

CAINOZOIC	**Quaternary** Major faulting in the Western Rift, renewed faulting in the Eastern Rift with grid faulting lava flows and volcanic within rift floor. Block faulting of Ruwenzori, Pare and Usambara. Changes in sea level with raised coral reefs and drowned creeks swamps and alluvial deposits.
	Tertiary Development of sub-Miocene pen plain followed by deformation with sediments laid down near the coast and Lake Victoria Basin Eastern Rift outlined and extensive lave flows of Kenya highlands. Development of end-Tertiary penetrate and subsequent warping.
MESOZOIC	**Cretaceous** Marine sediments in east, absent in Uganda. End-Cretaceous peneplain.
	Jurassic Marine sediments in east absent in Uganda. Beginning of coastal downwrap
	Karroo Mostly continental deposits basal tillites, sandstones, shales, coal measures.Formation of basins with partly faulted margins.
PALAEOZOIC	Major break in sequences - no record
	Mozambique Belt Intensely folded metamorphic rocks trend between NW and NE against eastern flank of Nyanza shield. Probably several systems (e.g. Usangara, Tanzania, Turoka, Kenya) Gneisses, schist's, often garnetiferous, quartzite, crystalline limestone.
PRE-CAMBRIAN	**Bukoban** Sediments overlying Nyanzashield. Mostly in west Tanzania but also Kenya (Kissii) and Uganda (Bunyoro).
	Karagwe-Ankolean Incompletely metamorphosed sediments with intrusive granites in western Tanzania and south western Uganda. 1300-1400 million years?
	Ubendian Metamorphic belt in south west Tanzania comparable with Mozambique Belt, NW - SE folds.
	Buganda Toro Intensely folded system extending east-west to the both of Lake Victoria 1800-2050 million years?
	Kavirondian Typically sandstones, conglomerates quartizites some volcanism and granite instrusions with gold bearing quartz venins. Unconformable on Nyanzian.
	Nyanzian Volcaninc rocks with interbeddedsediments . Intrusive gold bearing granite. East southeast trend 2600-3000 million years?
	Dodoman Metamorphic rocks in central Tanzania with east -southeast trending folds. More than 3000 million years?
	Gneiss complex of Uganda Metamorphic and granite rocks comprising a number of systems (e.g. Mirian, Aruan, Watian).

Figure 3-3: Stratigraphic Column of the Geology of Tanzania (after Barth 1990)

3.2 Regional Geological Setting of Lake Victoria Gold Fields

The Lake Victoria Gold comprises a number of E–W to NW–SE striking super-terranes that can be subdivided into terranes and belts (Kabete et al; 2008). The greenstone belts in the LVG are comprised of dominantly mafic volcanic rocks and (immature) sedimentary rocks that are assigned to the Late Archean Nyanzian Supergroup (Borg, 1990; Borg and Shackleton, 1997). The super group can roughly be divided into a Lower and Upper Series on the basis of a recognisable upward transition from mafic to felsic lavas, with minor tuffs and interbedded sedimentary rocks. A number of greenstone belts are found in Lake Victoria gold field such as:

Nzega greenstone belt: Greenstones of the Nyanzian Supergroup comprise felsic volcanics, BIF, and subordinate mafic volcanics and sedimentary rocks. Mineralization is hosted by BIF or felsic tuffs.

Iramba-Sekenke greenstone belt: Greenstone-belt gold prospects occur over a broad area concentrated around the Iramba Plateau. The Sekenke Gold Mine was discovered in 1907 and worked at an average grade of 15.4 g/t gold and 2.5 g/t silver. Several parallel quartz veins contain gold values close to the contact between greenstones and diorite. Other old mines in the belt include Kirondatal, Union Gold Mine, Kinyalele, and Kisamamba.

Geita greenstone belt: This is an east-west trending belt which hosts the world class Geita Gold mine with a resource of 20 million ounces grading on average 4.0 g/t. The greenstone belt is marked by high relief hills, ridges and a plateau underlain by steeply dipping Banded Iron Formation (BIF). The NyanzianSupergroup formations comprise pyroclastics overlying mafic volcanics. Laterite is well developed at the surface over mafic volcanic units. Gold mineralization occurs in native form, often in close association with pyrite, and pyrrhotite in fractures concordant with the bedding of banded iron formation units. Stratiform mineralization predominates although quartz reefs are mineralized at some deposits

Rwamagaza greenstone belt: This belt lies south of the Geita Greenstone belt and probably represents the same rocks on the other limb of an anticlinorium. Outcrops of massive mafic volcanics with some thin beds of tuff are notable. The principal gold mine used to be MaweMeru, which is high grade gold quartz vein containing much pyrite and chalcopyrite.

Kahama greenstone belt: The Bulyanhulu mine is a world class deposit with a resource estimated at 14.6 Million oz grading 15 g/t. The stratigraphy of Bulyanhulu is characterized by Lower NyanzianSupergroup volcano-sedimentary sequence largely comprised of bimodal mafic and felsic extrusive and intrusive rocks.

Musoma-Mara greenstone belt: Rocks of Nyanzian Supergroup host the gold mineralization and comprise a sequence of basic and felsic volcanics and tuffs with BIF. The Kiabakari, another old mine, is tabular, siliceous, with steeply dipping ore bodies in sericitic schist, overlain by laterite. It has been mined to a depth of 450 m. The main ore body has a grade of 6.7g/t and is under exploration. The mine was once the third largest gold producer in Tanzania.

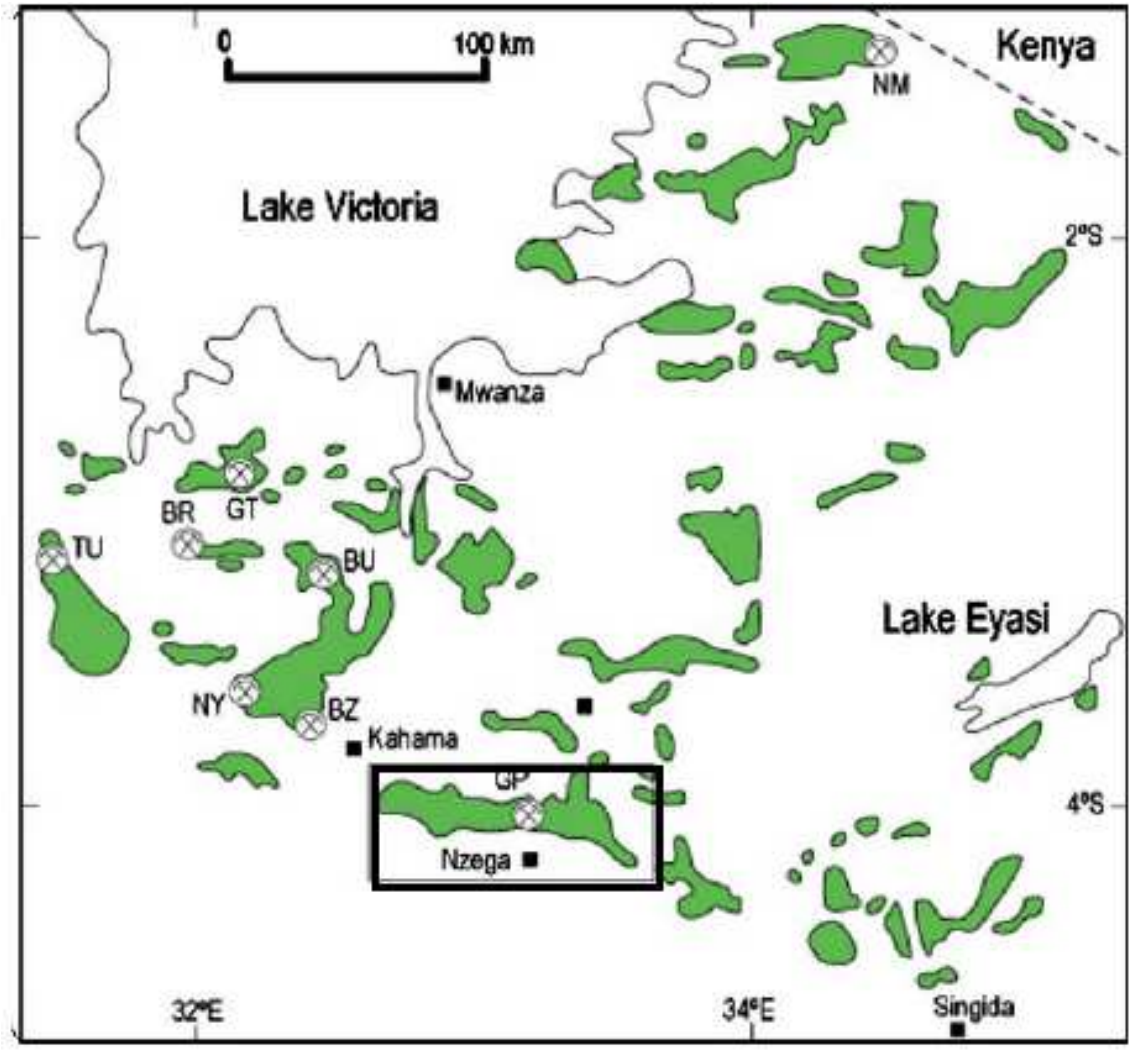

Figure 3-4: Overview map of greenstone belts (in green) and major gold deposits in the Lake Victoria Goldfields, northern Tanzania. Gold deposits indicated on map include: Tulawaka (TU), Geita (GT), Bulyanhulu (BU), Buck Reef (BR)

The Nzega greenstone belt differs from other greenstone belts in Tanzania in that volcanic rock of acidic composition are relatively abundant. BIF is well represented and appears to be a strike continuation of the same rocks at Geita. Domal features are reported to have been recognized within volcanic assemblage. The Geita Greenstone Belt forms the northern arm of the "Sukumaland" Belt.

It strikes east-west, is approximately 60km long by 15 km wide and consists of two west-southwest-east-northeast trending BIF ridge complexes. In between the Sukumaland greenstone belt, a combination of structure, alteration and lithology control the size and style of gold mineralisation. Borg 1994, created an interpretation map of a section of Barth's (1990) geological map of the Lake Victoria Goldfields.

This is shown in Figure 3-5. From this, it is clear that gold mineralisation clusters in areas where greenstone belts have been truncated by large-scale shear-zones, fault-zones and fracture zones which have also controlled the intrusion of the later dyke swarms described above (Technical Co-operation, 1992, Borg 1994). Gold is reported to occur both within strata-bound host rocks and in cross cutting veins (UNDP, 1986).

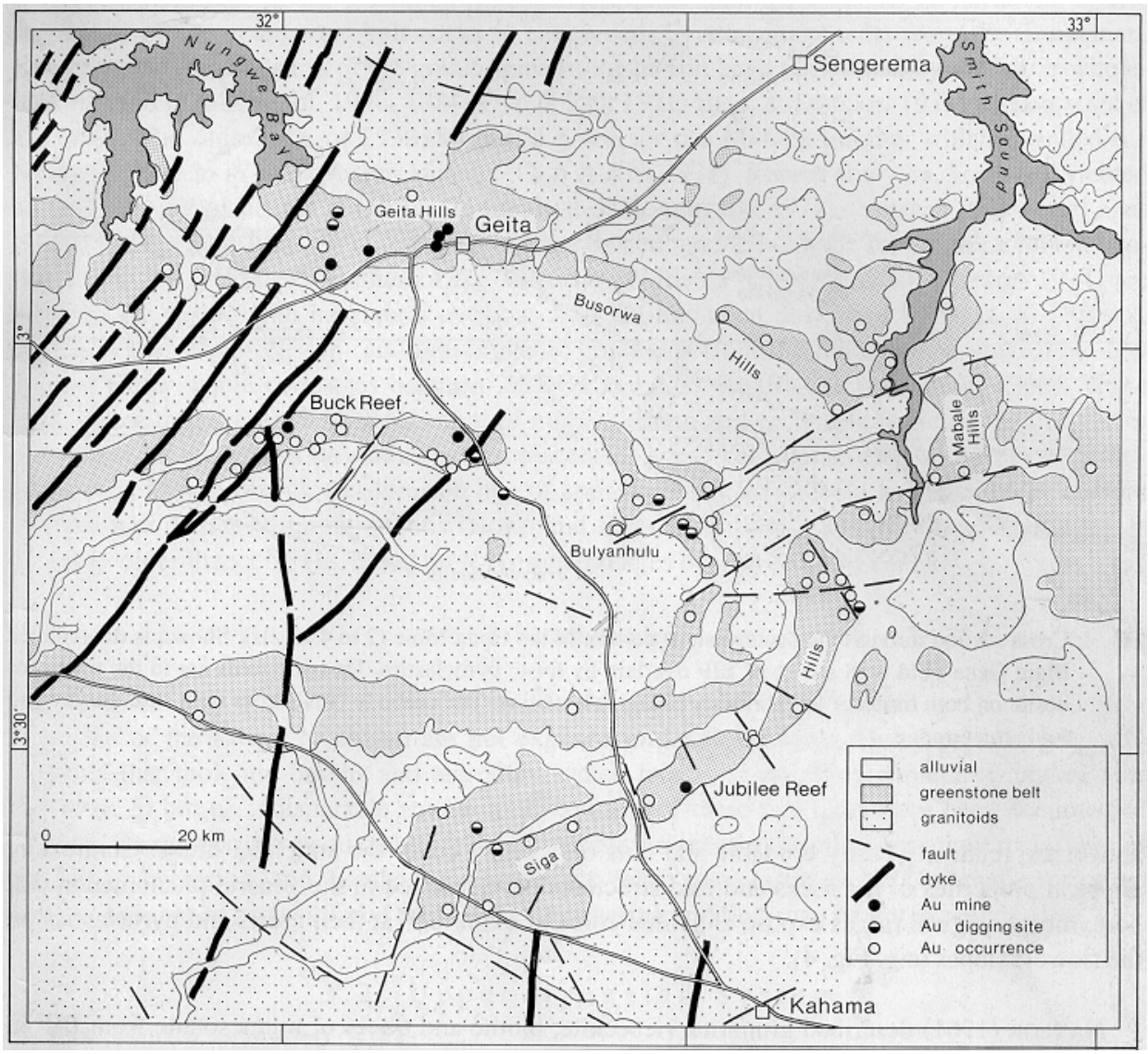

Figure 3-5: Interpretation of Regional Geological Map of Lake Victoria Gold Field (after Borg, 1994).

3.3 Local Geology

The study area (Nzega greenstone belt) a 2,800 square kilometres is characterized by a variety of lithological units, where it includes many types of igneous, metamorphic and sedimentary rocks. In addition, the location of the study area at the northern part of the Nzega gave the area more important setting.

Therefore, there are many different types of works and studies that have been conducted at the studied area. The study area is represented in sheet no. QDS 28, (Handley 1956). The geological map of the studied area (Figure 3-6) indicates that the area is covered by different varieties of basement and sedimentary rock formations.

The Nzega greenstone belt dominantly consists of rocks belonging to the Nyanzian sequence (as classified by Borg (1990) and in particular the Golden Pride area consists of meta-sedimentary rocks of the Upper Nyanzian Sequence (Figure 3-6). The greenstone belt is transected by a major, regional scale (~150km long) shear zone, the Bulangamirwa Shear Zone, in the hanging wall of which the Golden Pride mineralization has developed.

The uppermost part of the Nyanzian System is formed by a thick unit of felsic, mainly rhyolitic volcanic flows, which is only locally exposed and may be irregularly developed. These might represent a proximal facies equivalent to the upper felsic pyroclastics.

Stephenson (1981) estimated the total thickness of the Nyanzian stratigraphy as 7,500-9,000 m. The Nyanzian volcanics and BIFs were succeeded, probably unconformably, by clastic sediments of the Kavirondian. This unit consists of rather immature conglomerates and quartzites.

The former contain sub rounded clasts of laminated chert and oxide facies BIF. The accompanying quartzites are texturally and compositionally mature. The area has been intruded by syn- and post orogenic granites, minor syenites and several generations of felsic, intermediate and mafic dykes.

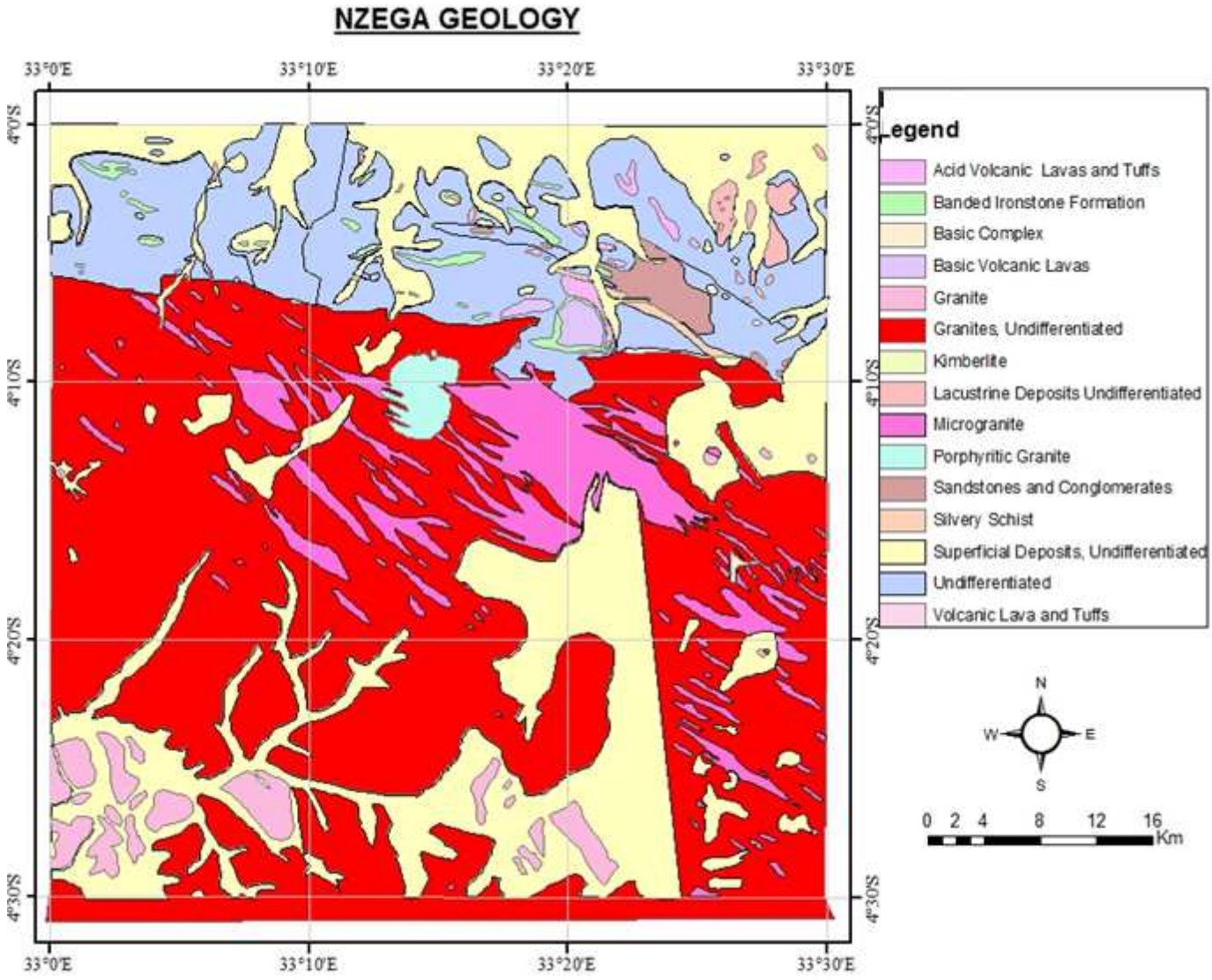

Figure 3-6: Geological Map of Tanganyika from Degree Sheet 28-Nzega North-West digitized from Handley (1956), UTM Zone 36 projection WGS 84 Datum.

3.4 Mineralization in the Lake Victoria Gold Fields

Archean lode gold mineralization within the Lake Victoria Greenstone belt is associated with the following geological features:

Structure

Mineralization is usually associated with second-order shear veins and conjugate shear sets and sites within shear zones where duplexing, inflection, en-echelon segmentation and pressure shadows occur. Regional metamorphism in known deposits is greenschist or less commonly, amphibolite facies. Deposits in higher metamorphic conditions are rare.

Granitoids

It is a plutonic rock that has between 20 percent and 60 percent quartz. Plutonic rocks cooled at depth very slowly from a hot, fluid state. A sure sign is well-developed, visible grains of various minerals mixed in a random pattern, as if they had been baked in a pan in the oven. They look clean, and they don't have strong layers or strings of minerals like those in sedimentary and metamorphic rocks. Granitoids indirectly control the location of Archean lode mineral deposits by their effect on the development of potentially mineralized structures during diapirism regional deformation.

Lithostratigraphy.

All major Archean rock types, especially the iron rich varieties are potentially host to economic gold mineralization. Highly favorable sites for hosting gold deposits are lithological boundaries, where there is a high degree of competency contrast between the adjacent rock units.

Hydrothermal alteration.

Alteration is an indication of potentially mineralized areas. Areas of iron oxide enrichment, resulting from the weathering of sulphide minerals that potentially host gold deposits are a guide, though the iron oxides may result from the normal weathering processes.

4 CHAPTER FOUR: MATERIALS AND METHODS

In order to reach objectives of the research and to answer the research questions, several steps were carried out. Raw aeromagnetic magnetic secondary data for Nzega greenstone belt was investigated, processed and interpreted. The research was carried in two major phases

4.1 Pre -field work

In the first instance literature review was carried out to extract the regional geology and mineralization of the study area as the information will guide on the aeromagnetic interpretation.

4.1.1 The study of Geological map by Barth (1990)

The 1:500,000 scale geological maps by Barth (1990) produced from geological compilation of 1:125,000 and 1:100,000 scale QDS maps available from the Geological Survey of Tanzania (GST 2005). The map shows the geology and selected mineral deposits of the Lake Victoria Goldfields.

Barth (1990) subdivides the geology of this region from older to younger, into Archean granitoid shield, Archean greenstone belt, Proterozoic–late Archean intrusive rocks, and Proterozoic and Cenozoic rocks including regolith, and Recent and proto-lake sediments.

The map of Barth (1990) produced during the onset of modern exploration in Tanzania, and, as such, it highlights Banded Iron Formations (BIFs) and late basins from other greenstones and associated regolith, and linear belts of late-kinematic granitoids in extensive granitoid-gneiss basement. The map clearly shows many gold prospects and old mines, although their spatial relationship with structures cannot be interpreted from the map.

This is despite the fact that the importance of structural controls on lode-gold deposits was already known in 1990 (e.g. Groves 1987). Other geological regions in Lake Victoria Gold Field were broadly explored. Other greenstone belts such as that one of Canadian Precambrian shield and Australia were studied. Projection of all the data sets used in the study to the same projection system was done during this phase of the research.

4.2 Post-field work

The major tasks of the study including detail processing, analysis and interpretation were conducted during this phase of the research. Data sets were analysed and interpreted both in separate and integrated approaches to extract lithological contacts, lineaments and other geological features. The underlying surface information was also achieved through qualitative interpretation applied on different aeromagnetic data layers.

Finally, all the acquired lithological and structural data sets were integrated and digitized to produce the structural maps of the area. Relationship between lithologies and structures was established qualitatively and their control towards the prevailing mineralization was assessed.

4.3 Resources/Materials

4.3.1 Airborne Magnetic data

The Ministry of Energy and Mineral Development of the Republic United of Tanzania has conducted airborne magnetic and radiometric surveys of the whole country. The data used in this study was acquired by Geological Survey of Tanzania in 2004 in Nzega area**.**

The main sources of data in this study are aeromagnetic survey grid data and formal studies, geological and geophysical interpretation maps. Airborne magnetic data were processed to map magnetic lineaments, lithology, faults and folds. Magnetic lineaments represent deep seated first order shears.

4.3.2 Geological map

The Geological map of Tanganyika now United Republic of Tanzania Nzega area, QDS 28 after (Handley, 1956) at a scale of 1:125,000 has been digitized and extracted non spatial information incorporated with it such as lithology and structures. World Geodedic System of 1984 (WGS84) with Universal Transversal Mercator Projection in zone 36 of southern Hemisphere was used.

4.3.3 Software and Hardware

In this research, the writer used different sets of software and hardware in accordance with the task to be done. These include image processing software to enhance images and delineate features; gridding and mapping programs to grid and map aeromagnetic data and word processing, spreadsheet and data base software (MS- OFFICE). Some of the software used is as follows:

i) Oasis Montaj Gridding, Processing and Mapping system (Geo-softInc, 2004)
ii) Surfer 9 from Golden Software
iii) Arc-Gis 8.2 Software from ESRInc.2000
iv) MS- OFFICE 2007 (Access, Excel and Word)

In addition to the various soft-wares different sets of hardware were used: One personal computer (Dell), Printers, Plotter and Scanner.

4.4 Aeromagnetic Data Processing

4.4.1 Data Processing

The aeromagnetic data used in this study was provided by the Geological Survey of Tanzania. The aeromagnetic data of Nzega Tanzania had a total of 60 line kilometers. The Nzega aeromagnetic survey was conducted in 2004 at the request of the Ministry of Energy and Minerals Tanzania. In processing aeromagnetic data, the effects of shallow masses of short wavelength are removed by filtering out (smoothening) short wavelength anomalies (high frequency).

The effects of deep wavelength are called regional anomaly. The geomagnetic gradient was removed from the data using the International Geomagnetic Reference Field formula (IGRF) of 2004.The data processing methods applied in aeromagnetic surveys includes minimum curvature gridding method, total magnetic intensity vertical derivative methods, field continuation continuations), analytical signal.

4.4.1.2 Geo-referencing

To start data processing, all the images (aeromagnetic, geological map) should have the same coordinate system and geo-reference to overlay, correct and extract information from them. The world Geodedic System was used. The Nzega data were gridded to the World Geodetic System (WGS, 1984) with Universal Transversal Mercator projection in zone 36 southern hemisphere.

4.4.1.3 Removal of earth's normal magnetic field

The procedure employed for the removal of the earth's normal magnetic field is stated, for the Nzega aeromagnetic data the International Geomagnetic Reference Field (IGRF) are already subtracted. The IGRF is a mathematical model of the normal magnetic field background of the earth. This model is a function of data location and elevation and the model is updated every five years based on magnetic observation from base station located throughout the world. A magnetic survey can be corrected for the IGRF by subtracting the IGRF model value at each point in the survey.

4.4.1.4 Image Enhancement

Image enhancement deals with the procedure of making a raw image better interpretable for a particular application using various enhancement techniques to improve the visual impact of the original data for the human eye. The magnetic field of the earth's surface contains anomalies from sources of various size and depth. To interpret these fields, it is desirable to separate anomalies caused by certain features from anomalies caused by others.

How to separate the anomalies depends on what type of feature is of interest to us. Anomalies could be separated by their wavelengths and certain features become visible that would be otherwise hidden. According to the interpreter interest, the type of filter can then be selected. Magnetic anomalies caused by geologic structures can also be enhanced using various filtering methods either in space or wave-number domain. Filtering refers to the isolating or enhancing data in the wave-number or frequency domain.

To perform wave-number filtering, it is necessary to convert anomalies in the magnetic field represented on X, Y coordinate system, to a two dimensional set of amplitudes over a range of frequencies or wave-numbers. This is done with the Fourier transform. The Fourier transform can be used to transform a data set from the space domain to the frequency or wave-number domain. Once in the wave-number domain, the proper filter can be applied. The filtered data in the wave-number domain can then be transformed back to the space domain in the same manner using the inverse of the Fourier transformation (Fargatts 1985).

The Fourier transform was done using magnetic map. Processing related to image enhancement was performed using Oasis Montaj data processing software and Surfer data analysis software. Wavelengths, relative amplitudes, geometry and directions are basic characteristics of magnetic anomalies reflecting the respective orientation of magnetic sources. Magnetic maps are most often dominated by large amplitude shallow depth anomalies which obscure subtle and deep seated anomalies. In the interpolation of structures from XYZ data different anomaly maps have been produced from various enhancement filters. Some of these are as follows:

4.4.1.5 Shaded Relief Grey-Scale Map

This is very useful in determining the geologic strike, structural boundaries, faults and near surface features that can be seen clearly in colour maps. Human eye can easily be deceived into seeing the magnetic variations as though they were physical topography. A simple positive anomaly which appears white or black in grey scale can be made to appear to the eye as a hill by calculating the first vertical derivatives in the direction of the supposed illumination (Reeves, 2001).

In order to calculate the first order horizontal derivative of the magnetic field, a computer algorithm in the space domain was used to illuminate light source in a specific direction at a given azimuth and angle from infinite distance. The resulting grid can be displayed in grey scale shading to emphasize the 3D effect. Due to the complex geology of the study area various shaded relief features were produced using different azimuth angles for the grid data.

4.4.1.6 Colour Shaded Relief Image

One of the most important aspects in the design of presentable maps is the selection of the most appropriate colours. Colour image shows anomaly magnitude and long wavelength features particularly well. However small and low magnitude anomalies may not be evident in colour images , the position of colour changes are not dependent only on the positions, magnitudes and widths of anomalous but also on how the data are assigned colours on image processing. Different colours lookup table effect different colour distribution in an image.

A grey scale image is more useful for showing fine details and locating anomaly boundaries even so they do not give much indication of the anomaly magnitude. The tri stimuli model of colour perception is generally accepted. This states that there is three degree of freedom in the description of colour (Bakker et al; 2001). Among various three- dimensional spaces used to describe and define colours are:

a) Red, Green and Blue (RGB) space based principles of colours

b) Hue, Saturation and Value (HSV) most related to our intuitive, perception of colour (Fig.4.1)

c) Yellow, Magenta and Cyan (YMC) space based on the subtractive one presentation to another according to need. When data have to be committed to paper and published, for example as a national map, then choices of presentation style will be far more critical.

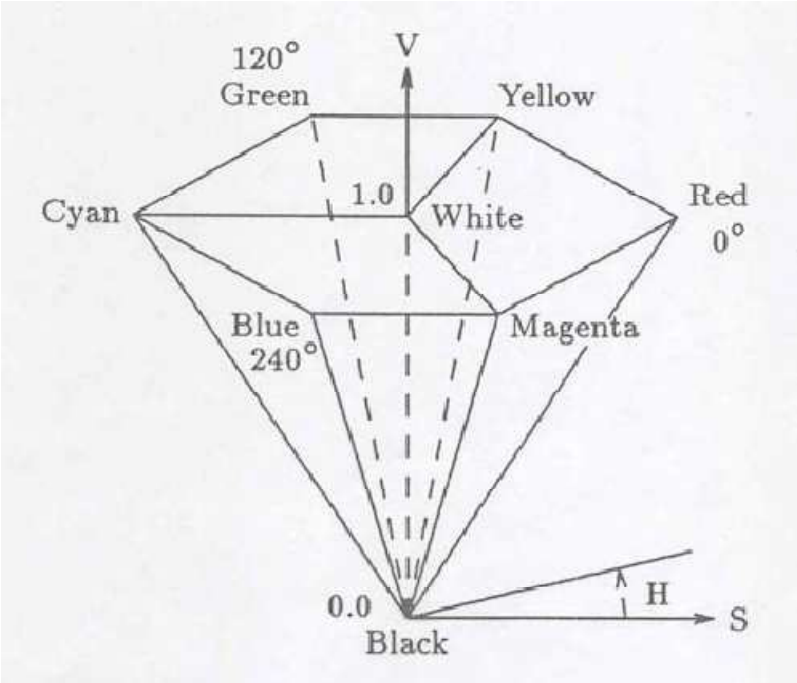

Figure 4-1: The HSV colour model (after Foley et al; 1990) H.S.V represent Hue, Saturation and Value, respectively Figure: The HSV colour model.

4.4.1.7 Vertical Derivatives

The first order vertical derivatives computation in an aeromagnetic survey is equivalent to observing the vertical gradient with a magnetic gradiometer and has the same advantages, namely enhances shallow sources suppressing deeper ones and giving better resolution of closely spaced sources. Low pass filter is also used with this filter to remove the high wavelength noise. Second, third and higher order vertical derivatives may also be computed to pursue this effect further, but usually the noise in the data becomes more prominent than the signal at above the second vertical derivative. The equation of the wave-number domain filter to produce n^{th} derivative is:

$$F(\omega) = \omega^n$$

F (w) is Fourier representation

w is the wave number

n is Order of derivatives.

4.4.1.8 Reduction to pole

The shape of any magnetic anomaly depends on the inclination and declination of the main fields of the earth. The same magnetic body will produce a different anomaly depending on where it happens to be. The reduction to pole filter reconstructs the magnetic field of a data set as if it were at the pole. This means that the data can be viewed in a map form with a vertical magnetic field and a declination of zero. In this way, the interpretation of the data is made easier and vertical bodies will produce induced magnetic anomalies that are centered on the body and symmetrically. The pole filter employs the phase as well as the amplitude spectrum

4.4.1.9 Analytical Signal

Analytical signal was calculated for the area (Figure 5-2) which positions the anomaly at the centre of the causative body by combining both vertical and horizontal derivatives. Analytical signal is considered better enhancement technique since dipolar effects are absent and even for small bodies the peaks merge resulting to an anomaly cantered above the causative body (Alsaud, 2008). It is also observed that the vertical derivative applied to the analytical signal has sharpened up and positioned the anomaly more exactly than the original analytical signal image (Figure 5-2).

5 CHAPTER FIVE: DATA PROCESSING AND INTERPRETATION

5.1 Introduction

Aeromagnetic data has played a prominent role in earth science through revealing subsurface information. Aeromagnetic maps generally show the variation in the magnetic field of the earth and hence reflect the distribution of magnetic minerals in the earth's crust. Mapping the variation of the crustal field, mainly due to susceptibility of crustal rocks, has greatly assisted in geological mapping and mineral prospecting specially in areas with limited outcrop Jaques et al., (1997); Porwal et al., (2006); Schetselaar and Ryan, (2009).

A publication by Grant, (1985) relates magnetic minerals with geology and mineralization. Areas where igneous and metamorphic rocks predominate generally show complex magnetic variations. Meanwhile in sedimentary regions, magnetic variations are small, mainly reflecting basement lithology Jaques et al., (1997).

In areas like Nzega greenstone belt, it is a challenge to fully establish the inter-relationship between lithology and structure due to complex tectonic history and several surficial factors (soil cover). As a result, integrated interpretation approach was followed believing that subsurface activities could fully and /or partly be manifested on the surface and so the relationship could be established.

The aim of this chapter is to provide the results of the processing and interpretation of the aeromagnetic data acquired over the Nzega area and performs a qualitative and quantitative investigation of regional and local litho magnetic domains and subsurface structural setting of the area. Interpretation of aeromagnetic survey data aims to map the subsurface regional structures (e.g., faults, contacts, magnetic bodies and mineralization).

This can be performed quantitatively using Euler de-convolution method to determine the depths of subsurface structures employing magnetic equation based on solving Euler's homogeneity equation. The processes data is presented in a final profile data in XYZ ASCII file Format imported and database generated in Oasis Montaj. It is the culmination of the data acquisition and compilation process and the start of procedures to visualize and interpret the result.

The interpretation is aided by the geology, expected target and possible parameters to select the best model that fits the data, as the measured data matches multiple models exactly or very closely. Prior information of the area in terms of geology and confirmation from other sources is crucial in generating correct and an accurate interpretation of magnetic data. The extraction of geological information from a survey is also known as interpretation.

The objective of interpretation is to use the observation made in the survey to; improve the description of the configuration of rocks in the ground that give rise to the anomalies of poorly exposed or unexposed areas. Set limits to the depth, size, aerial extent, etc. of each body causing an anomaly. There are two aspects for interpretation namely; qualitative and quantitative interpretation.

5.2 Qualitative Interpretation

A first step towards qualitative interpretation is the preparation of a “magnetic map” on which the intensity values at different stations are plotted and on which the contours of equal anomalies (isoanomalies) are drawn at suitable intervals.

Contouring especially of large scale surveys like airborne surveys is mostly done on automatic plotters using computer programs for interpolation. With the ready availability of contouring programs for implementation on desk-top computers (e.g. Surfer in windows environment, Oasis Montaj etc), manual contouring of even small maps has practically disappeared.

Geophysical anomaly maps are often coloured using suitable colour schemes and colour gradations for the area enclosed between successive contours. Colouring is a very valuable aid in the qualitative interpretation of geophysical maps in general and should not be underestimated. Many features of interest are first discernible when a map is suitably coloured.

The qualitative interpretation of a magnetic anomaly map begins with a visual inspection of the shapes and trends of the major anomalies. After delineation of the structural trends, a closer examination of the characteristic features of each individual anomaly is carried out.

These features are (Sharma, 1976):

a. The relative locations and amplitudes of the positive and negative contour parts of the anomaly,

b. The elongation and aerial extent of the contours and

c. The sharpness of the anomaly as seen by the spacing of contours. Accordingly, the foregoing items are taken in considerations during qualitative interpretation of the aeromagnetic map.

5.3 Quantitative interpretation

Quantitative interpretation aims at inferring the depth, shape, size and magnetic susceptibility of the object or geological structure that produces a magnetic anomaly and this is often carried out in the form of modeling of sources which could, in theory, replicate the anomalies recorded in the survey. Such interpretation is carried out with the aid of computer programs that do forward modeling and inversion.

A forward modeling program accepts depth, size, shape and magnetic susceptibility information as an input and output a predicted magnetic anomaly. The predicted magnetic anomaly can then be compared to the measured magnetic anomaly. When the two are different we can adjust the input parameters of the forward modeling program in order to get a better agreement between the measured and predicted anomaly.

The process is repeated until the predicted and measured anomalies are approximately identical. The possible interpretation of measured anomaly is to repeat the forward modeling many times until we find a satisfactory agreement between the predicted and observed magnetic anomaly. These programs repeat the forward modeling in order to find an optimal solution. In addition these programs use smart algorithms that determine how the model parameters; depth, shape, size and susceptibility need to be change in order to improve the agreement between the predicted and measured magnetic anomaly.

5.3.1 Interpretation of aeromagnetic data

The magnetic data interpretation is theoretically more difficult because of the dipolar nature of the magnetic field and possibility of remanence magnetization. However, it is often simpler than that of gravity due to small number of contributory sources which are likely one source, the magnetic basement. The bases of many applications of aeromagnetic surveying in that the interpretation of magnetic data assumes that magnetic sources must be below the base of the sedimentary sequence.

With exception of iron deposit, or dyke and sill emplace in the sediments or volcanic or pyroclastic sediments concealed within the sediments. The subsurface features mainly faults also have a distinctive effect on the total magnetic field. Therefore, the magnetic methods is applicable in mapping the thickness of the sedimentary sequence by systematically determining the depth of the magnetic sources (magnetic basement) over the survey area.

Nzega greenstone belt have been characterized by volcano-sedimentary deposits therefore, this study intended to map the subsurface structure of the survey area that may assist in locating potential gold mineral prospects.

The visualized results of the total magnetic intensity map, vertical derivatives contour map, analytical signal, shaded relief gray scale map and filtering magnetic maps of the study area are shown on Figures 5.1- 5.7 indicate several isolated magnetic anomalies which can be interpreted individually as a causative bodies.

Most of the magnetic anomalies observed in this study are related to mafic rocks intruding basement rocks. Other anomalies occur in areas where the basement rocks are overlain by sediments and the interpretation of such anomalies may indicate the thickness of sediments overlaying the causative bodies.

The major units interpreted from the images include anomalies which indicate the presence of volcanic, sedimentary rocks, metamorphic rocks, mafic and felsic intrusive and lineaments due to faults. The low intensity anomalies observed in areas with granite rocks where the high frequency anomalies were found to be indicative of the volcanic rocks. Areas covered with metasediments and sediments seem to be characterized by smooth anomalies of simple pattern.

ENHANCED AEROMAGNETIC IMAGES OF THE AREA OF STUDY

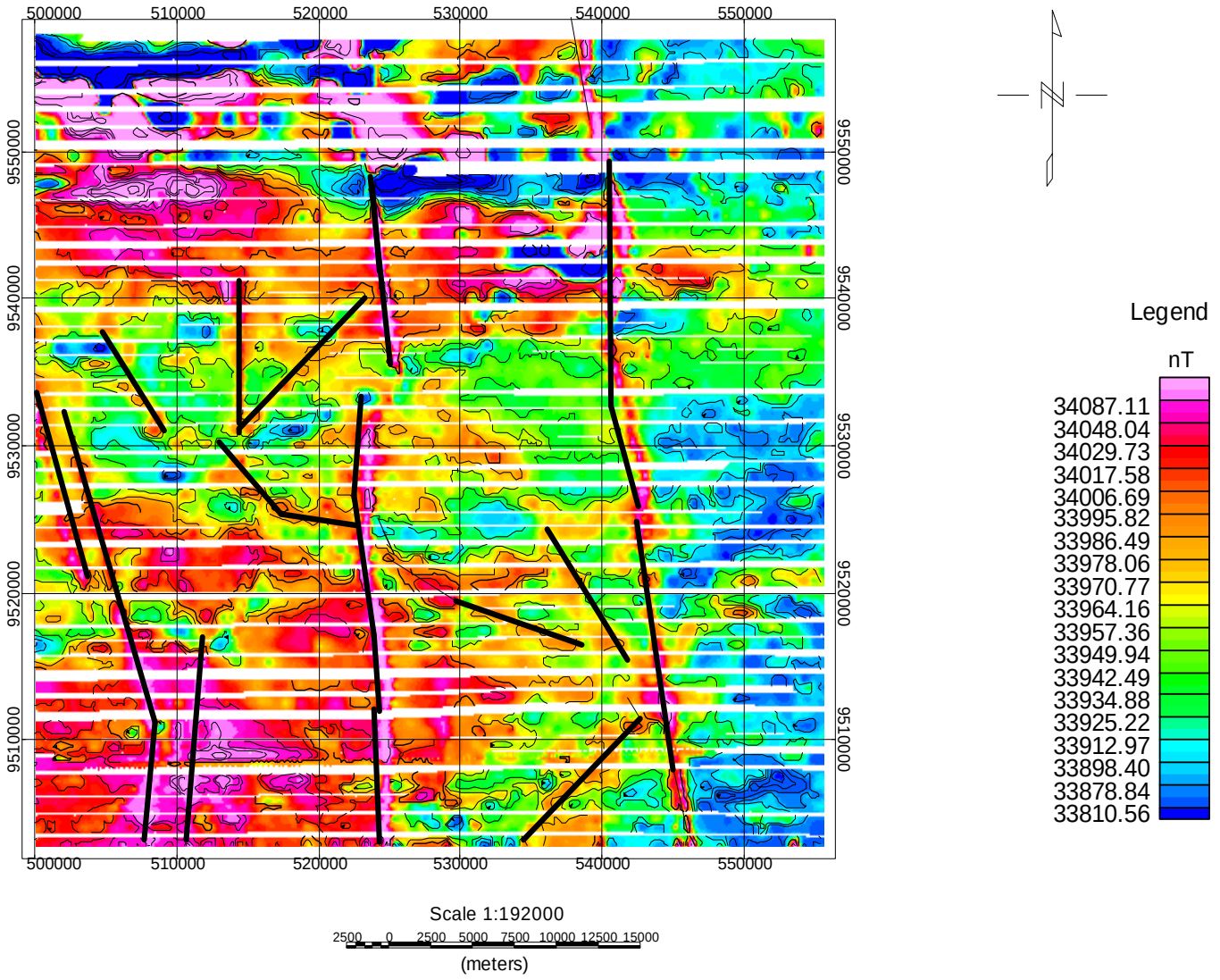

Figure 5-1: Total Magnetic Intensity (TMI) grid cell size 70 with Lines indicating identified magnetic faults.

Figure 5-1 Shows the enhanced TMI image of the area, the maximum magnetic field amplitude of about 34087.11nT indicating the variation of the magnetic intensity due to either lithological or topographical changes. The magnetic high and low are expressed by the colours, the magnetic high (Red) basic eruptive rocks and low (Blue) advertises the presence of less ferromagnetic rocks like acid volcanic or metasediments. The geologic lineament structures trending NW-SE and N-S direction are also observed on the map. Anomalies of high magnetic field intensity form a specified trend in the NW-SE and N-S direction, forming a linear structure (Fault) to the north and south, anomalies of low magnetic field intensity (33810.56nT) are to the north-west and eastern part of the area.

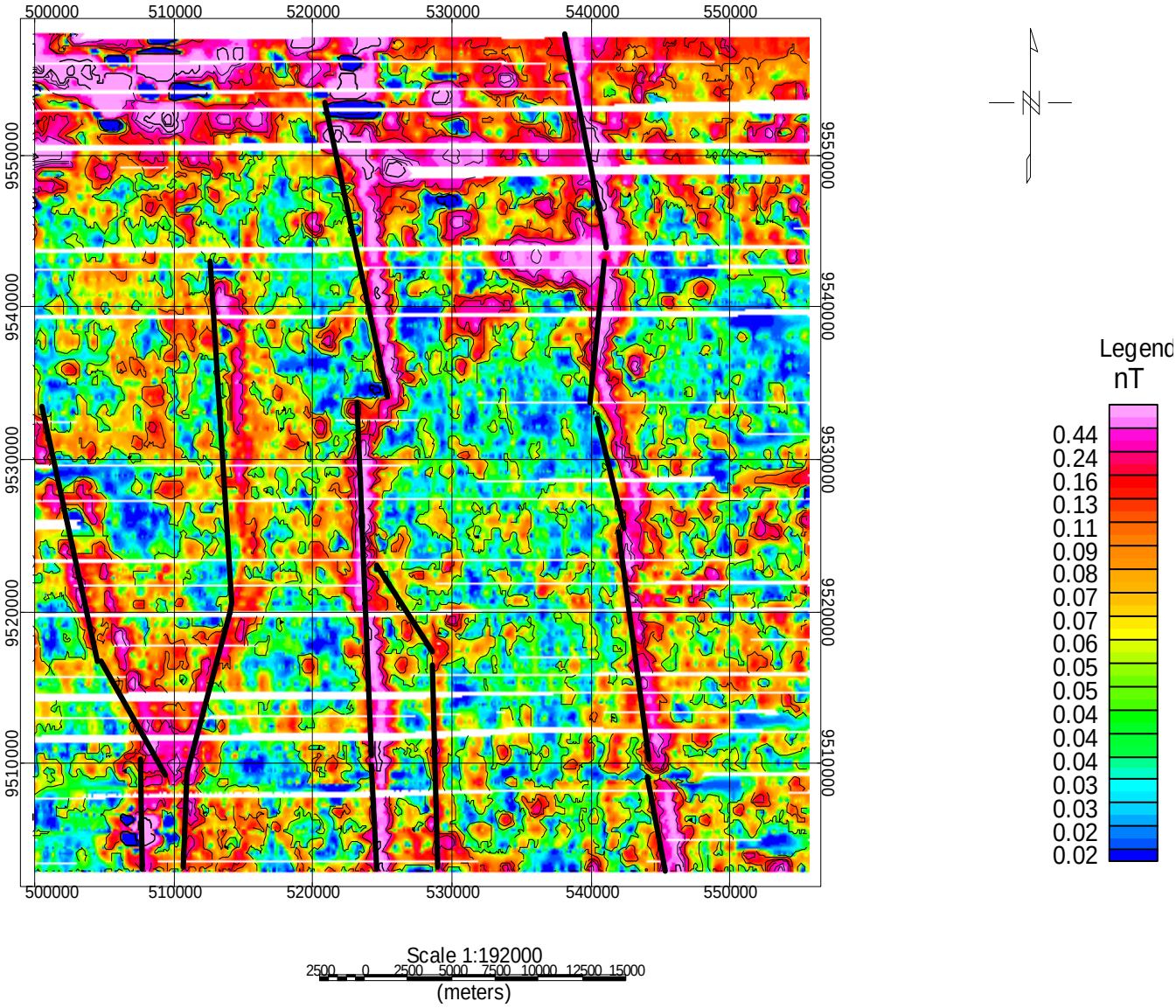

Figure 5-2: Analytical signal images with lines identifying the N-S magnetic faults anomalies.

Figure 5-2: Shows a plot of the analytic signal amplitude map of the magnetic anomaly. Warm red color represents highs (0.44nT) and cool blue colors represent lows (0.02nT). It positions the anomaly at the centre of the causative body. The magnetic map indicates that there might be some strong anomalies due to intrusive bodies' sources below the sedimentary cover such as the north-south magnetic fault of the study area on the map which shows strong analytical signal. Some examples of these faults structures are shown in a more detail on magnetic map in (Figure 5-1). The surface geology appears to give no indication of the source of this feature which means that the source of this anomaly lies below the sedimentary rocks. The linear geologic structures exhibit strong analytical signal trending NW-SE and N-S similar to that of horizontal derivatives.

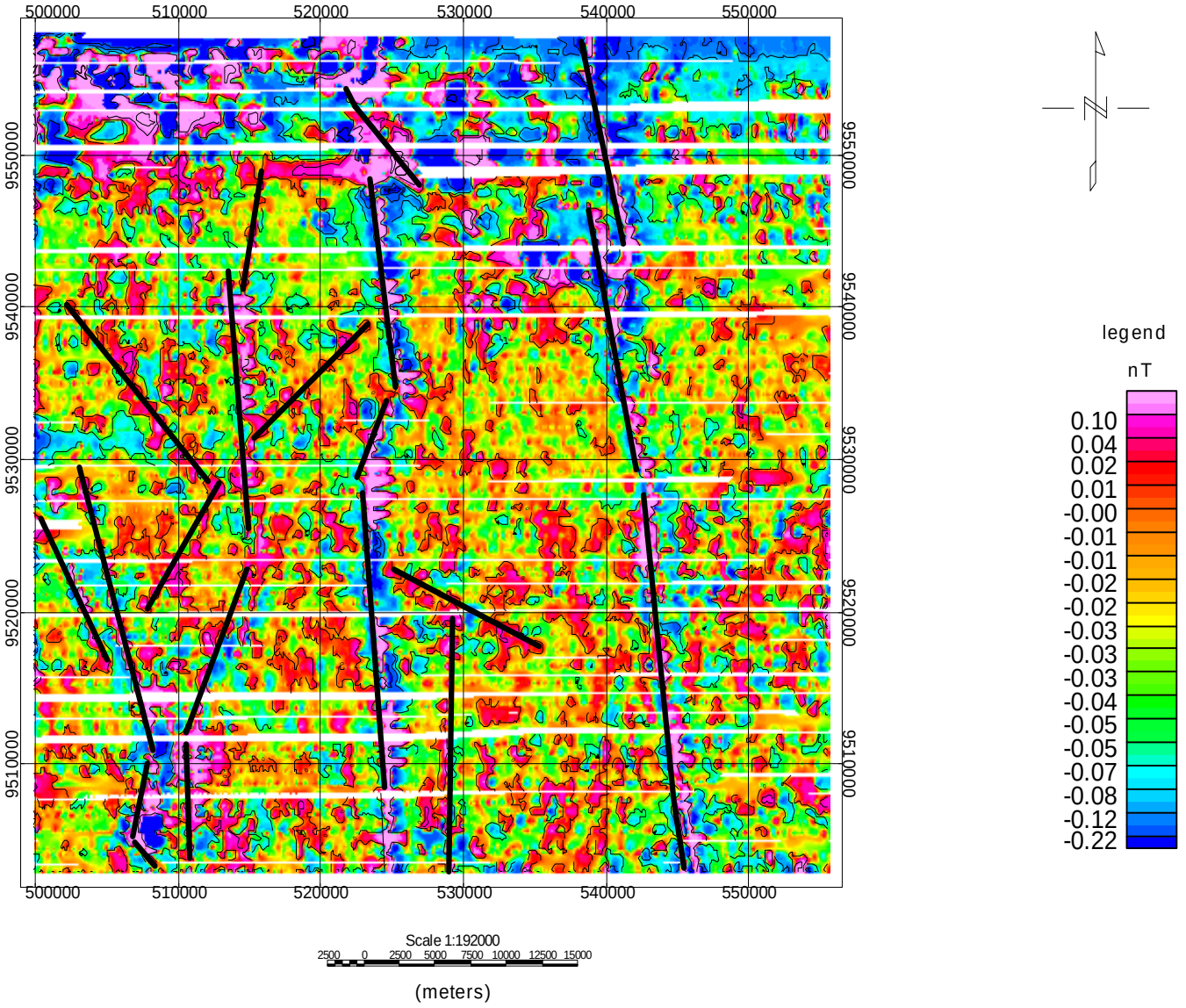

Figure 5-3: Vertical derivative maps using a grid cell of size 70, Lines identifying magnetic fault anomaly.

Figure 5-3: show**s** vertical Derivative (V.D) image enhances the shallower (short-wavelength) anomalies and attenuates the longer wavelength regional components of the potential field. V.D. has its zero values over the vertical edges of thick source bodies, positive values over positive anomalies, and negative values over negative anomalies. It emphasizes magnetic effects caused by relatively shallow and local subsurface features, such as magnetic basement structures and intra-sedimentary magnetized faults. V.D map lines of discontinuity often indicate the presence of cross-cutting faults or shear zones as shown on figure 5-3. Some of the structures which were showing in upward continuation map, total magnetic intensity and analytical signal are also marked in vertical derivative map, in which the geologic structures like the faults mentioned are more sharpened with high resolution as it enhances shallow anomalies more than the regional anomalies (high wavelength).

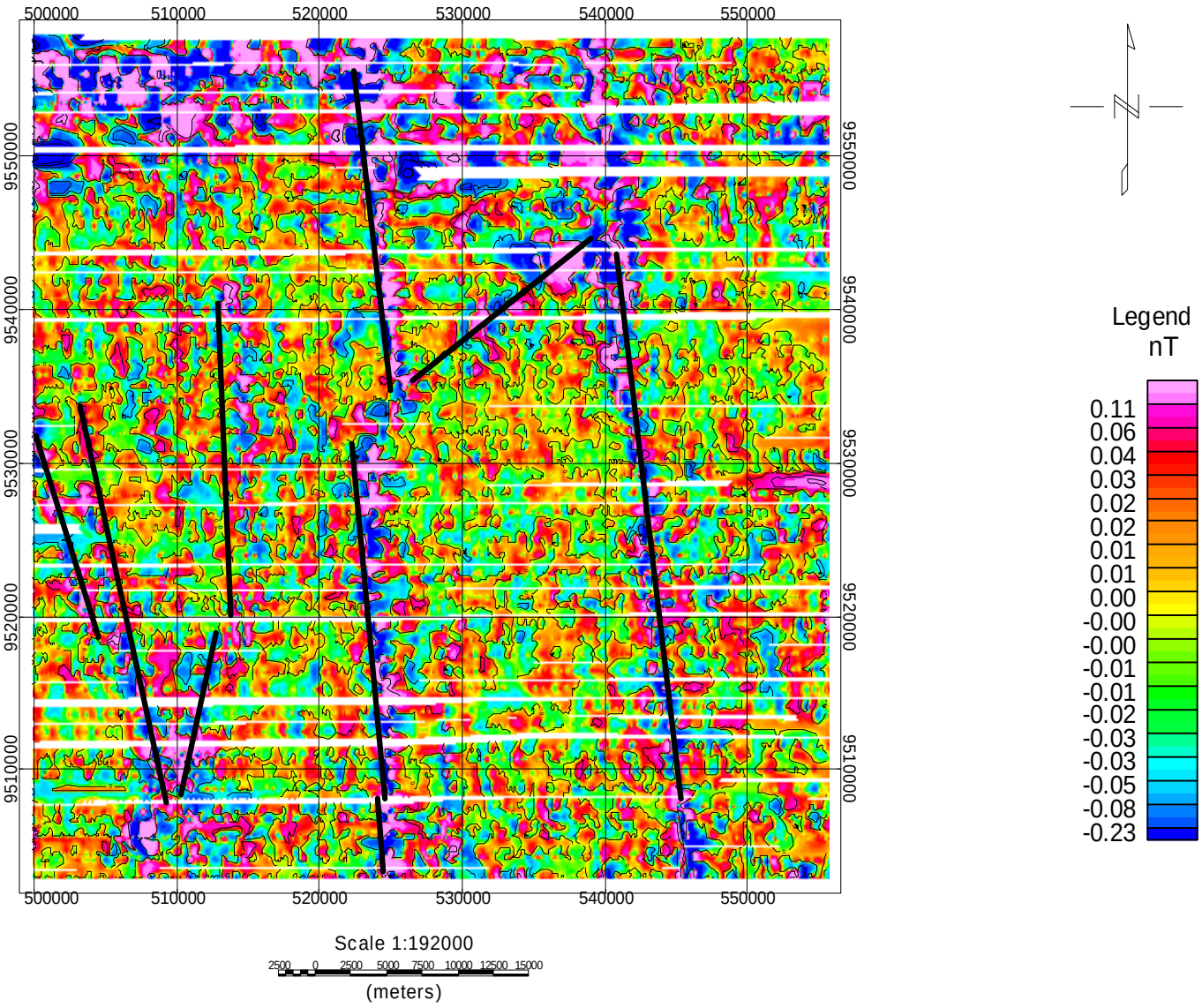

Figure 5-4: Horizontal derivative image of the first order of grid cell of size 70.

The filtered map, horizontal derivative (Figure.5-4), is used to trace easily the faults that characterized the study area. In general, the area is characterized by N-S and NW-SE trending faults direction. The horizontal derivative (HD) method is considered as the simplest approach to estimate the contact locations (e.g. faults). The derivatives are strongest in mostly part of the study area the linear fault trending seems to have strong as well as weak derivatives as shown on the map. The amplitude of the gradient reaches 0.11nT/m.

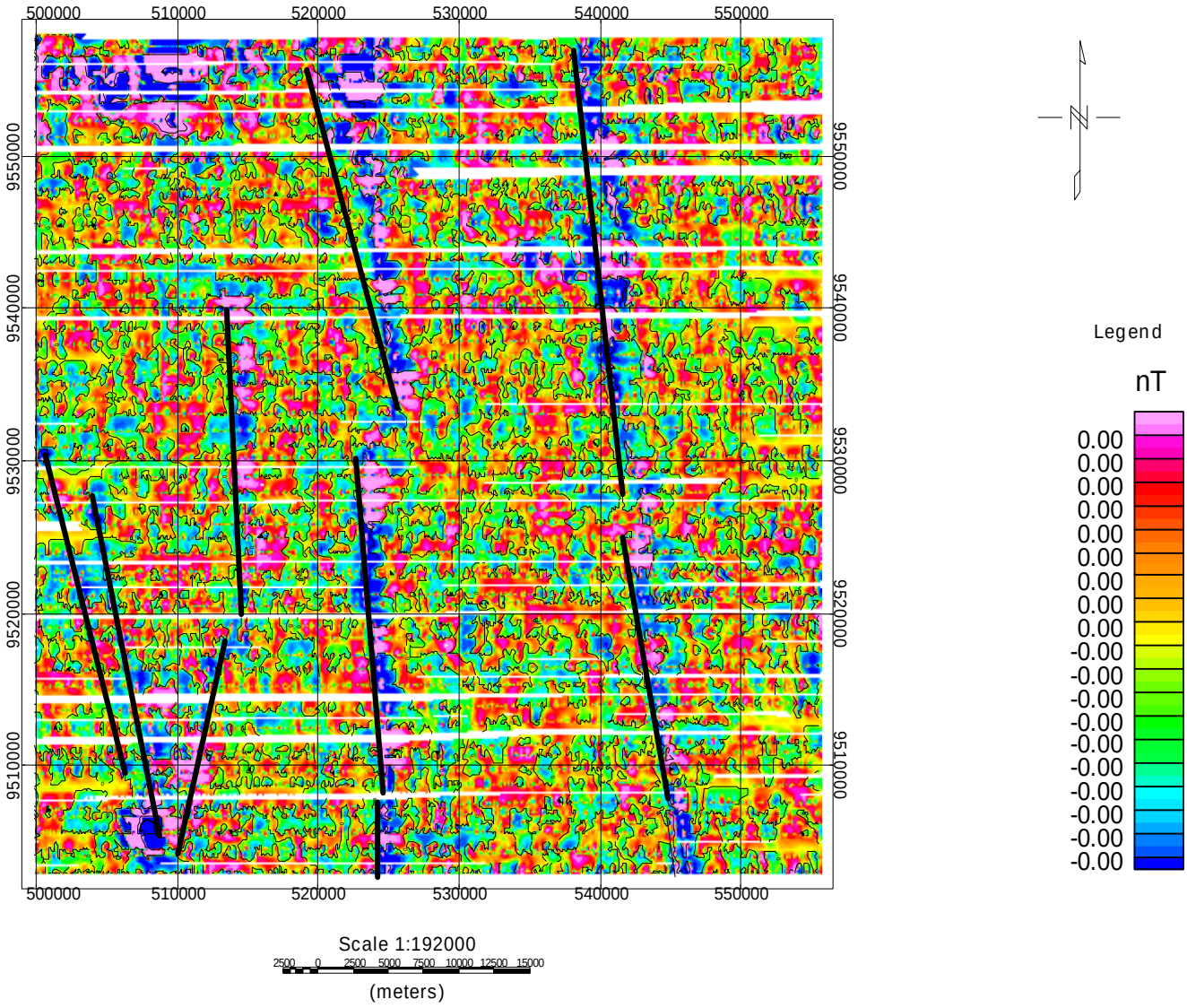

Figure 5-5: Second vertical derivative images of grid cell size 70.

The vertical derivative filter map (Figure 5.5) aids in defining the edge of the shallower aeromagnetic bodies. It measures the difference of magnetic values at different elevations. The high rate of vertical change of magnetic field characterized the shallower magnetic bodies from their deeper anomalous features. It has sharpened up and positions the anomaly more exactly than the analytical signal. It can be observed that the background field has been isolated by the higher frequency anomalies that have magnetic lineament trending which is NW-SE and N-S.

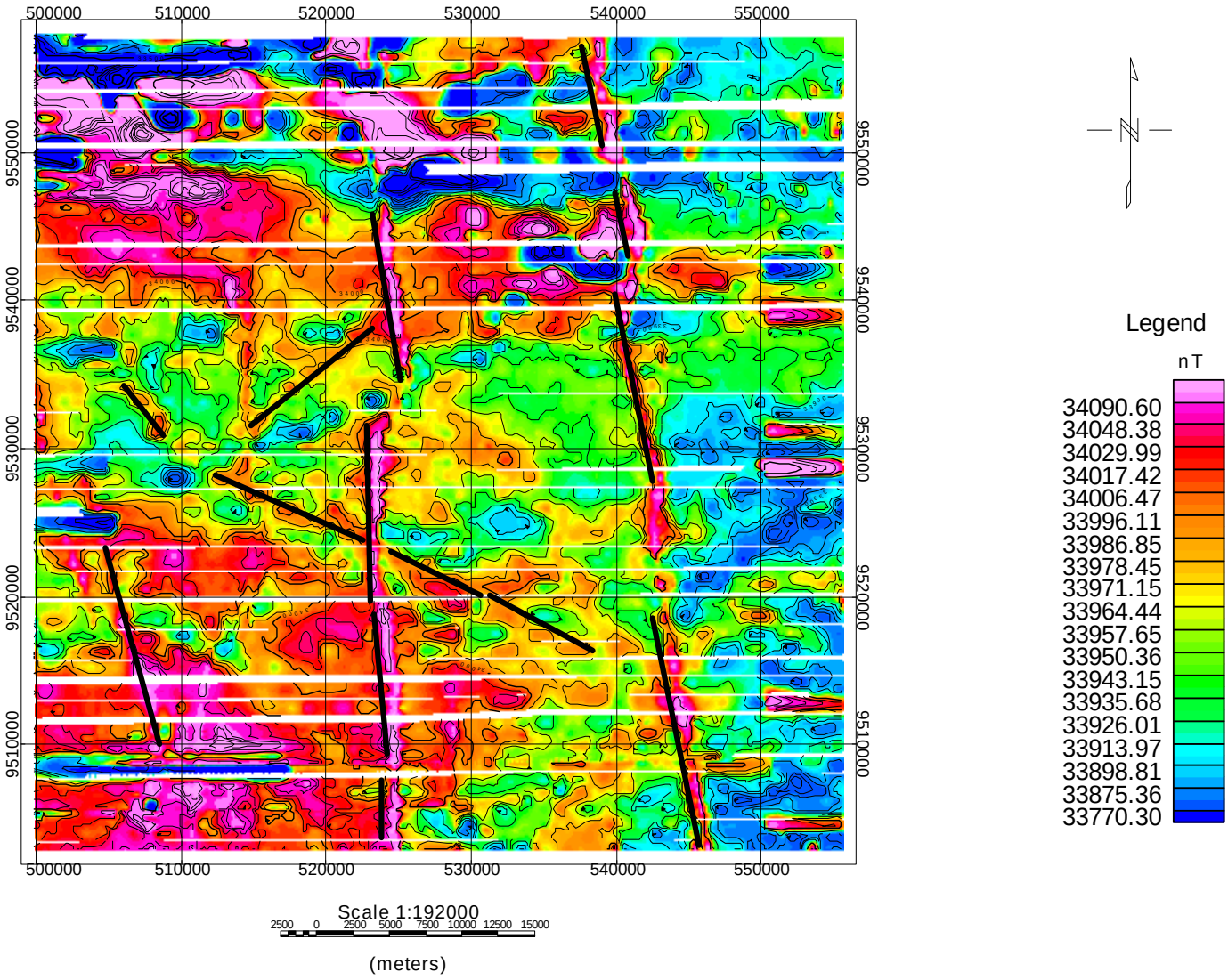

Figure 5-6: Upward continuation (1Km) map of grid cell size of 70.

Upward continuation is a way of enhancing large scale (usually deep) features in the survey area. It attenuate anomalies with respect to wavelength; the shorter the wavelength, the greater the attenuation. The magnetic bodies with high magnetic values range between 34090.60nT on the map (Figure 5-6) can be interpreted as intrusive bodies whereas that of low magnetic bodies with low magnetic values 33770.30nT can be due metasediments accumulation. Lines on the map shows regional structural trending NW-SE and N-S. When the upward continuation map and total magnetic intensity anomaly map are compared it is clear that upward continuation technique is best in suppressing the near surface anomalies, and enhances the regional anomalies or deep seated anomalies.

5.3.2 Structural features from aeromagnetic imagery

Magnetic properties of rocks are mostly a direct result of the presence or absence of magnetite in the rocks. Aeromagnetic imagery is therefore a useful tool for mapping subsurface geological and structural differences made visible by the variations in magnetic susceptibility. Structural discontinuities can be detected from aeromagnetic images because of sharp gradients in magnetic intensity between the structural discontinuities and their surroundings.

Oxidation in fractures, faults and shear zones during weathering destroys magnetite. This results in narrow zones with markedly less magnetic variations than the surrounding rocks in which they occur. Structures can therefore be delineated in suitably enhanced aeromagnetic images. In this study, aeromagnetic imagery is used to extract deep-seated planar structures which are probably conduits for mineralizing fluids.

Airborne magnetic data covering the Nzega greenstone belt were windowed in from a larger data-set obtained from the Tanzania Geological Survey (Appendix 1). The grid cell size is 325m X 325m. The average magnetic field inclination and declination in the study area are -33^0 and 2^0, respectively.

A shaded-relief aeromagnetic image of the study area was generated (Figure 5.7). The shaded-relief image is an effective representation of complex textural and linear features. Grey scale shaded-relief images were created from which lineaments were interpreted. Successful representation of lineaments in shaded-relief images depends on the illumination azimuth, illumination angle above the horizontal and vertical scale exaggeration.

General structural trends in the area are variable, therefore a series of grey scale shaded relief images of the total magnetic intensity data are generated. Four images with illumination angle above the horizontal of 0^o and illumination azimuths of 045^0, 090^o, and 135^0, respectively, exhibited the sensible lineament definition and these were used for structural interpretation.

The lineaments were digitized as segments and labeled by orientation NW-SE, N-S, and NE-SW as shown on Figure 5-8 of the grey scale shaded-relief images. The TMI map (Figure 5-1) displays several dominant trends NW-SE and N-S that do not occur at random but rather are generally aligned along definite and preferred axes that can be used to define magnetic provinces.

The horizontal derivatives maps (Figure 5-4) aided in defining the location of linear features which in turn, are related to the trend of the faults in the area. Faults can be traced easily along these linear features which prove the effectiveness of these filters in the interpretation. The faults were traced along both maps and compared with the surface faults from the geology.

Topography and surface geology maps were used to evaluate the correlation between the deep-rooted faults and faults identified on the surface. The Nzega greenstone belt structural complex is in the NW-SE and NE-SW direction trending of the area. Interpreted structural elements are shown on Figures 5-9, 5-10 and 5-11 and were also overlain in the geological map of the area to see their trends as shown in Figure and 5-16.

5.4 Structural features

5.4.1 Interpretation of magnetic lineaments

Gay (1972) and Gunn et al. (1997) reported on the various criteria used for identifying magnetic lineaments which were used in this study. Some of these criteria which were used in this study are: offset of apparently similar magnetic units, abrupt change in linear gradient and linear narrow magnetic highs and lows. Lineament interpretations were carried on the various layers of enhanced images among which a large number of lineaments were identified from the shaded relief image.

Magnetic faults mainly due to offset of similar magnetic gradients, were identified from total magnetic intensity (TMI), analytical signal, first and second vertical derivatives and horizontal derivatives (HD) images**.** A very prominent fault with high magnetic signature was identified from all the data layers trending N-S as shown Figures 5-1 to 5-7).

Very noticeable magnetic lineaments were identified from different illumination directions applied in tilt shaded relief image (Figure 5-7). Likewise, other magnetic lineaments were extracted through close inspection of various layers of enhanced images and a lineament magnetic map produced.

The structural framework of the study area as interpreted from the magnetic data (Figures 5-2, 5-4 and 5-7) is shown on Figures 5-10, 5-11 and 5-16. Three main groups of lineaments were identified. Most of these magnetic lineaments seemed to affect the Nzega greenstone belt and found less dominant in the Precambrian basement rocks.

The dominant orientation of magnetic anomalies of the area appears to be consistent with such trending structures. In addition, these structures have served as conduits for different subsurface dykes/structures found in the area. Structure is the single most important control factor on the spatial location of the dominantly epigenetic orogenic deposits.

Structural features are therefore a valuable evidence for predictive mineral potential. In the Nzega greenstone belt, most mineral deposits exhibit clear structural controls. The deposits typically occur in or close to deformation and shear zones, fold axial traces, faults and fractures and zones with high foliation/shear fabric density.

An important aspect of using structural analysis during area selection in mineral exploration is the scale invariance or fractal nature of the structural patterns produced during deformation which implies that the same geometries are identifiable at all scales from local (deposit) scale to regional scale.

Most of the mineralization in the late Archean greenstone belts was formed during the main deformation, metamorphism and syn-to late-kinematic emplacement of granitoid. Orogenic mineral deposits in the study area are hosted by shear and deformation zones. These are typically linear to curvilinear features. Zones of strain contrast during deformation are important sites of mineralization.

Foliations and shear fabrics are useful measures of strain suffered by the different rock units. Shear and deformation zones, foliation and shear fabrics occur as lineaments on gray scale image as shown in Figure 5-7. The Nzega greenstone belt is predominantly of low deformation strain, with dominantly northerly trending structural features (NW-SE to NE-SW) and it can be suggested that the area has been subjected to an important regional tectonic field stress.

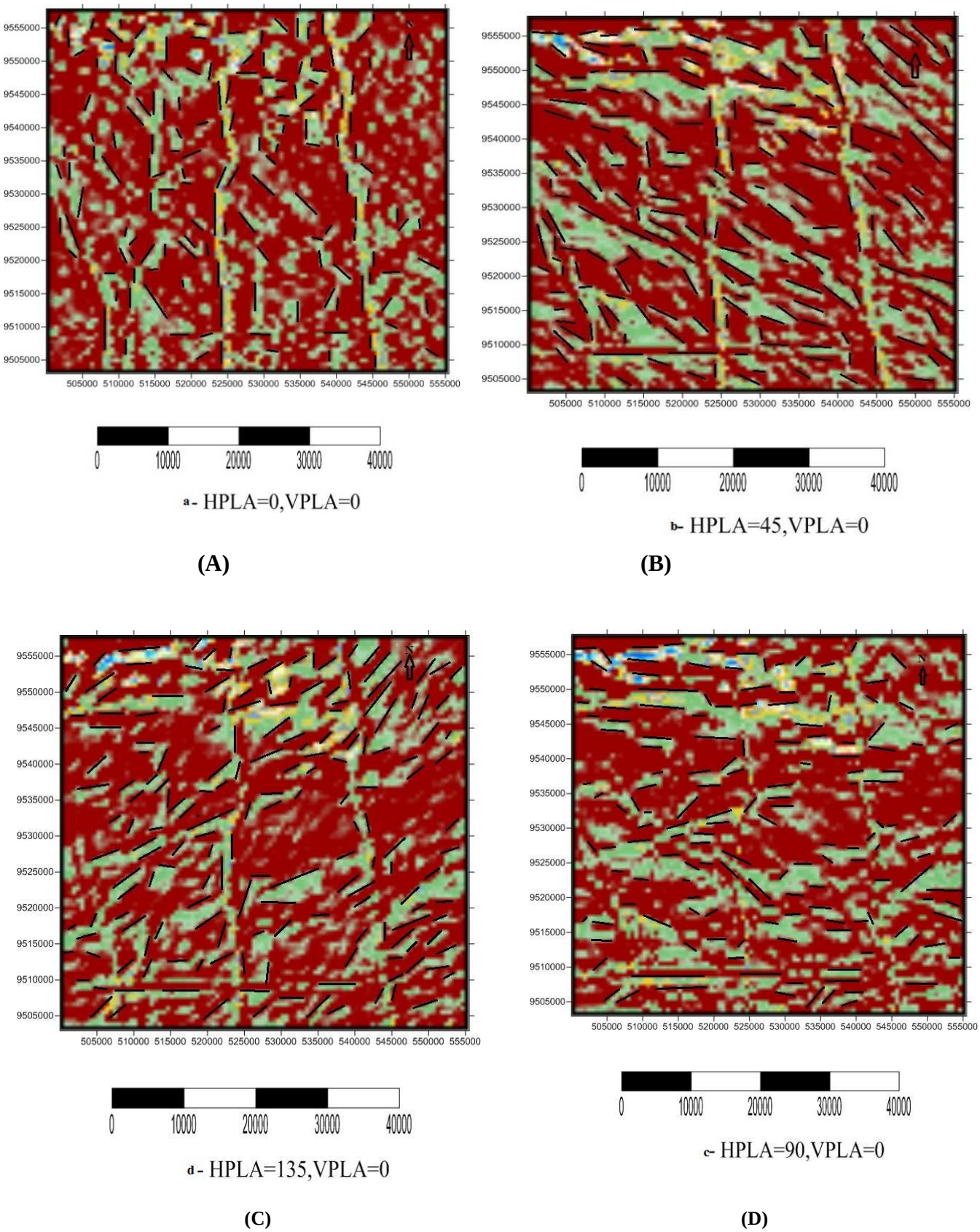

Figure 5-7: Shading relief map of total magnetic intensity, to show the main structural trends affecting the study area: A) N-S, B) NW- SE, C) ENE and D) NE-SW trends. HPLA= Horizontal Light Positioning Angle. VPLA= Vertical Light Positioning Angle.

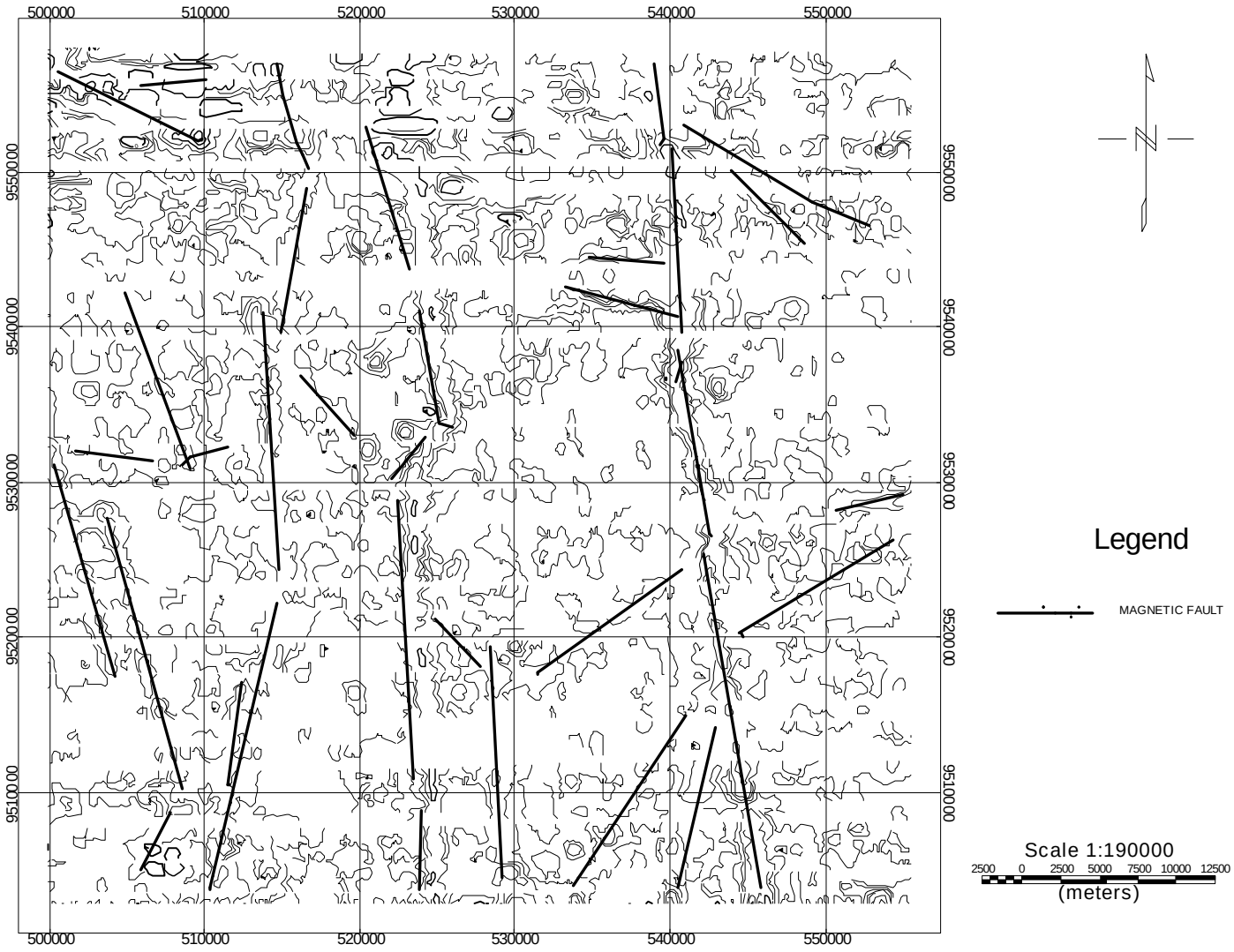

Figure 5-8: The interpreted structural lineament map of the study area based upon analytical signal and horizontal gradient methods.

Figure 5-8: Shows structural lineament map with no geology, indicate trend directions dominating the study area NW-SE and N-S magnetic faults.

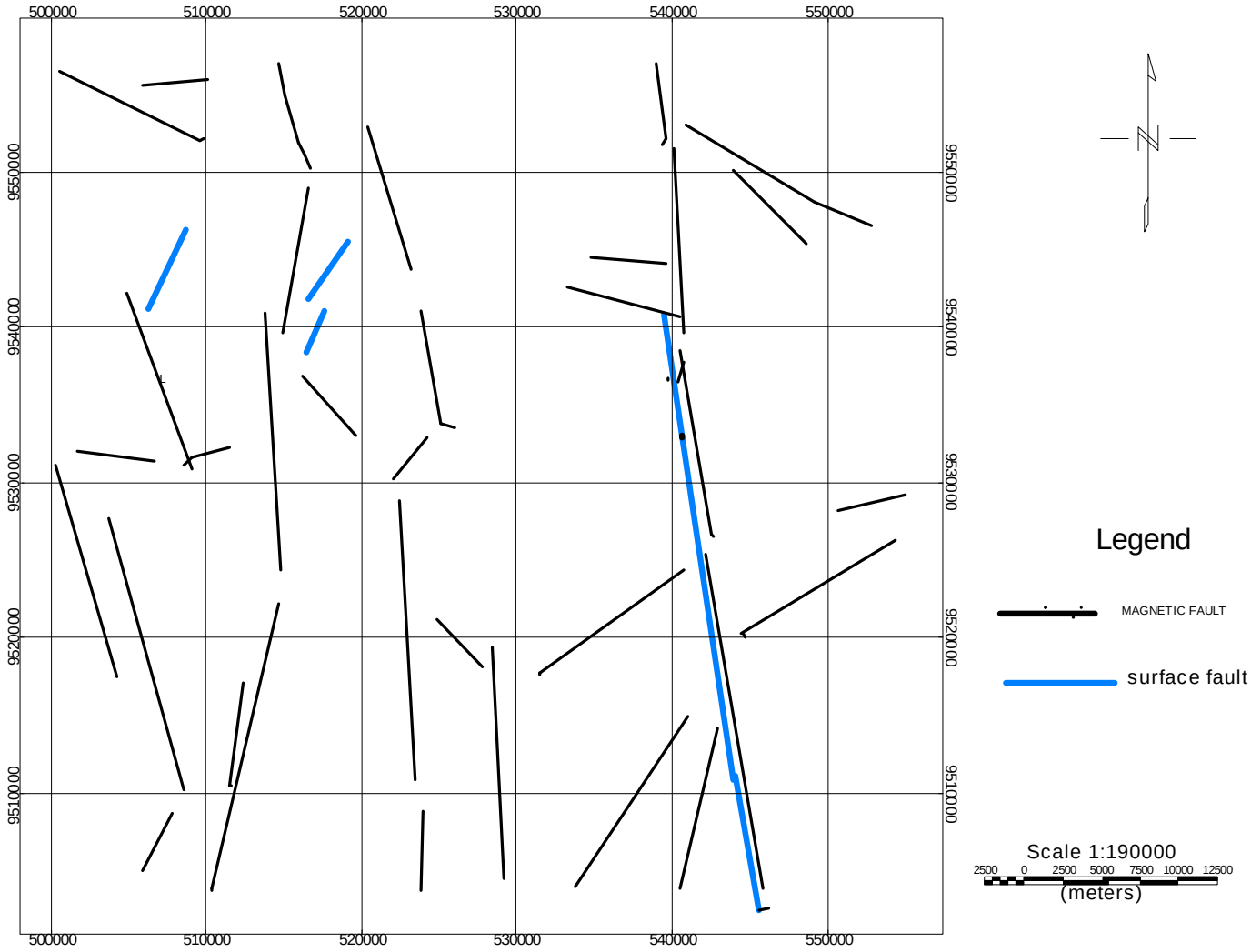

Figure 5-9: The interpreted structural lineament map of Nzega showing surface and subsurface geologic structures with no geology.

The three sets of structures locations resulting from the analysis of the magnetic data by horizontal derivatives, analytic signal and Euler de-convolution methods combined to aid in the final interpretation of geological structures location as shown on Figure 5-9.

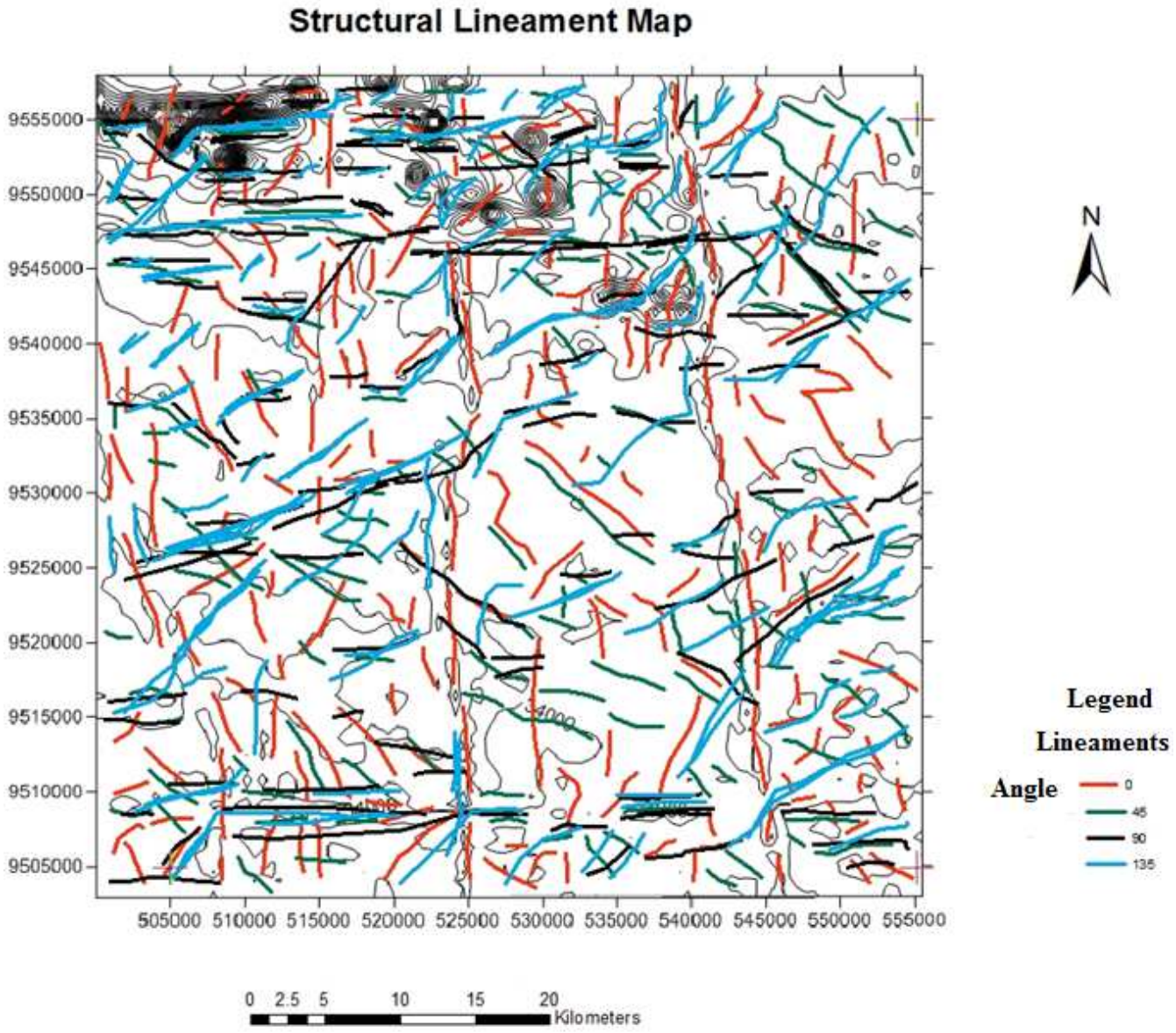

Figure 5-10: The interpreted surface structural lineament map of the study area from shaded relief image map.

Figure 5-10 shows structural lineament map, the colour lines indicate three trend directions dominating the study area NW-SE, NE-SW and N-S, The structural lineaments were extracted from shaded relief image on Figure 5-8.

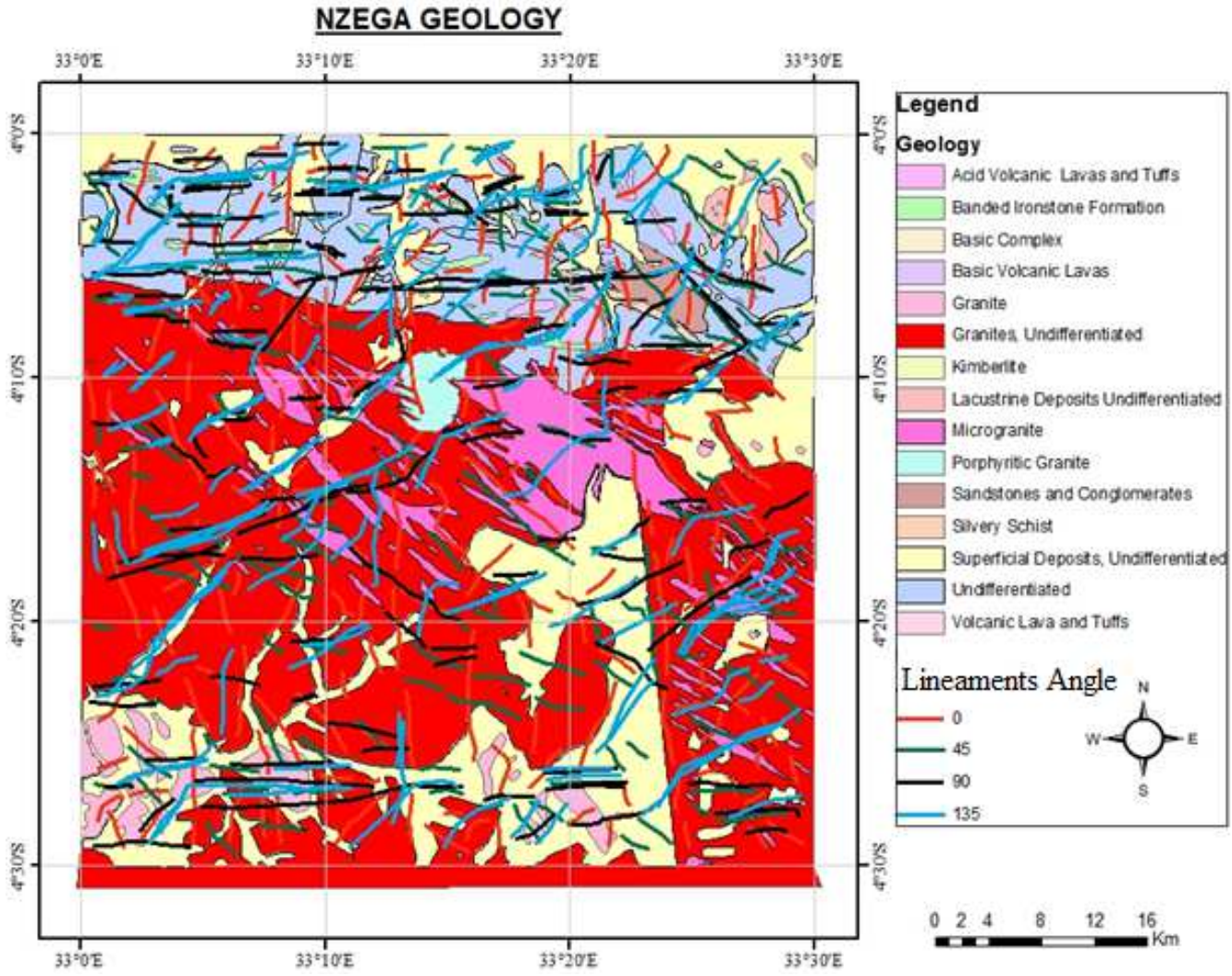

Figure 5-11: Geology and surface structural interpretation of shaded relief image map.

Figure 5-11 shows the geology and surface structural interpretation of shaded relief image map, the colour lines indicate three trend directions dominating the study area NW-SE, NE-SW and N-S. The enhanced image data visualized as if were a surface extracted from shaded relief image and overlain on the geology from different angle of illuminations.

5.4.2 Geological features indicative of mineralization from the geological map

This section describes the extraction of the geological features indicative of late Archean greenstone mineralization deposit. Qualitative knowledge on the spatial associations of mineral occurrences with the different geological features is the basis of most exploration programmes.

In this study, the qualitative and quantitative knowledge of the spatial associations between geological features and mineralization deposits is used to judge the importance of the different geological features for mineralization in the study area. The geological features examined are lithology, granitoids, structures and alteration zones.

5.4.2.1 Lithology

Different lithological units are identified from the previous published geological map. The boundaries of these lithological units could also be recognized from the various enhanced images but with different boundary shapes. This implies that there exist good agreement between the published map and interpretations acquired from aeromagnetic data used in this study. The interpretations used to compile a modified geological lineament map of the greenstone belt as shown on Figures 5-13 and 5-16. Geological maps are used for recognition of lithologies and hence the names of different lithologies used in the map.

The Nzega greenstone belt is covered by QDS 28 of the Geological Survey of Tanganyika geological map sheets of variable quality of Figure 3.6. This map was used as the reference map during map compilation. The scanned geological maps were geo-referenced and digitized on screen as segment maps. The resultant geological map was overlaid on the processed aeromagnetic image lineament structures of the study area and geological contacts were slightly adjusted according to the aeromagnetic intensity variations on the image.

The Nzega greenstone belt dominantly consists of rocks belonging to the Nyanzian sequence felsic volcanics, Banded Iron Formation (BIF), and subordinate mafic volcanics and sedimentary rocks. Mineralization is hosted by BIF or felsic tuff (as classified by Borg in 1990) and, in particular the Golden Pride area consists of meta-sedimentary rocks of the upper Nyanzian sequence (Figure 3-6). The Greenstone Belt is transected by a major, regional scale (150 km long) shear zone

.

5.4.2.2 The granite-greenstone contact

The exact role played by the granitoids in mineralization (source of gold bearing fluid and/or heat source driving hydrothermal circulation of fluids in adjacent discontinuities) is uncertain. Forceful granitoid diapirism influenced the local and regional structure of the Nzega greenstone belt. At the margins of the greenstone belt, gold-hosting structures with mainly reverse dominated movement and dipping away from the granitoid contacts are common. This is evidence for a genetic link between the granitoids and gold mineralization. The granite greenstone contacts from the geological maps covering the Nzega greenstone belt tend to occur close to the granite-greenstone contacts.

5.4.2.3 Geological structural from the geological map

Structural features are valuable evidence for mineral localization, in the Nzega greenstone belt; most mineral deposits exhibit clear structural controls. The deposits typically occur in or close to deformation and shear zones, fold axial traces, faults and fractures and zones with high foliation/shear fabric density.

An important aspect of using structural analysis during area selection in mineral exploration is the scale invariance or fractal nature of the structural patterns produced during deformation which implies that the same geometries are identifiable at all scales from local (deposit) scale to regional scale.

The Nzega greenstone belt is predominantly of low deformation strain, with dominantly trending structural features (NW to NE and W-E) similar to greenstone belts in the Lake Victoria Gold fields shown on Figures 5-11 and 5-16. The gold mineralization is generally associated with the late stage Archean deformation of the granite-greenstone terrain. (Figures 3-5 and 3-6 in chapter three).

``

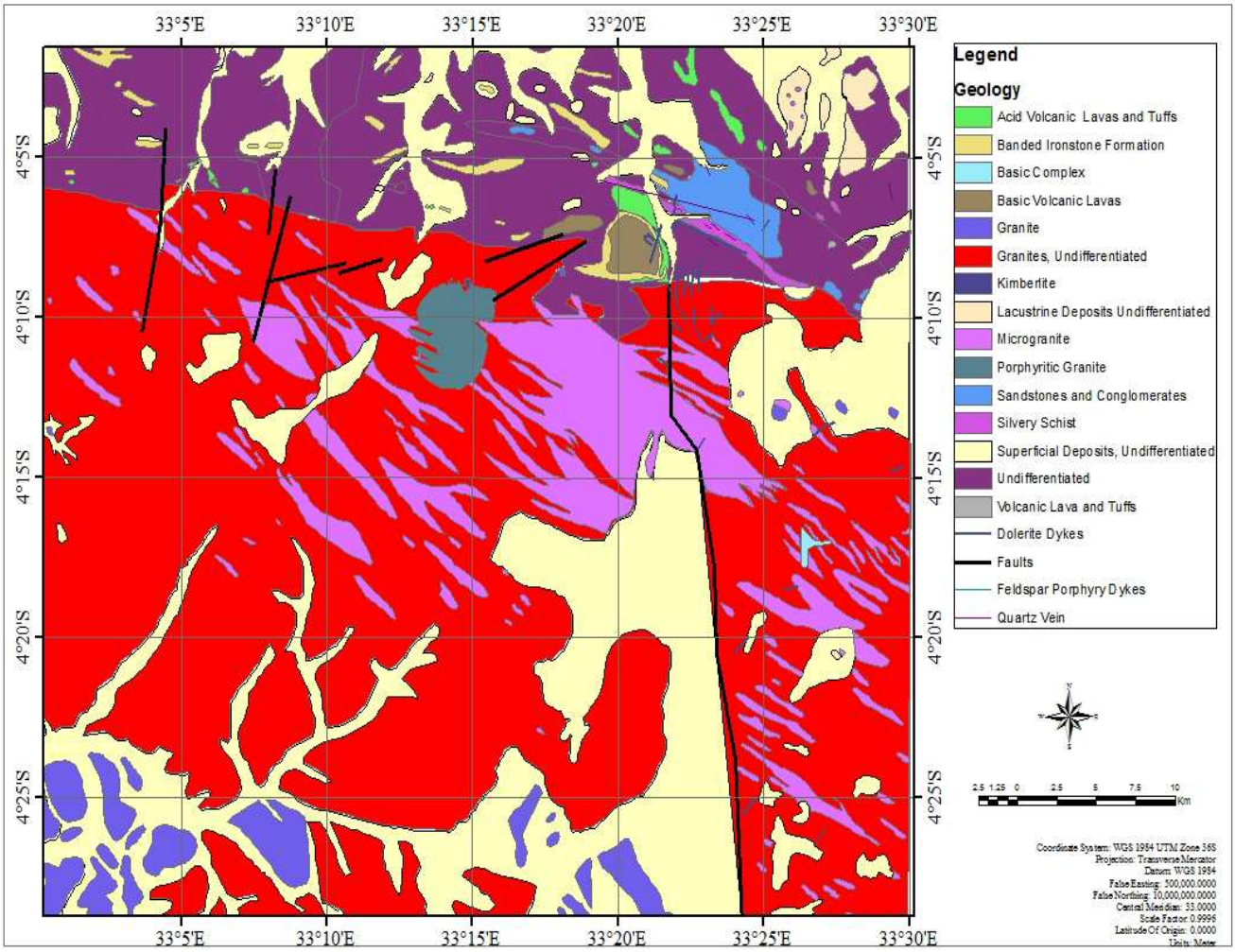

Figure 5-12: Litho-logical map of the study area compiled from the Geological Survey of Tanganyika after (Handley, 1956) UTM zone 36S projection, WGS 84 Datum.

Geological features such as faults, lithological boundaries, and river channels with superficial deposits crosscutting other composite units such as dykes, borders of intrusions are shown on the geological maps which must be possible areas of hosting Archean mineralization.

5.5 Quantitative Interpretation of Magnetic data

5.5.1 Trend Analysis

The magnetic signatures shown on Figures 5-1 to 5.8 in chapter five characterizing the present picture of the Nzega greenstone belt were mainly produced during the latest regional metamorphism, resulting both in broad regional anomalies with smooth gradients, and folded, high-frequency magnetic anomaly bands. The magnetic anomaly strikes mainly follow systematic orientations as a response to the regional stress field during the latest ductile deformation stage. Post-metamorphic tectonic and hydrothermal processes tend to disrupt or destroy the previously continuous magnetic patterns.

This result in offsets or terminations of magnetic signatures as shown on Figures 5-1 to 5.8 represent fault and fracture zones, or zones of broken and gradually disappearing anomaly patterns and reduced anomaly amplitudes. These highly fractured zones are also susceptive for fluid injection and chemical alteration, which affects also the magnetic minerals. In general, later tectonic stress is preferably released by development of dense fracturing along the old structural weakness zones.

5.5.2 Depth estimation

The quantitative interpretation of aeromagnetic survey data can be so complex. However, rigorous analysis is carried out on a routine basis only when simple geometric models are utilized to represent the subsurface sources. In this study, depth estimation by Euler de-convolution technique was used for delineating geologic contacts. This technique provides automatic estimates of source location and depth.

Therefore, Euler de-convolution is both a boundary finder and depth estimation method. Euler de-convolution is commonly employed in magnetic interpretation because it requires only a little prior knowledge about the magnetic source geometry, and more importantly, it requires no information about the magnetization vector (Thompson, 1982; Reid et al., 1990). Euler de-convolution is based on solving Euler's homogeneity equation (Reid et al., 1990) as:

$$(x - x_0)\frac{\partial F}{\partial x} + (y - y_0)\frac{\partial F}{\partial y} + (z - z_0)\frac{\partial F}{\partial z} = -NF'$$

Equation…….01

Where F' is the regional value of the total magnetic field and (x_0, y_0, z_0) is the position of the magnetic source, which produces the total magnetic field F measured at (x, y, z). N is so called structural index. For each position of the moving window, on over-estimated system of linear equations is solved for the position and depth of the sources (Thompson, 1982; Reid et al., 1990).

The most important parameter in the Euler de-convolution is the structural index, N (Thompson, 1982). This is a homogeneity factor relating the magnetic field and its gradient components to the location of the source. N measures the rate of change of the fields with distance from the source (fall-off-rate) and is directly related to the source dimensions. Therefore, by changing *N*, we can estimate the geometry and depth of the magnetic sources. A poor choice of the structural index has been shown to cause a diffuse solution of source locations and serious biases in depth estimation.

Thompson (1982) and Reid et al. (1990) suggested that a correct N gives the tightest clustering of the Euler solutions around the geologic structure of interest. For magnetic data, physically plausible N values range from 0 to 3. N = 3 for sphere, N = 2 for pipe, N =1 for thin dyke and N = 0 for magnetic contact**.** Values less than zero imply a field strength that increases with distance from the source (and is infinite at infinity).

The map of magnetic basement depth (Figure 5-13) has been compiled primarily from the Euler de-convolution. The map illustrates aspects of the interpretation contours of depth to magnetic basement. The magnetic basement depth contours indicate some depressions ranging from 1.6 km to 2.2 km. The depth results obtained helped greatly in interpreting the relief and structure of the buried magnetic basement surface.

The studied area is represented by numerous series of near surface structures (Figures 3-5 to 3-6 and Figures 5-1 to 5-8) showed that the depth range of near surface basement structures beneath the studied area, is 1.1 to 1.8 km. Meanwhile, the deep- seated basement structures are varying in depth between 1.6 km to 2.3 km. These near surface and deep-seated zones cut across and displace each other with different dislocations and different directions.

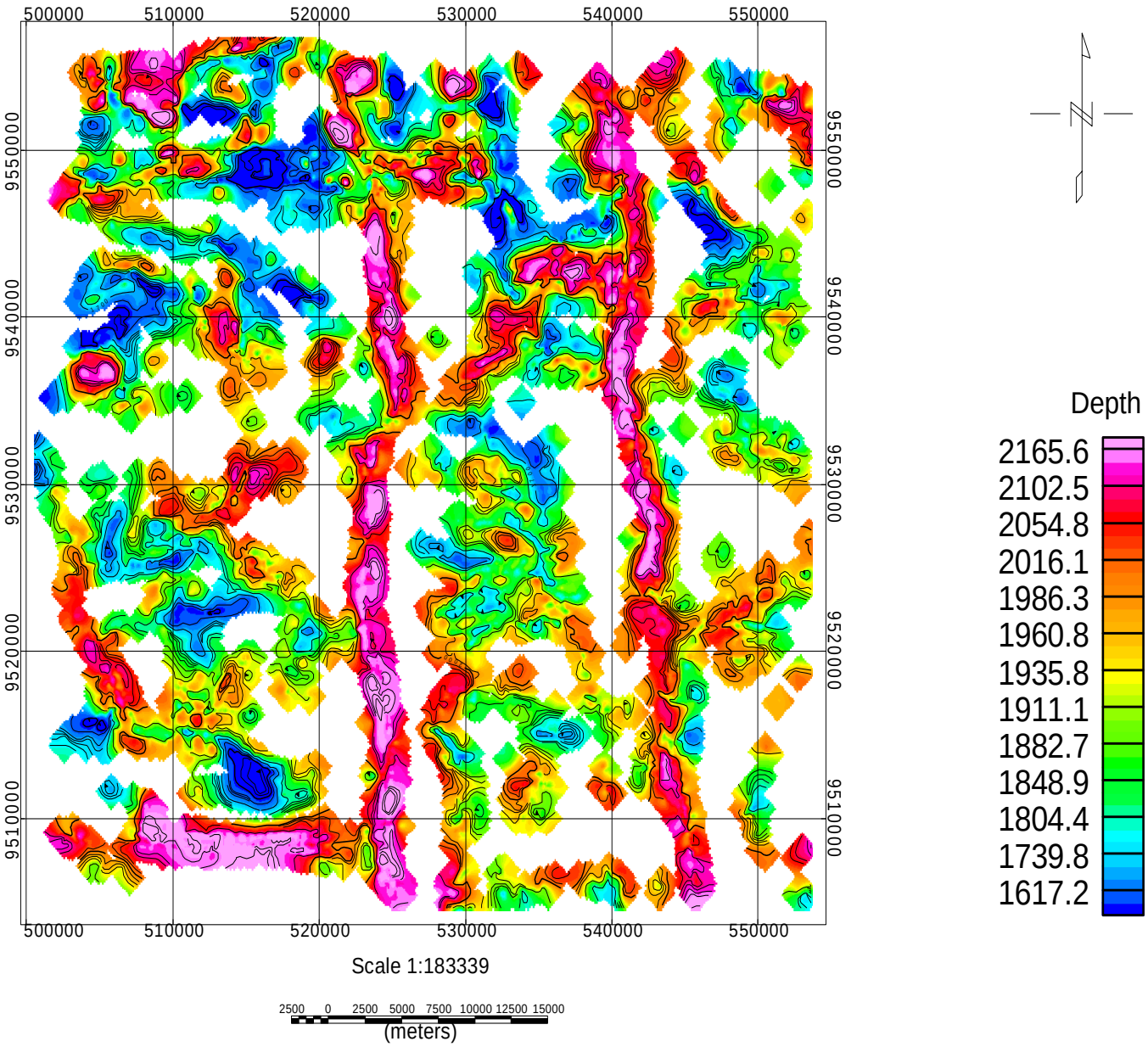

Figure 5-13: Magnetic depth coloured map as a result of Euler de-convolution of the total aeromagnetic intensity data.

The 3D Euler de-convolution magnetic depth map (Figure 5.13) shows that the area has a depth to basement ranging from 2.2 – 1.6 km. The N-S part records an average depth to basement ranging from 1.9 –to 2.0 km with some section showing great depth to basement of about 2.1 - 2.2 km. The western and eastern section records depth to basement varies from 1.6 – 2.0 km. The central part of the study area shows the deepest section in the area trending in N-S to depth basement.

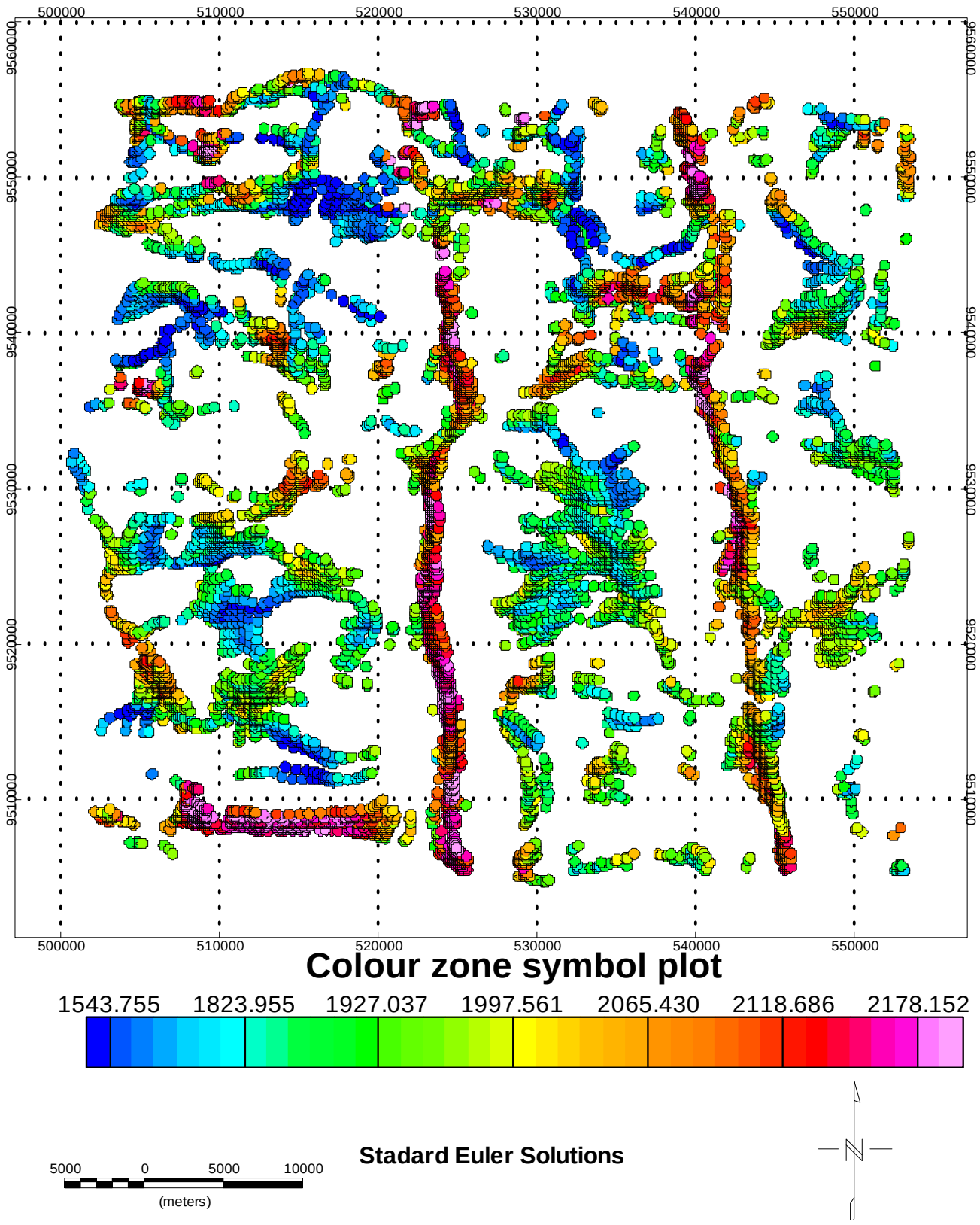

Figure 5-14: Plot of the Euler solutions of the magnetic anomaly and structural index one representing linear intrusive). Figure 5-14: Euler depth solutions, gridded and plotted as an image, with shallow solutions represented by blue to deep solutions represented by red. The depth estimates of the Euler solutions are depicted in the color scale bar in meter.

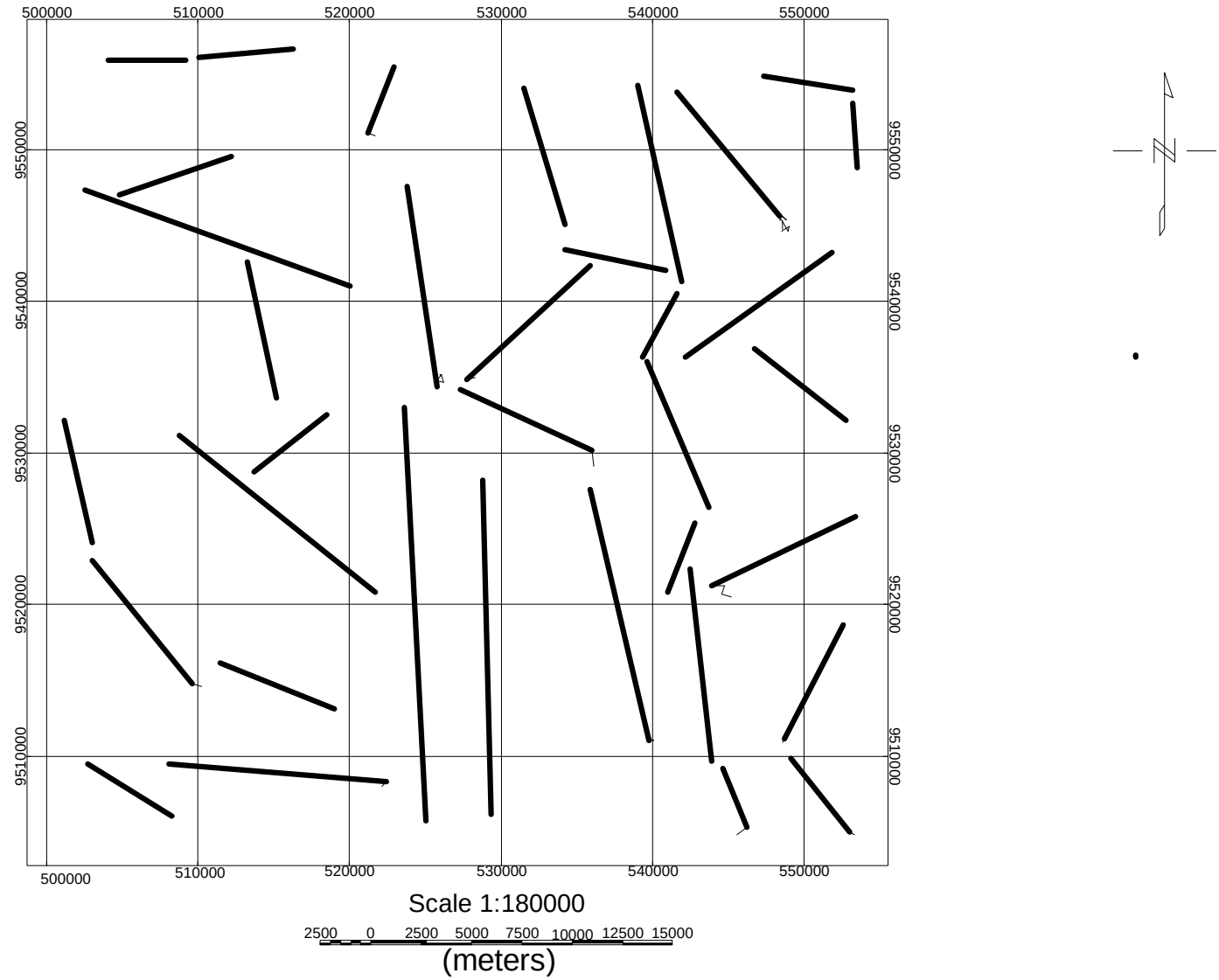

Figure 5-15: Estimated locations of Magnetic faults contacts according Euler de-convolution methods.

Euler de-convolution methods were combined with analytical signal and horizontal derivatives to aid in the final interpretation of structural map of the study area shown in Figure 6-1.

5.6 The structural map of the study area deduced from magnetic interpretation

This section deals with compilation of structural map of the area of study. Various derived images from aeromagnetic data such as analytical signal, horizontal derivative and Euler de-convolution methods are used to create a structural geological map of Nzega greenstone belt. The compilation involves the extractions of structures enhanced by different filtered images (Figures 5-2, and 5-15) obtained from aeromagnetic data.

The three sets of structure locations resulting from the analysis of the magnetic data by horizontal derivatives, analytic signal and Euler de-convolution methods were combined to aid in the final interpretation of geological structure location as shown on Figure 5-16. The colour lines indicate three major trend directions dominating the study area in NW-SE, NE-SW and N-S,directions.

The observed faults appear to cross-cut the Nzega greenstone belt and therefore they should be post-dated (younger). The faults are found to depth of up to 2.2 km. This was revealed from the Euler basement depth maps in Figure 5-13. The Nzega rocks are also influenced by the subsurface magnetic lineament because there is a correlation between surface and subsurface lineament. Aeromagnetic lineaments superimposed on the geology suggest that the area has been subjected to an important regional field tectonic stress.

The study has revealed more faults than known before from surface geological mapping. Since faults in the area are associated with known gold mineralization, this means there are more locations to focus on in this context than has hither to be known. More minor magnetic trends are observed in the enhanced aeromagnetic data even though they are not shown on the final structural map of the study area. But several faults inferred from aeromagnetic anomalies in Nzega are in NW-SE, N-S direction, indicating that there is a significant tectonic stress affecting their orientations.

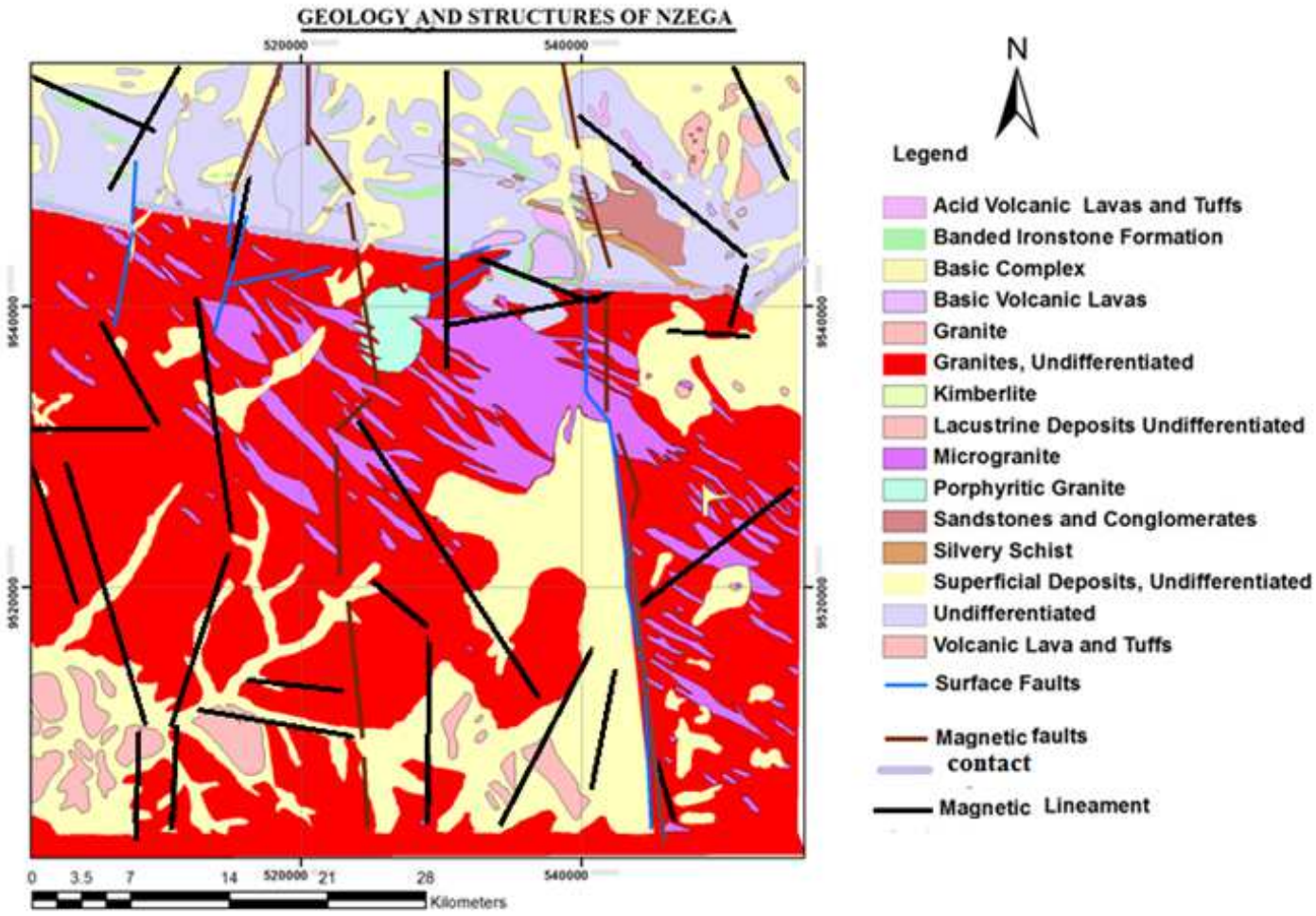

Figure 5-16: Structural map from the synthesis of geology, structure and aeromagnetic interpretation data.

6 CHAPTER SIX: DISCUSSION AND CONCLUSIONS

6.1 Discussion

The magnetic method is a powerful tool that can be successfully applied in structural studies. Since magnetic provide a relatively direct mapping of the abundance of magnetic minerals, it also serves as a useful indicator of lithology, structure, weathering and alteration processes. The method is mature and inexpensive technology. Airborne and ground magnetic have various advantages and disadvantages but airborne magnetic will be the method of choice unless subtle near surface anomalies are crucial. There are several variations on enhancement and presentation methods that need to be selectively applied depending on both the data and the aim of the project. Specialized enhancements have been developed for dealing with regolith materials.

Qualitative interpretation is based on recognition of spatial patterns within the data. Many geological entities such as faults, folds and intrusions can often be easily identified. Direct lithological interpretation is usually not possible without additional information. Airborne geophysical study is utilized to delineate the subsurface structure which controls the anomalous mineralization zones of the studied area.

In this study, aeromagnetic data and the regional geological map are considered as the main sources of information. According to visual inspection of the various geological and aeromagnetic maps, the subsurface basement tectonic map of the studied area is constructed. The depth to the top of the intrusive causative targets was calculated from the aeromagnetic map using Euler de-convolution method. It was found that the computed depths range between 1.6 and 2.2 km. The relatively large depth values are observed mainly above Nyanzian, Kavirondian and observed their trends at many localities.

These depths values correspond to the occurrence of the intrusive igneous rocks. The relatively shallow depth values correspond to the mountainous areas. Euler de-convolution shows the same main trends as the other previous filtering methods. These results agree well with both topographical and geological maps of the studied area. The interpreted depths helped greatly in the interpretation basement relief. Shading relief magnetic maps, analytical signal as well as horizontal gradient helped to delineate NE, NW and E-W trends, which are the dominant trends affecting the Nzega greenstone belt area. The Euler plots in (Figure 5.14) clearly define the solution for depths that range from 1.5 km to 2.2 km.

Most of the Euler solutions in the central part show shallow depth of about 1.5 km for the possible causative sources. The depths in some parts of the area are not uniform. In the north-eastern part, the solutions are situated at shallow depth with increasing depth, and in the north southern part the solutions are situated at deep depth of about 2.1 km to 2.2 km meaning the fault is at great depth. In the northwestern part of the area, Euler plots also show non-uniform depth distribution from shallow to deep depths. The total aeromagnetic images (Figure 5.1) successfully mapped magnetic lineaments which can be verified well on the geological map of the study area. Appropriate processing using the directional horizontal derivative (Figure 5-4) and analytic signal map (Figure 5-2), vertical derivatives (Figure 5-3) clearly revealed the subtle geologic anomalies mainly fault which is prominent in all the magnetic data processed. Specifically, the negative vertical derivatives signal in (Figure 5-3) reflects zones of low magnetization which is a pointer to faults/fractures that are associated with possible depletion of magnetite.

A lineament is observed trending N-S starting at 520500, 955000 and running south to 520000, 951000. This is interpreted as a possible shear zone or fault with a clear evidence of displacement of magnetic units as shown on all the Figures in chapter five. The N-S structures in the study area are due to extensional faulting in the Precambrian crystalline basement giving rise to alternating system of down warp and epeirogenic uplift. There is also a clear magnetic distinction between the north-eastern and south-western half of the grid separated by a magnetic low running from south-east to north-west part of the grid as shown on total magnetic signature and upward continuation.

A low magnetic signature running Eastern part of the study area is very prominent. The N-S magnetic fault high structure seems to be associated with both magnetic high and low (possibly that there is an intrusion a dyke into a fault contact between meta-sediments and mafic/felsic meta volcanic units, if not then there is a geologic unit devoid of magnetic material (eg. quartz veining, faults, shearing etc). due to erosion or weathering. The three sets of geological structures resulting from the analysis of the magnetic data by horizontal derivatives, analytic signal and Euler de-convolution methods were combined to aid in the final interpretation of subsurface structures. The combined map of structural zoning of the study area is shown in Figure 5-16 on chapter five which revealed more faults/lineaments which indicate that more work need to be done on these structures to see whether they host auriferous fluids. Magnetic lineaments were traced by overlaying the structures from the horizontal derivative and analytical signal map in addition to Euler solutions.

The down warp in this study represents syncline/basin while the structural high anomalies are interpreted to be the focal points for the mineral fluids pathways. Further investigation into regional structural setting on the area with the aid of airborne magnetic images revealed the presence of a NE-SW, NW-SE and N-S trending large scale lineament. This lineament or shear zone should be regarded as possible pathways for migrating auriferous fluids. Similar shear zones are favourable areas for Au mineralization within the Lake Victoria Gold Fields.

6.2 Conclusions

The enhanced images of the study area such as total magnetic intensity , analytical signal, horizontal derivative and vertical derivative maps, upward continuation show that the magnetic bodies of high intensity are common in the study area than those of low bodies , a clue that the area is highly enclosed with mafic volcanic rocks . The study revealed a lineaments structures trending NW-SE and N-S which are considered to be related to subsurface crustal structures. Several lineaments not mapped on surface before were revealed by aeromagnetic interpretation in this study. The fault which is a result of tectonic movement is found in almost all the filtered images of the study area.

The geological features useful for hosting Archean lode gold potential in the Nzega greenstone belt include, the granite-greenstone contact, surface linear structures, lithology as derived on the geologic map should be considered as path ways to hydrothermal fluids carrying metals. Total magnetic intensity map, analytical signal, 3D Euler solutions, Contour depth map, upward continuation maps successfully mapped magnetic lineaments which has been demonstrated on the surface geological map of the study area Quarter degree sheet (QDS 28). With the magnetic it was possible to define the major lithologic units'. The more outstanding signatures are: volcanic units and intrusive which were observed to have strong magnetic signature.

The structural map obtained for the area is dissected by linear faults, which have different directions indicating a complex tectonic history and several events of deformation. The major linear structures in the basement trending NW-SW, N-S to NE-SW and it is very likely that this stress field is associated to some tectonic movement. Finally, it could be concluded that, the application of aeromagnetic survey combined with geological studies provide a powerful tool in delineating the lithological and structural setting which may control the mineralization in the greenstone belt. The recognition of this structural control should be built into regional targeting or modes for gold/mineralization in the Nzega greenstone belt and elsewhere in the Lake Victoria Gold Fields.

7 CHAPTER SEVEN: RECOMMENDATIONS

- This study has better defined the tectonic setting of Nzega greenstone belt through integrated analysis of surface and subsurface data which trending NW-SE, NE-SW and the N-S magnetic fault. I therefore recommend drilling and trenching to be carried out in the area where the anomalous features and trends have been identified in this study. The N-S trending magnetic faults have a characteristic positive response and are thought to be related to mafic volcanic rocks and can be associated with gold mineralization.

- There is a need to follow up new faults/lineaments found in this study to see their potential in terms of gold mineralisation in the study area.

- Detail ground geophysics and high resolution geophysical data interpretation are recommended for further understanding of the anomalous target areas especially those revealed from this study. The ground magnetic method appears to be adequate in locating magnetic anomalies which could be attributed to such low/high magnetic source such as shear zone, fault, intrusions, dyke and quartz veining identified by aeromagnetic surveys.

- Soil geochemistry is also advised, the soil geochemistry, along with ground magnetic is a valuable tool to determine the location of the trenches. This can then be followed up with drilling once the targets are identified.

- Deep pitting and trenching to understand the soil profile, depth to the bedrock and nature of mineralization.

REFERENCES

Aero service cooperation, 1974: Understanding the use of Werner De-convolution in aeromagnetic cooperation.

Alida S. 2007: Classification of Birimian Gold occurrences - Using their Geological and Geochemical Attributes: Case study in south Ashanti Belt Ghana. M.Sc. Thesis International Institute for Geo-Information Science and Earth Observation the Netherlands.

Alsaud, M. M. 2008: Structural mapping from high resolution aeromagnetic data in west central Arabian Shield, Saudi Arabia using normalized derivatives. 129-136.

Association of African Geological Surveys and United Nations Educational scientific and Cultural Organisation (ASGA / Unesco), 1968: International tectonic map of Africa (1:5,000,000), Sheets 5 and 6. Printed by the Instuit Geographique National (France).

Bakker, W.H., Gorte G.H., Horn, J. A., Janssen, L.L.F., Pohl, C., Prakash, A., Reeves C.V Weir, M.J & Woldai, T., 2001: Principles of Remote sensing Editors: Janssen, L.L.F and Huurneman.G.C., An introductory textbook, ITC, Enschede, the Netherlands.

Barley M.E. & Goldfarb R.J. 1996: Exploration Guides: Global Tectonic Setting of Mesothermal Gold deposits abstracts to accompany a short course.

Barth, H. 1990: “Explanatory Notes on the 1:500 000: Provisional Geological Map of the Lake Victoria Goldfields, Tanzania”, Geologisches JahrbuchReihe B, Regional GeologieAusland Heft 72.

Batterham, P.M., Bullock, S.J. & Hop good D.N., 1983, Tanzania: “integrated interpretation of aeromagnetic and radiometric maps for mineral exploration”. Trans. Instn. Min, Metall. (Sect.B: Appl. Earth sci.), 92, p. B83 – B92.

Bell, K. & Dodson, M.H., 1981: “The geochronology of the Tanzanian Shield”. Journal of Geology Vol. 89, p. 109-128.

Berry, L. & Berry, E. 1969: Land Use in Tanzania, Bralup Research Paper No.6, University of Dar es Salaam.

Booth, B. 1954: “A note on the structural geology of the Geita Mine”, Rec. Geol. Surv.Tanganyika Vol. 1 pp 20 –21.

Borg G 1990: A preliminary report on the geology of the Siga Hills, NW Tanzania. Part I: Regional geology, geophysics, geochemistry and distribution of gold within the project area: Tanzanian– German Technical Cooperation, BGR internal report, Archive no. 108564. pp77.

Borg, G. 1994: "The Geita Gold Deposit in NW Tanzania – Geology, Ore-Petrology, Geochemistry and Timing of Events", Geol. Jb. D 100, 545-595.

Borg G & Krogh T 1999: Isotopic age data of single zircons from the Archaean Sukumaland Greenstone Belt, Tanzania. Journal Africa Earth Science 29:301–312.

Borg G & Shackleton R M 1997: The Tanzania and NE Zaire cratons. In: DeWit M, Ashwal LD (eds) Greenstone belts. Oxford University Press, Oxford, pp 608–619.

Borg, G. & Masola S.M.B., 1991: "The litho types of the Sukumaland Greenstone Belt, NW Tanzania. Geology and genetic evolution in Gold and platinoids in Central Africa", IGCP No. 255 final meeting, 11; 13/9/91, Bujumbura. Extended abstracts volume.

Borg, G., Lyatuu, D.R & Rammlmair, D. 1990: "Genetic aspects of the Geita and Jubilee Reef Archean BIF-hosted gold deposits, Tanzania", Geologische Rundschau Vol. 79/2, pp. 355-371.

Brian F. Windley 1984: "The Evolving Continents" (2nd Edition) Wiley, London.

Cahen, L., Delhal, J. & Lavreau, J. 1976: The Archean of Equatorial Africa: A Review in the early history of the earth. Editor Windley B. E, Wiley and Sons, London, 489-498.

Cahen, I., Snelling, N.J., Dehal, J., & Vail, J.R., 1984: The Geochronology and Evolution of Africa. Clarendon Press, Oxford, 512 pp.

Campbell, S.D.G. & Pitfield, P.E.J., 1994: "Structural controls of gold mineralisation in the Zimbabwe Craton, Exploration Guidelines Zimbabwe Geological Survey" Bulletin No. 101.

Chamberlain CM & Tosdal RM 2007: "U–Pb geochronology of the Lake Victoria Greenstone Terranes". Confidential report to project sponsors. Mineral Deposits Research Unit, University of British Columbia, Vancouver, BC 81p.

Charles J. Moon, Michael E.G. Whitely & Antony M. Evans. 2006:"Introduction to Mineral Exploration" 2nd Edition Blackwell publisher.

Clarke, D.A., 1997: Magnetic petrophysics and magnetic petrology: aids to geological interpretation of magnetic surveys. AGSO Journal of Geology and Geophysics 17: 83-103.

Costech 1991: Proceedings of the Annual Seminar of the Research and Advisory Committee of the Commission for Science and Technology, 2-4 July 1991.

Dobrin, M. B. 1976: Introduction to Geophysical Prospecting, McGraw-Hill Book Company, New York, 630p.

Doell, R. & Cox, A., 1967: Magnetization of Rocks in: SEG Mining Geophysics Volume Editorial Committee (Editors), Mining Geophysics, Volume 2: Theory. Society of Exploration Geophysicists, Tulsa pp. 446-453.

Doyle, A.G. 1934: "Sanza Goldfield, Tanganyika Territory" The Mining Magazine October 1934.
.
Doyle H.A. 1986: Geophysical exploration for gold: a review, Exploration Geophysics 17(4) 169 – 180.

Euler 1.00 (C) G. R. J., Cooper 2001: School of Geosciences, University of Witwatersrand, South Africa.

Forgat, & Timoth M., 1985, : Wave-number filtering of gravity data and its application to interpreting structure in the Western Transverse Ranges of southern California, Ms Thesis, University of Southern California, USA 296p.

Gay, S. P. (1972): Fundamental characteristics of aeromagnetic lineaments thier geological significances and their significance to geology. Salt Lake City, Utah.

George H. Davis & Stephen J.Reynolds 1996: "Structural Geology of Rocks and Minerals"2nd edition Wiley London.

Geological Survey of Finland (GTK), 2003: Airborne magnetic, electromagnetic and radiometric data flown over selected areas of Mpanda, Kahama, Biharamulo, and Mara on behalf of the Government of Tanzania.

Geological summary of Finland Special paper 48, 2008, ISBN 978-952-217-047-7 (PDF)

Geo-survey (Geo-survey International GmbH), 1971–1980: Country-wide airborne geophysical imagery flown on behalf of the Government of Tanzania.

Geo-survey International Ltd. 1983: "Regional Geology and Mineral Potential of the Geita Greenstone Belt, NW Tanzania", (A report prepared for the Ministry of Minerals, United Republic of Tanzania).

Geo-survey International (1984): "A land sat Interpretation of the Structural Geology and Geomorphology of Tanzania", Plate 6; 1:2,000,000 scale coloured map produced for the Ministry of Minerals, United Republic of Tanzania

Geo-survey, 1983a: "Geophysical and mineral potential atlas of Tanzania".Geo-survey, G.m.b.H, Munchen.

Geo-survey, 1983c: "The investigation of the Nzega east greenstone belt". Technical report number 198/4/83. Unpublished report to the Ministry of Water, Energy and Minerals, Tanzania.

Geo-survey, 1983b: Regional geology and mineral potential of the Geita Greenstone Belt, N.W. Tanzania. Report ref: 196/10003 Unpublished report to the Ministry of Water, Energy and Minerals, Tanzania.

Geo-survey, 1983d: Regional geology and mineral potential of the Nzega greenstone belt, northwest Tanzania. Technical report number 199/4/83. Unpublished report to the Ministry of Water, Energy and Minerals, Tanzania.

Geo-tech Airborne Limited (2006): Report on a Helicopter- Borne Versatile Time Domain Electromagnetic (VTEM) Geophysical Survey Lake Victoria Gold Fields Project Northern Tanzania for Barrick Africa Exploration Limited by Geo-tech Airborne Limited, December 2006.

Gilbert, J.M. & Park, C.F., 1986: The Geology of Ore Deposits. W.H. Freeman and Company, U.S.A.

Goodwin, A.M., 1996: Principles of Precambrian geology. Academic Press, London.

Goodwin, A.M., 1991: Precambrian geology, the dynamic evolution of the continental crust. Academic press, Toronto 666p.

Grant, F. S. 1985: Aeromagnetic, geology and ore environments. Magnetite in igneous, sedimentary and metamorphic rocks: An overview Geo-exploration, *23*, 303-333.

Groves, D.I., & Phillips, G.N., 1987: The genesis and tectonic control on Archean gold deposits of the Western Australian Shield: a metamorphic replacement model. Ore Geol. Rev. 2, 287–322.

Groves, D.I., & Barley, M.E, 1997: "Archean Mineralisation", In A Short Course Handbook - Archean Gold Deposits: Geological Setting, Nature and Conceptual Exploration

Gunn, P. J., Maidment, D., & Milligan, P. R. 1997: Interpreting aeromagnetic data in areas of limited outcrop. 17(2), 175-185.

Hageman SG & Cassidy KF 2000: "Archaean orogenic lode gold deposits". Rev Econ Geol 13:9–68.

Hester, B. (1998): "Opportunities for Mineral Resource Development Tanzania", 3rd Edition; prepared by Brian W. Hester Inc for the govt. of the United Republic of Tanzania, update of Barnard, F., Hester, B., Johnson A (1991);108 pgs.

Hobbs, B.E., Means, W.D., & Williams, P.F. 1976: "An Outline of Structural Geology".

Horsfall, K.R., 1997: Airborne magnetic and gamma-ray data acquisition. AGSO Journal of Geology and Geophysics 17: 23-30.

Hsu H. D. & Tilbury l. A. 1977: A magnetic interpretation program based on Werner deconvolution.Bureau of Mineral Resources. Geology and Geophysics, Record 1977/50 (unpubl.).

Hunting Geology and Geophysics ltd: Report on Airborne magnetic and electromagnetic survey in the Musoma District of Tanzania. -- Rep. No. S/8014, London 1966.

Ikingura, J. R., Reynolds, P. H., Watkinson, D. H., & Bell, K. (1992): 40Ar/39Ar dating of micas from granites of NE Kibaran Belt (Karagwe-Ankolean), NW Tanzania. Journal of African Earth Sciences (and the Middle East), 15(3-4), 501-511.

Jaques, A. L., Wellman, P., Whitaker, A., & Wyborn, D. (1997): High resolution geophysics in modern geological mapping.17 (2), 159-173.

Kabete J.M, Groves DI, McNaughton NJ, & Mruma A. H (2008): A new tectonic subdivision of the Archean of Tanzania and its significance to gold metallogeny. SEG-GSSA 2008 Africa Uncovered Conference—Abstr Vol, pp 21–25.

Makowiecki, L.Z., King, A.J. & Cratchley, C.R.: "A comparison of three airborne electromagnetic methods of mineral prospecting "-- results of test surveys in East Africa. -- Geol. Surv. Canada, Pap. 65-66, 1965.

Mathew Purr 1994: Interpretation of airborne geophysical data over the Aarons pass Granite

Maund, N.H.,& Bowie, E. 1997: "Report in the detailed geologic mapping of the Geita Prospect, Lake Victoria Goldfields, Tanzania" Internal SAMAX Ltd. report.

Mcharo, BA & Mutalemwa, ES, 1993: The exploration database in Tanzania, ITC Journal 1993-2, pp140-148.

Merrill, R.T., McEthinny, M.W. & McFadden, P.L., 1996: The magnetic field of the earth: Paleomagnetism, the core and the deep mantle. Academic Press, San Diego, 531 pp.

Mohamed, S.A. & Mwalyosi, R.B.B. 1991: "Country Environmental Profile for Evaluation of the Special Grant for Environment and Development" Phase II. Report to NORAD, 30 pp + Five Maps.

Mwaipopo, A. 1997: "History of Gold Production from the past mining in Geita", Internal Ashanti Report.

Mwalyosi, R. & Mohamed, S. (Eds) 1992: "A Resource Assessment Strategy for Lake Manyara Catchment Basin, Tanzania". Proceedings of a Workshop, Arusha, Tanzania.Institute of Resource Assessment, University of Dar es Salaam.

Naylor, W.L 1959-1960: Quarter Degree Sheet (QDS) 32, Geological Survey of Tanganyika scale 1:125.00.

Ntulanalwo, V.B., 1985: Ground geophysical surveys in Nzega. Ministry of Water, Energy and Minerals. Unpublished internal report.

Parasnis, D. S. 1966: Mining Geophysics, Elservier Publishing Co., Amesterdam, London, New York.

Parker, M. 1992: The Mining Industry in Tanzania, country review prepared by Applied Geophysical Services for the govt. of the United Republic of Tanzania, 114 pgs.

Parker, M., 1991: Review of airborne geophysical surveys in Tanzania, ESAMRDC report 91/TECH/67, 49p.

Parker, M, 1992: Using older geophysical surveys: Problems and solutions, ESAMRDC report 92/TECH/74, 22p.

Paterson, Grant & Watson Ltd., 2003: Report on the Geophysical Interpretation Itilima Gold and Diamond Project Shinyanga, Tanzania. Prepared for Midlands Minerals Corporation, p.39.

Paterson, Grant & Watson Limited, 1999: High-resolution airborne magnetic and radiometric data in an area of sedimentary cover: Calama West, northern Chile**.**

Petters, Sunday W. 1991: Regional Geology of Africa, Lectures Notes in Earth Sciences; Springer Verlag, Berlin Heidelberg.

Pilikinton, M. & Roest, W.R. 1992: "Drapping aeromagnetic data in areas of rugged topography; journey of applied geophysics, v 29, p.135-142.

Pittard K. & Bourne B. 2009: The Geophysical Response of the Tusker Gold Deposit, Lake Victoria Gold Fields, Tanzania. Australian Society of Exploration Geophysicists Conference, February 2009, Adelaide.Extended Abstracts.

Porwal, A., Carranza, E. J. M., & Hale, M. 2006: Tectono-stratigraphy and base-metal mineralization controls, Aravalli province (western India): New interpretations from geophysical data analysis. Ore Geology Reviews, 29 (3-4), 287-306.

Quennell, A.M., McKinlay, A.M. & Aitken, A.G., 1959: Summary of the geology of Tanganyika, part I, Introduction and Stratigraphy. Geological Survey of Tanganyika, Memoir, **1**, 264pp.

Quennell, A.M., 1960: Summary of the Geology of Tanganyika, Part II: Geological Map. Tang. Geol. Surv., Memoir 1, Part 2. Dar es Salaam, Government Printer.

Reeves C.V; 1993: New Horizon for Airborne Geophysical mapping: ITC journal special issue, 2, p 149-155.

Reeves C V 2001: The role of airborne geophysical reconnaissance in exploration geoscience.First Break, vol 19.9, pp. 501-508.

Samki, J.K. 1977: A Provisional Soils Map of Tanzania. Surveys and Mapping Division, Ministry of Lands, Dar es Salaam, Tanzania.

Sandy M. Archibald, 2011 Report on: Exploration programs, Handeni project area.

Schalk, W Van Der Merwe 1998: "Structural Investigation of the Geita Gold Deposit", report prepared for Ashanti Exploration Ltd.

Schandl, E.S, 1999, "A Petrographic Study of the Geita Hill Gold Deposit, Tanzania", Report commissioned by Ashanti Goldfields.

Schetselaar, E. M., & Ryan, J. J. 2009: Remote predictive mapping of the Boothia mainland area, Nunavut, Canada: an iterative approache using landsat ETM, aeromagnetic and geological field data. Canadian Journal of Remote Sensing, 35, S72-S94.

Shackleton, R. M. 1976: Pan-African Structures. 280, 491-497.

Sharma, P. V. 1976: Geophysical Methods in Geology, Elsevier Scientific Publishing Company, Amsterdam-Oxford-New York, 428 p.

Smith, A. 2002: Mabale Hills Exploration Proposal, May 2002, Private company report for Sub-Sahara Resources NL, 42 pgs.

Sowerbutts W. T. C. 1987: Magnetic mapping of the Butterton Dyke: an example of detailed Geophysical survey, volume 144, pp 29-35

Stephenson, J. E 1981: Geology and mineralization of Archean greenstone belts south of Lake Victoria, northwest Tanzania. - Geosurvey International Limited for the Ministry of Minerals, Dodoma, 86 p.

Stockley, G.M., 1947: The geology of the country around Mwanza Gulf. Department of Land and Mines, Geological Division, Short Paper No. 29. Government Printer, Dar es Salaam.

Stuart, H., Cowley, P., 1998: Feasibility Study, Vol. 2,"Geology and Mining."

Technical Cooperation project no. 84.2053.1 1992: "The Archean, BIF-hosted Geita Gold Deposit, NW Tanzania. Geology, Ore-Petrology, Geochemistry and Timing of Events".

Telford, W. M., Geldart, L. P. and Sheriff, R. E. 1990: “Applied Geophysics, Second Edition, Cambridge University Press”.

Thompson, D. T., 1982. Euldph: A technique for making computer –assisted depth estimates from magnetic data, Journal of Geophysics, 47, 31-37.

Tyler, W.H. 1937: “The South-West Mwanza Goldfield, Tanganyika”, The Mining Magazine March 1937.

United Nations Development Programme (UNDP), 1986: The investigation of the Nzega west greenstone belt. Draft technical report No. 8. United Nations Development Programme, Project No.URT/81/035.Unpublished report to the Ministry of Water, Energy and Minerals, Tanzania. (C2250).

United Nations Development Programme (UNDP) 1987: “Final Report on the Geita Gold Prospects “(unpub. rep.), Technical Report no. 12, Ministry of Energy and Minerals, Dar es Salaam.

Van Straaten, H.P., 1982: Gold mineralisation in Tanzania - A Review. Proceedings of the symposium Gold 82: The Geology, Geochemistry and Genesis of Gold Deposits. Gological Society of Zimbabwe, Special Publication No. 1.

Vos, I. M. A., Bierlein, F. P., Standing, J. S. & Davidson, G. 2009: The geology and mineralization at the Golden Pride gold deposit, Nzega Greenstone Belt, Tanzania. Mineralium Deposita, Volume 44, Issue 7, pp.751-764.

Walraven, F., Pape, J. & Borg, G., 1994**:** Implications of Pb-isotopic composition at Geita gold deposit, Sukumaland Greenstone Belt, Tanzania. Journal of African Earth Sciences, **18**, 2, 111-121.

Werner, S. 1953: Interpretation of magnetic anomalies at sheet-like bodies, Sver. Geol. Undersok., ser. C. C. Arsbok. , no. 06.

West D. & Witherly K. 1995: Geophysical exploration for gold in deeply weathered terrains; two tropical cases Exploration Geophysics 26(3) 124 – 130.

APPENDICES

Aeromagnetic Total Magnetic Intensity (TMI) data used in the study

Easting's Line 1181	Northing's	TMI	Easting's Line 1181	Northing's	TMI
500048.51	9502941.1	34025	502472.5	9502953	34044
500099.01	9502941.1	34025	502523	9502953	34042
500149.51	9502941.1	34024	502573.5	9502953	34038
500200.01	9502942.1	34026	502624	9502953	34038
500250.5	9502942.1	34029	502674.5	9502953	34038
500301	9502942.1	34031	502725	9502954	34039
500351.5	9502942.1	34034	502775.5	9502954	34039
500402	9502942.1	34036	502826	9502954	34040
500452.5	9502943.1	34035	502876.5	9502954	34040
500503	9502943.1	34035	502927	9502955	34041
500553.5	9502943.1	34034	502977.5	9502955	34040
500604	9502943.1	34033	503028	9502955	34040
500654.5	9502944.1	34032	503078.5	9502955	34039
500705	9502944.1	34031	503129	9502956	34041
500755.5	9502944.1	34030	503179.5	9502956	34044
500806	9502944.1	34029	503230	9502956	34046
500856.5	9502945.1	34028	503280.5	9502956	34048
500906.99	9502945.1	34031	503331	9502957	34050
500957.49	9502945.1	34031	503381.5	9502957	34050
501007.99	9502945.1	34034	503432	9502957	34051
501058.49	9502946.1	34034	503482.5	9502957	34049
501108.99	9502946.1	34035	503533	9502958	34050
501159.49	9502946.1	34038	503583.5	9502958	34048
501209.99	9502946.1	34039	503634	9502958	34049
501260.49	9502947.1	34039	503684.5	9502958	34050
501310.99	9502947.1	34039	503735	9502959	34049
501361.49	9502947.1	34038	503785.5	9502959	34048
501411.99	9502947.1	34035	503836	9502959	34048
501462.49	9502948.1	34036	503886.5	9502959	34047
501512.99	9502948.1	34036	503937	9502960	34045
501563.49	9502948.1	34037	503987.5	9502960	34045
501613.98	9502948.1	34036	504038	9502960	34046
501664.48	9502949.1	34039	504088.5	9502960	34047
501714.98	9502949.1	34038	504139	9502961	34048
501765.48	9502949.1	34042	504189.5	9502961	34048
501815.98	9502949.1	34043	504240	9502961	34049
501866.48	9502950.1	34044	504290.5	9502961	34050
501916.98	9502950.1	34045	504340.9	9502962	34052
501967.48	9502950.1	34047	504391.4	9502962	34051
502017.98	9502950.1	34049	504441.9	9502962	34053

Easting's Line 1182	Northing's	TMI	Easting's Line 1182	Northing's	TMI
555456.6	9504011	33820	553066.4	9504042	33873
555406.8	9504012	33826	553016.6	9504043	33876
555357	9504012	33828	552966.9	9504043	33875
555307.3	9504013	33830	552917.1	9504044	33876
555257.4	9504014	33830	552867.3	9504044	33874
555207.6	9504014	33831	552817.5	9504045	33872
555157.8	9504015	33833	552767.7	9504046	33869
555108.1	9504015	33833	552717.9	9504046	33867
555058.3	9504016	33835	552668.1	9504047	33864
555008.4	9504017	33836	552618.3	9504048	33862
554958.6	9504017	33837	552568.5	9504048	33860
554908.9	9504018	33840	552518.7	9504049	33857
554859.1	9504019	33843	552469	9504050	33855
554809.3	9504019	33845	552419.1	9504050	33851
554759.5	9504020	33848	552369.3	9504051	33849
554709.7	9504021	33851	552319.5	9504052	33848
554659.9	9504021	33854	552269.9	9504052	33847
554610.1	9504022	33857	552220.1	9504053	33847
554560.3	9504023	33860	552170.2	9504053	33846
554510.5	9504023	33862	552120.5	9504054	33847
554460.7	9504024	33864	552070.7	9504055	33848
554411	9504025	33866	552020.9	9504055	33848
554361.1	9504025	33866	551971.1	9504056	33849
554311.3	9504026	33866	551921.3	9504057	33850
554261.5	9504026	33865	551871.5	9504057	33851
554211.8	9504027	33865	551821.7	9504058	33855
554162	9504028	33867	551771.9	9504059	33860
554112.1	9504028	33867	551722.1	9504059	33867
554062.4	9504029	33868	551672.3	9504060	33877
554012.6	9504030	33869	551622.5	9504061	33889
553962.8	9504030	33871	551572.7	9504061	33902
553913	9504031	33873	551522.9	9504062	33914
553863.2	9504032	33875	551473.1	9504062	33922
553813.4	9504032	33876	551423.3	9504063	33930
553763.6	9504033	33876	551373.5	9504064	33934
553713.8	9504034	33875	551323.7	9504064	33936
553664	9504034	33874	551273.9	9504065	33935
553614.2	9504035	33872	551224.2	9504066	33932
553564.4	9504035	33870	551174.4	9504066	33923
553514.6	9504036	33868	551124.5	9504067	33909
553464.8	9504037	33868	551074.7	9504068	33895
553415	9504037	33869	551025	9504068	33885
553365.2	9504038	33869	550975.2	9504069	33880

Easting's Line 1200	Northing's	TMI	Easting's Line 1200	Northing's	TMI
555424	9504432	33855	553129.5	9504446	33930
555374.1	9504432	33852	553079.6	9504446	33933
555324.3	9504433	33847	553029.8	9504447	33934
555274.4	9504433	33848	552979.9	9504447	33934
555224.5	9504433	33851	552930	9504447	33933
555174.6	9504433	33854	552880.1	9504448	33933
555124.8	9504434	33857	552830.3	9504448	33932
555074.9	9504434	33859	552780.4	9504448	33929
555025	9504434	33858	552730.5	9504449	33927
554975.1	9504435	33860	552680.6	9504449	33923
554925.2	9504435	33861	552630.8	9504449	33921
554875.3	9504435	33862	552580.8	9504449	33917
554825.4	9504436	33861	552531	9504450	33915
554775.6	9504436	33861	552481.1	9504450	33912
554725.7	9504436	33863	552431.2	9504450	33914
554675.8	9504437	33863	552381.3	9504451	33914
554626	9504437	33864	552331.4	9504451	33917
554576.1	9504437	33865	552281.7	9504451	33920
554526.2	9504437	33866	552231.8	9504452	33921
554476.3	9504438	33867	552181.9	9504452	33920
554426.4	9504438	33869	552132.1	9504452	33918
554376.6	9504438	33872	552082.2	9504453	33916
554326.6	9504439	33875	552032.3	9504453	33915
554276.8	9504439	33879	551982.4	9504453	33914
554226.9	9504439	33880	551932.5	9504453	33912
554177	9504440	33884	551882.6	9504454	33912
554127.1	9504440	33883	551832.7	9504454	33911
554077.3	9504440	33885	551782.9	9504454	33912
554027.4	9504441	33886	551733	9504455	33913
553977.5	9504441	33887	551683.1	9504455	33912
553927.6	9504441	33887	551633.2	9504455	33913
553877.8	9504441	33885	551583.4	9504456	33909
553827.9	9504442	33886	551533.5	9504456	33908
553778	9504442	33887	551483.6	9504456	33907
553728.1	9504442	33887	551433.7	9504457	33907
553678.2	9504443	33889	551383.8	9504457	33907
553628.3	9504443	33893	551333.9	9504457	33909
553578.4	9504443	33898	551284.1	9504457	33911
553528.6	9504444	33901	551234.2	9504458	33915
553478.7	9504444	33903	551184.3	9504458	33919
553428.8	9504444	33905	551134.4	9504458	33924

Easting's Line 1220	Northing's	TMI	Easting's Line 1220	Northing's	TMI
500002.6	9505699	34046	502275.1	9505710	34034
500053.1	9505699	34046	502325.6	9505710	34033
500103.6	9505699	34045	502376.1	9505710	34033
500154.1	9505699	34042	502426.6	9505710	34032
500204.6	9505700	34041	502477.1	9505711	34033
500255.1	9505700	34039	502527.6	9505711	34034
500305.6	9505700	34036	502578.1	9505711	34033
500356.1	9505700	34036	502628.6	9505711	34031
500406.6	9505701	34034	502679.1	9505712	34030
500457.1	9505701	34033	502729.6	9505712	34028
500507.6	9505701	34033	502780.1	9505712	34029
500558.1	9505701	34033	502830.6	9505712	34028
500608.6	9505702	34032	502881.1	9505713	34027
500659.1	9505702	34033	502931.6	9505713	34028
500709.6	9505702	34032	502982.1	9505713	34028
500760.1	9505702	34033	503032.6	9505713	34027
500810.6	9505703	34033	503083.1	9505713	34027
500861.1	9505703	34032	503133.6	9505714	34027
500911.6	9505703	34033	503184.1	9505714	34027
500962.1	9505703	34034	503234.6	9505714	34025
501012.6	9505703	34035	503285.1	9505714	34026
501063.1	9505704	34037	503335.6	9505715	34027
501113.6	9505704	34036	503386.1	9505715	34026
501164.1	9505704	34037	503436.6	9505715	34026
501214.6	9505704	34038	503487.1	9505715	34027
501265.1	9505705	34040	503537.6	9505716	34027
501315.6	9505705	34039	503588.1	9505716	34026
501366.1	9505705	34040	503638.6	9505716	34027
501416.6	9505705	34038	503689.1	9505716	34027
501467.1	9505706	34037	503739.6	9505717	34029
501517.6	9505706	34036	503790.1	9505717	34030
501568.1	9505706	34036	503840.6	9505717	34029
501618.6	9505706	34035	503891.1	9505717	34028
501669.1	9505707	34034	503941.6	9505718	34028
501719.6	9505707	34033	503992.1	9505718	34027
501770.1	9505707	34031	504042.6	9505718	34029
501820.6	9505707	34029	504093.1	9505718	34028
501871.1	9505708	34029	504143.6	9505719	34027
501921.6	9505708	34031	504194.1	9505719	34028
501972.1	9505708	34033	504244.6	9505719	34029
502022.6	9505708	34032	504295.1	9505719	34028
502073.1	9505709	34032	504345.5	9505720	34027

Easting's Line 1221	**Northing's**	**TMI**	**Easting's** Line1221	**Northing's**	**TMI**
500045.5	9505497	34029	502924	9505511	34020
500096	9505498	34030	502974.5	9505512	34019
500146.5	9505498	34031	503025	9505512	34019
500197	9505498	34032	503075.5	9505512	34018
500247.5	9505498	34033	503126	9505512	34018
500298	9505499	34033	503176.5	9505513	34018
500348.5	9505499	34031	503227	9505513	34019
500399	9505499	34030	503277.5	9505513	34018
500449.5	9505499	34029	503328	9505513	34018
500500	9505500	34027	503378.5	9505514	34017
500550.5	9505500	34027	503429	9505514	34017
500601	9505500	34025	503479.5	9505514	34018
500651.5	9505500	34026	503530	9505514	34019
500702	9505501	34025	503580.5	9505514	34022
500752.5	9505501	34027	503631	9505515	34021
500803	9505501	34028	503681.5	9505515	34022
500853.5	9505501	34027	503732	9505515	34023
500904	9505502	34027	503782.5	9505515	34023
500954.5	9505502	34026	503833	9505516	34025
501005	9505502	34027	503883.5	9505516	34025
501055.5	9505502	34027	503934	9505516	34024
501106	9505502	34030	503984.5	9505516	34022
501156.5	9505503	34029	504035	9505517	34021
501207	9505503	34030	504085.5	9505517	34021
501257.5	9505503	34030	504136	9505517	34020
501308	9505503	34031	504186.5	9505517	34021
501358.5	9505504	34032	504237	9505518	34021
501409	9505504	34032	504287.5	9505518	34020
501459.5	9505504	34032	504337.9	9505518	34021
501510	9505504	34033	504388.4	9505518	34020
501560.5	9505505	34031	504438.9	9505519	34019
501611	9505505	34032	504489.4	9505519	34018
501661.5	9505505	34031	504539.9	9505519	34017
501712	9505505	34033	504590.4	9505519	34018
501762.5	9505506	34032	504640.9	9505520	34018
501813	9505506	34032	504691.4	9505520	34016
501863.5	9505506	34031	504741.9	9505520	34017
501914	9505506	34031	504792.4	9505520	34017
501964.5	9505507	34031	504842.9	9505521	34016
502015	9505507	34030	504893.4	9505521	34013
502065.5	9505507	34030	504943.9	9505521	34012
502116	9505507	34030	504994.4	9505521	34010

Easting's Line 1240	Northing's	TMI	Easting's Line 1240	Northing's	TMI
555465.1	9506877	33907	546057.3	9506914	33917
555415.1	9506877	33905	546007.3	9506915	33922
555365	9506877	33905	545957.2	9506915	33926
555315	9506877	33902	545907.2	9506915	33936
555265	9506877	33900	545857.2	9506915	33948
555214.9	9506878	33900	545807.1	9506915	33961
555164.9	9506878	33899	545757.1	9506916	33979
555114.8	9506878	33901	545707.1	9506916	34001
555064.8	9506878	33902	545657	9506916	34032
555014.8	9506878	33903	545606.9	9506916	34066
554964.7	9506879	33902	545556.9	9506916	34104
554914.6	9506879	33900	545506.9	9506917	34135
554864.6	9506879	33897	545456.8	9506917	34146
554814.6	9506879	33894	545406.8	9506917	34133
554764.5	9506879	33889	545356.8	9506917	34101
554714.5	9506880	33884	545306.8	9506917	34064
554664.4	9506880	33877	545256.7	9506918	34038
554614.4	9506880	33872	545206.7	9506918	34020
554564.4	9506880	33868	545156.6	9506918	34011
554514.3	9506880	33863	545106.6	9506918	34008
554464.3	9506881	33860	545056.6	9506918	34010
554414.3	9506881	33855	545006.5	9506919	34019
554364.2	9506881	33851	544956.5	9506919	34029
554314.1	9506881	33847	544906.5	9506919	34041
554264.1	9506881	33842	544856.4	9506919	34050
554214.1	9506882	33840	544806.3	9506919	34049
554164	9506882	33838	544756.3	9506920	34043
554114	9506882	33837	544706.3	9506920	34031
554064	9506882	33837	544656.2	9506920	34018
554013.9	9506882	33838	544606.2	9506920	34003
553963.9	9506883	33839	544556.2	9506920	33991
553913.8	9506883	33840	544506.1	9506921	33980
553863.8	9506883	33842	544456.1	9506921	33972
553813.8	9506883	33843	544406	9506921	33964
553763.7	9506883	33843	544356	9506921	33956
553713.6	9506884	33842	544306	9506921	33951
553663.6	9506884	33842	544255.9	9506922	33945
553613.6	9506884	33840	544205.8	9506922	33941
553563.5	9506884	33840	544155.8	9506922	33936
553513.5	9506884	33840	544105.8	9506922	33932
553463.4	9506885	33839	544055.7	9506922	33929
553413.4	9506885	33839	544005.7	9506923	33927
553363.4	9506885	33840	543955.6	9506923	33924

Easting's Line 1250	Northing's	TMI	Easting's Line 1250	Northing's	TMI
546219.1	9508672	33879	548592.5	9508683	33883
546269.5	9508672	33879	548643.1	9508684	33885
546320.1	9508672	33879	548693.5	9508684	33884
546370.5	9508673	33879	548744.1	9508684	33885
546421.1	9508673	33878	548794.5	9508684	33886
546471.5	9508673	33878	548845.1	9508685	33885
546522.1	9508673	33880	548895.5	9508685	33884
546572.5	9508674	33884	548946.1	9508685	33883
546623.1	9508674	33885	548996.5	9508685	33883
546673.5	9508674	33885	549047.1	9508686	33882
546724.1	9508674	33883	549097.5	9508686	33882
546774.5	9508675	33880	549148.1	9508686	33879
546825.1	9508675	33875	549198.5	9508686	33880
546875.5	9508675	33871	549249.1	9508687	33880
546926.1	9508675	33869	549299.5	9508687	33879
546976.5	9508676	33867	549350.1	9508687	33880
547027.1	9508676	33866	549400.5	9508687	33880
547077.5	9508676	33867	549451.1	9508688	33880
547128.1	9508676	33867	549501.5	9508688	33879
547178.5	9508677	33870	549552.1	9508688	33876
547229.1	9508677	33870	549602.5	9508688	33877
547279.5	9508677	33872	549653.1	9508689	33876
547330.1	9508677	33872	549703.5	9508689	33876
547380.5	9508678	33874	549754.1	9508689	33876
547431.1	9508678	33873	549804.5	9508689	33874
547481.5	9508678	33873	549855.1	9508690	33873
547532.1	9508678	33871	549905.5	9508690	33871
547582.5	9508679	33871	549956.1	9508690	33869
547633.1	9508679	33871	550006.5	9508690	33869
547683.5	9508679	33869	550057.1	9508691	33870
547734.1	9508679	33870	550107.5	9508691	33867
547784.5	9508680	33871	550158.1	9508691	33867
547835.1	9508680	33868	550208.5	9508691	33867
547885.5	9508680	33866	550259.1	9508692	33865
547936.1	9508680	33864	550309.5	9508692	33865
547986.5	9508681	33863	550360.1	9508692	33863
548037.1	9508681	33864	550410.5	9508692	33864
548087.5	9508681	33866	550461.1	9508693	33864
548138.1	9508681	33868	550511.5	9508693	33863
548188.5	9508682	33872	550562.1	9508693	33863

Easting's Line 1260	Northing's	TMI	Easting's Line 1260	Northing's	TMI
501326	9508658	33948	503447	9508668	34011
501376.5	9508658	33948	503497.5	9508668	34014
501427	9508658	33948	503548	9508669	34018
501477.5	9508659	33948	503598.5	9508669	34026
501528	9508659	33949	503649	9508669	34032
501578.5	9508659	33950	503699.5	9508669	34036
501629	9508659	33954	503750	9508670	34041
501679.5	9508660	33956	503800.5	9508670	34044
501730	9508660	33957	503851	9508670	34046
501780.5	9508660	33962	503901.5	9508670	34046
501831	9508660	33966	503952	9508671	34046
501881.5	9508661	33970	504002.5	9508671	34047
501932	9508661	33972	504053	9508671	34047
501982.5	9508661	33974	504103.5	9508671	34047
502033	9508661	33976	504154	9508672	34048
502083.5	9508662	33979	504204.5	9508672	34047
502134	9508662	33983	504255	9508672	34048
502184.5	9508662	33984	504305.5	9508672	34050
502235	9508662	33988	504355.9	9508673	34053
502285.5	9508663	33994	504406.4	9508673	34055
502336	9508663	33997	504456.9	9508673	34056
502386.5	9508663	33998	504507.4	9508673	34057
502437	9508663	33999	504557.9	9508674	34058
502487.5	9508664	34001	504608.4	9508674	34056
502538	9508664	34001	504658.9	9508674	34055
502588.5	9508664	34002	504709.4	9508674	34053
502639	9508664	34000	504759.9	9508675	34052
502689.5	9508665	34000	504810.4	9508675	34049
502740	9508665	34003	504860.9	9508675	34046
502790.5	9508665	34004	504911.4	9508675	34042
502841	9508665	34006	504961.9	9508676	34039
502891.5	9508666	34008	505012.4	9508676	34037
502942	9508666	34008	505062.9	9508676	34038
502992.5	9508666	34005	505113.4	9508676	34039
503043	9508666	34003	505163.9	9508677	34042
503093.5	9508667	34003	505214.4	9508677	34044
503144	9508667	34003	505264.9	9508677	34047
503194.5	9508667	34002	505315.4	9508677	34050
503245	9508667	34002	505365.9	9508677	34050

Easting's Line 1262	Northing's	TMI	Easting's Line 1262	Northing's	TMI
555464.7	9510064	33917	549474	9509977	33927
555415.2	9510064	33915	549424.5	9509977	33925
555365.6	9510063	33914	549375	9509976	33924
555316.1	9510062	33913	549325.5	9509975	33920
555266.6	9510061	33912	549276	9509974	33919
555217.1	9510061	33912	549226.4	9509974	33917
555167.6	9510060	33910	549176.9	9509973	33918
555118.1	9510059	33909	549127.4	9509972	33919
555068.6	9510059	33907	549077.9	9509971	33921
555019.1	9510058	33906	549028.4	9509971	33925
554969.6	9510057	33905	548978.9	9509970	33926
554920.1	9510056	33904	548929.4	9509969	33928
554870.6	9510056	33904	548879.9	9509969	33930
554821.1	9510055	33905	548830.4	9509968	33930
554771.5	9510054	33905	548780.9	9509967	33931
554722	9510053	33905	548731.4	9509966	33930
554672.5	9510053	33905	548681.9	9509966	33929
554623	9510052	33907	548632.3	9509965	33926
554573.5	9510051	33908	548582.8	9509964	33922
554524	9510051	33910	548533.3	9509964	33918
554474.4	9510050	33913	548483.8	9509963	33915
554425	9510049	33917	548434.3	9509962	33914
554375.4	9510048	33921	548384.8	9509961	33915
554326	9510048	33922	548335.2	9509961	33915
554276.4	9510047	33923	548285.7	9509960	33917
554227	9510046	33925	548236.2	9509959	33918
554177.4	9510046	33924	548186.7	9509959	33917
554127.9	9510045	33925	548137.2	9509958	33921
554078.4	9510044	33925	548087.7	9509957	33924
554028.9	9510043	33924	548038.2	9509956	33927
553979.4	9510043	33923	547988.7	9509956	33931
553929.9	9510042	33922	547939.2	9509955	33935
553880.3	9510041	33923	547889.7	9509954	33936
553830.8	9510041	33922	547840.2	9509953	33937
553781.3	9510040	33921	547790.7	9509953	33936
553731.8	9510039	33921	547741.1	9509952	33935
553682.3	9510038	33921	547691.6	9509951	33933
553632.8	9510038	33919	547642.1	9509951	33930
553583.3	9510037	33918	547592.6	9509950	33927
553533.8	9510036	33917	547543.1	9509949	33925
553484.3	9510036	33918	547493.6	9509948	33922

Easting's Line 1266	Northing's	TMI	Easting's Line1266	Northing's	TMI
500006.6	9508385	34081	507258	9508460	34012
500055.9	9508385	34083	507620.8	9508465	34011
500105.3	9508386	34078	507983.7	9508471	34008
500154.8	9508386	34076	508346.5	9508476	34007
500204.1	9508386	34076	508709.3	9508481	34004
500253.6	9508386	34078	509072.1	9508487	34001
500302.9	9508387	34075	509435	9508492	34000
500352.3	9508387	34076	509797.8	9508498	34000
500401.8	9508387	34078	510160.6	9508503	33999
500451.1	9508387	34078	510523.5	9508508	33998
500500.6	9508388	34080	510886.3	9508514	33997
500549.9	9508388	34081	511249	9508519	33996
500599.3	9508388	34081	511611.8	9508524	33995
500648.8	9508388	34078	511974.7	9508530	33995
500698.1	9508389	34078	512337.5	9508535	33994
500747.6	9508389	34078	512700.3	9508541	33992
500796.9	9508389	34077	513063.1	9508546	33992
500846.3	9508389	34076	513426	9508551	33993
500895.8	9508390	34074	513788.8	9508557	33991
500945.1	9508390	34070	514151.6	9508562	33990
500994.6	9508390	34065	514514.5	9508567	33989
501043.9	9508390	34064	514877.3	9508573	33989
501093.3	9508390	34062	515240.1	9508578	33988
501142.8	9508391	34059	515602.9	9508583	33985
501192.1	9508391	34059	515965.8	9508589	33983
501241.6	9508391	34059	516328.6	9508594	33981
501290.9	9508391	34058	516691.4	9508600	33979
501340.3	9508392	34055	517054.2	9508605	33979
501389.8	9508392	34053	517417.1	9508610	33977
501439.1	9508392	34052	517779.9	9508616	33977
501488.6	9508392	34051	518142.6	9508621	33977
501537.9	9508393	34049	518505.5	9508626	33977
501587.3	9508393	34050	518868.3	9508632	33978
501636.8	9508393	34050	519231.1	9508637	33978
501686.1	9508393	34050	519593.9	9508642	33981
501735.6	9508394	34050	519956.8	9508648	33983
501784.9	9508394	34050	520319.6	9508653	33987
501834.3	9508394	34051	520682.5	9508659	33990
501883.8	9508394	34054	521045.3	9508664	33991
501933.1	9508395	34057	521408.1	9508669	33993
501982.5	9508395	34059	521770.9	9508675	33994